eISSN 2345-0630
ISBN 978-609-457-959-2
eISBN 978-609-457-958-5

VILNIUS GEDIMINAS TECHNICAL UNIVERSITY

OCTOBER 20–22, 2016, DRUSKININKAI, LITHUANIA

PROCEEDINGS OF 11TH INTERNATIONAL CONFERENCE BIOMDLORE 2016

EDITED BY
MEČISLOVAS MARIŪNAS
JULIUS GRIŠKEVIČIUS
GEDIMINAS GAIDULIS

SPONSORS

VGTU LEIDYKLA TECHNIKA
Vilnius 2016

Proceedings of 11th International Conference BIOMDLORE 2016

October 20–22, 2016, Druskininkai, Lithuania

The Conference organized by Vilnius Gediminas Technical University (Lithuania), Kaunas University of Technology (Lithuania), Bialystok University of Technology (Poland), Lithuanian Society of Biomechanics and IFToMM National Committee of Lithuania.

Edited by Mečislovas Mariūnas, Julius Griškevičius and Gediminas Gaidulis

All papers were qualified on the basis of critical reviews.

The Conference is focused on the issues of biomechanics, gait and locomotion, orthopaedics and traumatology, assistive technologies, rehabilitation, medical diagnostics, biosignals analysis, mathematical modelling.

VGTU press TECHNIKA scientific book No. 2384-M
eISSN 2345-0630
ISBN 978-609-457-959-2
eISBN 978-609-457-958-5
http://leidykla.vgtu.lt

PREFACE

On behalf of the Lithuanian Society of Biomechanics, we are pleased to welcome you to the 11th International Conference BIOMDLORE 2016. This year's Conference is being hosted by Vilnius Gediminas Technical University (VGTU), more specifically by the Department of Biomechanics, which celebrates 20th Anniversary in 2016, as it was founded in 1996 at Faculty of Mechanics of VGTU. Vilnius Gediminas Technical University is a state university, which is one of the largest higher education institutions in Lithuania, and one of the leading universities in the Baltic States.

The contents of the Proceedings largely reflect the issues which are currently explored within the field of biomedical engineering and biomechanics. These issues include investigating the biomechanical properties of various soft and hard biotissues, dynamics and modelling of musculo-skeletal system, development of various medical diagnostic tools, processing of biosignals etc. The results of the research are of interest to experts in engineering, medicine, rehabilitation, orthopaedics and other fields.

We believe that the materials which will be presented at the Conference will provide a comprehensive overview of the achievements of researchers from Poland, Latvia, Estonia, Ukraine, Belarus, Russia, United Kingdom, United States of America and Lithuania. Moreover, for the very first time in history of BIOMDLORE conference, we, organizers, are very pleased having two keynote speakers dr. James Shippen and dr. Patrick Mark Aubin presenting at the Conference. We believe that the presentations delivered by the participants of BIOMDLORE 2016 will not only inspire new avenues for research in biomedical engineering and biomechanics, but will open doors for possible cooperation in joining research forces and form new teams.

We would like to take this opportunity to express our gratitude to the persons and institutions that have helped organize the Conference, reviewers for evaluating the articles, and all authors for submitting their work.

It is our special privilege and great pleasure to welcome you to the 11th International Conference BIOMDLORE 2016. We hope that the Conference will provide an arena for fruitful discussions and building new friendships. BIOMDLORE 2016 is not only about presentation and publication. We hope that it can be something more – BIOMDLORE 2016 is about to strengthen existing relationships and form new ones.

JULIUS GRIŠKEVIČIUS
Chair of Organizing Committee

MEČISLOVAS MARIŪNAS
Chair of Scientific Committee

SCIENTIFIC COMMITTEE

Chairman:
Prof. M. MARIŪNAS (Lithuania)

Co-chairman:
Assoc. Prof. J. GRIŠKEVIČIUS (Lithuania)

Secretary:
Assoc. Prof. ŠEŠOK (Lithuania)

Members:
Dr. P. M. AUBIN (USA)
Prof. J. BROŽAITIENĖ (Lithuania)
Assoc. Prof. A. DARDZIŃSKA-GŁĘBOCKA (Poland)
Prof. C. FRIGO (Italy)
Prof. V. GRIGAS (Lithuania)
Assoc. Prof. A. JAKŠTAS (Lithuania)
Prof. A. JUOCEVIČIUS (Lithuania)
Prof. R. KAČIANAUSKAS (Lithuania)
Prof. K. KĘDZIOR (Poland)
Assoc. Prof. A. KILIKEVIČIUS (Lithuania)
Prof. N. KIZILOVA (Ukraine)
Prof. I. KNETS (Latvia)
Prof. V. LAURUŠKA (Lithuania)
Prof. V. LAURUTIS (Lithuania)
Prof. A. RUGGIERO (Italy)
Assoc. Prof. D. SATKUNSKIENĖ (Lithuania)
PD Dr. K.-U. SCHMITT (Switzerland)
Dr. J. SHIPPEN (United Kingdom)
Prof. T. TOLOČKA (Lithuania)
Prof. V. TREGUBOV (Russia)
Prof. K. J. VAN ZWIETEN (Belgium)
Prof. A. VĒTRA (Latvia)
Prof. P. ŽILIUKAS (Lithuania)

ORGANIZING COMMITTEE

Chairman:
Assoc. Prof. J. GRIŠKEVIČIUS (Lithuania)

Co-Chairman:
Assoc. Prof. J. PAUK (Poland)

Secretary:
Assoc. Prof. K. DAUNORAVIČIENĖ (Lithuania)

Members:
Assoc. Prof. A. ŠEŠOK (Lithuania)
G. GAIDULIS (Lithuania)
G. JONAITIS (Lithuania)
J. ŽIŽIENĖ (Lithuania)
O. ARDATOV (Lithuania)
A. LINKEL (Lithuania)
D. LUKŠYS (Lithuania)
Dr. A. DOMEIKA (Lithuania)

CONTENTS

11TH INTERNATIONAL CONFERENCE
BIOMDLORE 2016
OCTOBER 20–22, 2016, DRUSKININKAI, LITHUANIA
BIOMDLORE.VGTU.LT

eISSN 2345-0630
ISBN 978-609-457-959-2
eISBN 978-609-457-958-5
DOI: 10.3846/biomdlore.2016.01

Computer simulation of the pulsating blood flow in arteries with stenosis, aneurysms and plaques

Vladimir Tregubov
Saint-Petersburg State University, Russia
E-mail: *v.tregubov@spbu.ru*

(Received 19 February 2016; accepted 8 April 2016)

Abstract. The stenosis, aneurysms and plaques are the most common types of the blood vessel pathology. To study their influence on the pulsating blood flow and the internal pressure the mechanical models of pulsating blood flow and the above mentioned pathology of blood vessels were developed. The blood was considered as non-Newtonian liquid. As the boundary condition on the vessel wall the semi-slip regime was chosen. Computer simulation was executed using Finite element method, which was realized by means of the system ABAQUS. As results the pressure and velocity distributions were obtained for the four kinds of pathology in each time moment of the pulse cycle.

Keywords: computer simulation, non-Newtonian liquid, plaque, stenosis, aneurism.

Introduction

Stenosis of blood vessels is the narrowing of their lumen, which causes poor circulation and tissue nutrition. This leads to the hypertrophy of left ventricle and the heart attack and stroke.

An aneurysm is a dilatation of the blood vessel to an area with thinning and weakening of its walls. This extension may be saccular or fusiform shape. An aneurysm is dangerous because the vessel in this place can break at any moment, causing massive bleeding, or haemorrhage. In addition, an aneurysm is a convenient place for the formation of blood clots.

Cholesterol plaques are formed on the rough walls of blood vessels as layers of fat that appears as a result of metabolic disorders. Thus there is an overgrowth of muscle cells and connective tissue that leads to reduced blood flow. This disease can affect arteries of large and medium size. In the area of plaque there is a possibility of the protective endothelium damage, which contributes to the formation of parietal thrombi and the further reduction of blood flow. In the future, these thrombi are often destroyed, and their particles are carried to the small blood vessels, causing the embolism, apoplectic stroke or heart attack.

The majority of authors model the blood by non-Newtonian fluid [1]. This allows, at least partially, to take into account the complexity of the internal blood structure, containing a large number of blood cells. The modelling of pulsating flow of blood as non-Newtonian liquid for deformable arteries without pathologies was presented in [2]. The mathematical model of atherosclerosis plaque formation was proposed in [3], where the blood was considered as an incompressible non-Newtonian fluid with shear-thinning viscosity. The wall shear stress and blood velocity behaviour in a vessel with two plaques in different positions were obtained. The numerical simulation of Non-Newtonian blood flow in a stenosis vessel was presented in [4]. The vessel was considered as two-dimensional channel and plaque area is modelled as a homogenous porous medium. The non-Newtonian micropolar fluid was used in [5] for mathematical modelling of the arterial blood flow through a composite stenosis.

But even in all these cases, pointed above, the blood can be considered as a liquid only in large and medium arteries. A number of researches attempt to model the blood as two-phase liquid. Thus, in [6] both phases are liquids with different properties. The two-phase non-linear model was used in [7] for the modelling of flow through the stenosed blood vessels. The most difficulty of

this approach consists in that mechanical properties of blood cells are not clearly understood as yet.

Mechanical model and computer simulation

Four kinds of pathology were considered in the proposed model: saccular and fusiform aneurysms, stenosis and plaque. They were modelled by means of non-deformable cylinders with a diameter 2 cm and spheres with smooth connections, as it is shown in Fig. 1. The blood was considered as non-Newtonian liquid with the power law dependence of the stress tensor **T** from the strain velocity tensor **D**. The governing equations in this case can be written as follows:

$$\begin{cases} \rho \dfrac{d\mathbf{v}}{dt} = \nabla \cdot \left(- p\mathbf{I} + \mathbf{T} \right), \\ div\, \mathbf{v} = 0, \\ \mathbf{T} = 2k \left| I_2 \right|^{\left(\frac{n-1}{2} \right)} \mathbf{D}, \end{cases} \tag{1}$$

where **v** is the velocity vector, ρ is the density, p is the pressure, **I** is the unit vector, I_2 is the second invariant, k and n are the coefficients, which define the specific kind of power law. The pulsating velocity profile was set at the entrance cross-section of the considered artery segment.

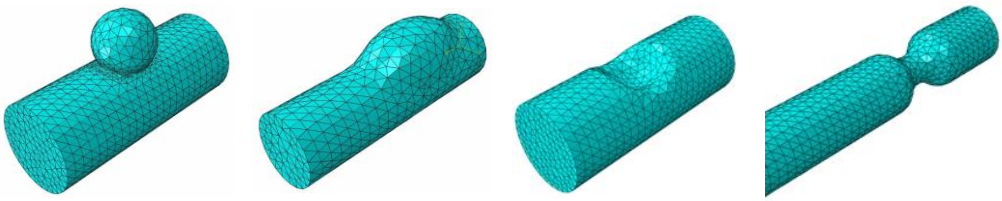

a b c d

Fig. 1. The mechanical models of a) saccular aneurysm, b) fusiform aneurysm, c) plaque, d) stenosis

In distinction to the papers cited above the so called “semi-slip” condition was used as a boundary condition at the vessel wall. This allows us to take into account the specificity of the interaction of the blood cells and plasma with the vessel wall. It can be written as follows:

$$v_\tau \Big|_{wall} = -b \left(\frac{\partial v_\tau}{\partial n} \right) \Bigg|_{wall}, \tag{2}$$

where v_τ is the tangent velocity, n in the normal to the vessel inner surface, b is the coefficient.

Computer simulation was executed using Finite element method, which was realized by means of the system ABAQUS, which has high-powered means for the creation of a model geometry and visualization of the results. For this purpose, the meshes of the first order were used, as it is shown in Fig. 1.

Results

As results the pressure and velocity distributions were obtained for the four kinds of pathology in each time moment of the pulse cycle. The examples of the pressure distribution are shown in Fig. 2 and of the velocity distribution in Fig. 3. It is also possible to construct the velocity profiles in any cross-section.

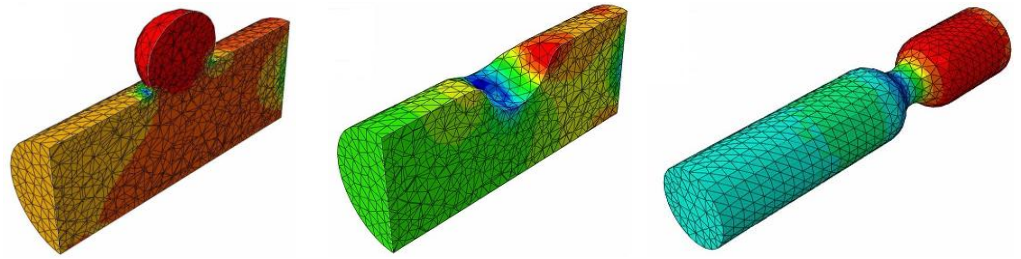

a b c

Fig. 2. The pressure distribution in time moment 0.5 sec in a) saccular aneurism, b) plaque, c) stenosis

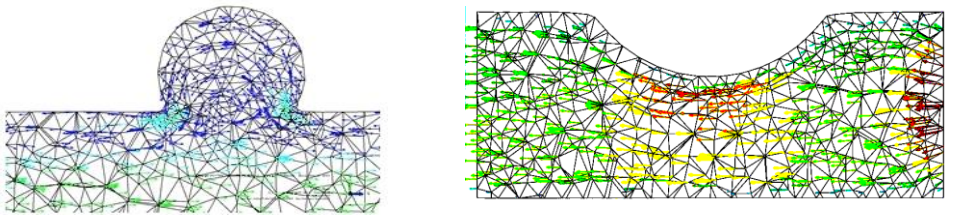

a b

Fig. 3. The velocity distribution in in time moment 1 sec in a) saccular aneurism, b) plaque

Conclusion

The information, received by means of computer simulation, make it possible to demonstrate how the pulse blood flow and pressure are changed in the presence of certain types of vascular pathology. In particular, the origin and disappearance of vortexes, the return wall-adjacent blood flow and the appearance of the critical pressure areas were observed. The obtained results allow also us to construct the velocity profiles in each cross-section.

References

[1] Dutta, A.; Tarbell, J. M. 1996. Influence of non-Newtonian behavior of blood on flow in an elastic artery model, *Journal of Biomechanical Engineering* 118(1): 111–119. http://dx.doi.org/10.1115/1.2795936

[2] Ratkina, S. V.; Tregubov, V. P. 2010. Mathematical simulation of a blood stream in large arteries, in *Biomechanics 2010: International Conference of Polish Society of Biomechanics. Book of abstracts,* August 25–28, 2010, Warsaw, Poland. Warsaw: Warsaw University of Technology, 187–188.

[3] Silva, T., *et al*. 2013. Mathematical modeling of atherosclerotic plaque formation coupled with a non-Newtonian model of blood flow, *Conference Papers in Mathematics* 2013: 405914. http://dx.doi.org/10.1155/2013/405914

[4] Shojaeizadeh, M.; Yeganegi, A. R. 2015. Effects of the non-Newtonian viscosity of blood on flow field in a constricted artery with a porous plaque. *International Journal of Science and Engineering Investigations* 4(38): 15–18.

[5] Ellahi, R., *et al*. 2014. A mathematical study of non-Newtonian micropolar fluid in arterial blood flow through composite stenosis, *Applied Mathematics & Information Sciences* 8(4): 1567–1573. http://dx.doi.org/10.12785/amis/080410

[6] Srivastava, V. P. 1996. Two-phase model of blood flow through stenosed tubes in the presence of a peripheral layer: applications, *Journal of Biomechanics* 29(10): 1377–1382. http://dx.doi.org/10.1016/0021-9290(96)00037-1

[7] Sankar, D. S.; Lee, U. 2007. Two-phase non-linear model for the flow through stenosed blood vessels, *Journal of Mechanical Science and Technology* 21(4): 678–689. http://dx.doi.org/10.1007/BF03026973

11TH INTERNATIONAL CONFERENCE
BIOMDLORE 2016
OCTOBER 20–22, 2016, DRUSKININKAI, LITHUANIA
BIOMDLORE.VGTU.LT

eISSN 2345-0630
ISBN 978-609-457-959-2
eISBN 978-609-457-958-5
DOI: 10.3846/biomdlore.2016.02

BoB – biomechanics in MATLAB

James Shippen[1], Barbara May[2]
[1, 2] Coventry University, United Kingdom
E-mails: [1] *j.shippen@coventry.ac.uk (corresponding author)*, [2] *barbara.may@coventry.ac.uk*

(Received 22 February 2016; accepted 28 April 2016)

Abstract. Biomechanics is a maturing discipline with numeric analysis of kinematic and kinetic data becoming widespread within academic research institutions and commercial organisations. Many engineers and scientists engaged in biomechanical analysis already routinely use MATLAB as it provides an environment that is productive for a broad range of analysis, facilitates rapid code development and provides sophisticated graphical output. Therefore, a biomechanical package which is based within the MATLAB environment will be familiar to many analysts and will inherit much of the analysis capabilities of MATLAB. This paper describes BoB (Biomechanics of Bodies) which is a biomechanical analysis package written in MATLAB M-code, capable of performing inverse dynamics analysis, using optimization methods to solve for muscle force distribution and produces sophisticated graphical image and video output.

Keywords: inverse dynamics, muscle force distribution, MATLAB.

Introduction

With the increased power and capabilities of technical computing, simulations of human movement have been able to provide the opportunity to learn how components interact to produce coordinated movement [1]. Several software programmes have been designed to simulate human movement but each system has defined the parameters of the musculoskeletal system differently. The number of muscles which have been included in the individual programmes, the ease of use and outputs in terms of graphics and muscle forces vary considerably.

For example, "OpenSim" which was developed at Stanford National Institute of Health Centre for Biomedical Computation is an open source software system which allows users to build models of musculoskeletal structures, create dynamic simulations of movement and determine the forces that muscles and bones exert during movement [2]. Another package "LifeMOD" could be scaled to the measurements of the test subject and included 19 body segments, 18 joints but only 38 muscles of the body [3]. "The AnyBody Technology" [4] software was developed for biomechanics and computer-aided ergonomics and marketed for use in product design in the automotive, medical and aerospace industries. It was also used in sports to maximise performance and to enable exercises to be devised targeted at strengthening precise points on the body.

However, many engineers and scientists engaged in biomechanical analysis routinely operate within MATLAB which provides an environment that accommodates a broad range of analysis, facilitates rapid code development and provides sophisticated graphical output. The Biomechanics of Bodies (BoB) biomechanical software is based within the MATLAB environment and inherits much of the analysis capabilities of MATLAB. BoB is written in MATLAB M-code, is capable of performing inverse dynamics analysis, uses optimization methods to solve for muscle force distribution, can run user developed m-code packages and produces sophisticated graphical image and video output.

Methods

BoB is capable of undertaking an inverse dynamics analysis of a subject's movement to calculate the torques occurring at the joints followed by an optimization approach to distribute the loads in the corresponding muscles which traverse the joints. The body of the subject is assumed

to be composed of a number of rigid segments, each with associated mass and rotational inertia properties. These segments are interconnected by joints. Forces act between these segments due to muscles which cross one or more joints. Additionally, external forces, for example ground reaction forces, act on the subject. BoB also contains a muscle model comprising approximately 600 muscle units including the major locomotor muscles of the body.

Inverse dynamics is used to calculate the torques at the joints corresponding to the observed motion and external forces from which the muscles loads are calculated. However, there is not a unique solution as the number of muscles is greatly in excess of the number of joints and hence the number of torques. Therefore, it is necessary to select the one solution for the infinite possible solution which minimises a cost function. Numerous cost functions have been proposed [5]; by default, BoB uses the sum of the square of the muscle activations for the cost function where muscle activation is defined as the muscle force divided by the muscle maximal isometric load. This function has the effect of reducing the maximum muscle activation which will reduce the propensity to fatigue and hence the function can be physiologically justified; however arbitrary user defined cost functions can also be implemented. The optimised solution must also satisfy a set of equality conditions (the external torques due to external forces and segmental inertial forces must equal the torque due to the surrounding muscles at each joint) and inequality conditions (the load in each muscle must be positive as the muscle cannot push and the load must be less than the maximum force the muscle can generate). The minimization of the cost function, subject to equality and inequality constraints, is solved using the interior-point-convex algorithm implemented in the MATLAB QUADPROG [6] function. The interior-point-convex algorithm attempts to follow a path that is strictly inside the constraints. It uses a presolve module to remove redundancies, and to simplify the problem by solving for components that are straightforward. If the cost function is a higher order than quadratic the Interior Point algorithm is implemented in the FMINCON [7] function.

To undertake the inverse dynamics analysis, the time history of the joint articulations, and their time derivatives, must be available. BoB can accept joint angles as closed form equations which are a function of time however this is typically limited to idealized situations such as teaching examples. More realistic joint angle time histories are obtained from motion capture systems – BoB has an interface to read motion capture data directly from C3D files as produced by optical tracking systems Vicon, Qualisys and CodaMotion systems and MVNX files from the Xsens magneto-inertial system. As an example of an application of the BoB biomechanical analysis software, the loads in the lumbar region of the back were calculated for 7 amateur and 4 professional horticulturalists during hedge trimming. The movements of the subjects were measured using a 12 camera Vicon optical tracking system. The ground reaction forces were measured using 2 AMTI OR6-7 forceplates.

Results

Following the measurement of the subjects' movements and external forces, BoB was used to calculate the torques occurring at each of the major joints and the muscle force distribution as described above. Figure 1 shows an example of the muscle loading distribution. The joint contact loads were calculated by the vector summation of the forces of constraint at the joints and the forces in the muscles traversing the joint. Figure 2 shows typical joint contact forces occurring between the sacrum and L5 vertebra for amateur and professional horticulturalists.

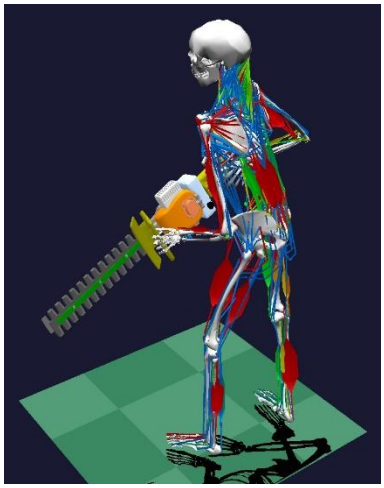

Fig. 1. Muscle activations are indicated by the shading and bulging

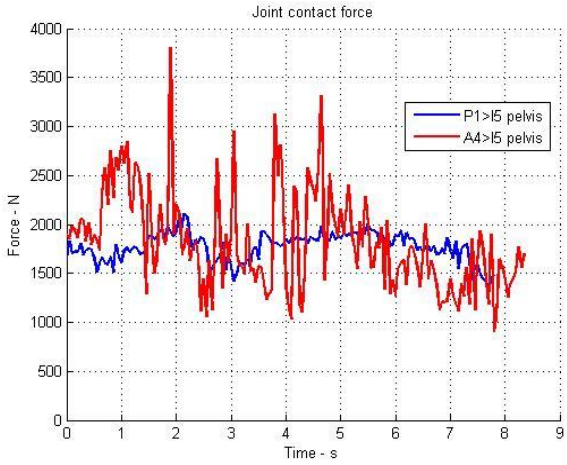

Fig. 2. Typical joint contact forces between the sacrum and L5 vertebra for professional (blue) and amateur (red) horticulturalists

Conclusions

A biomechanical analysis package called BoB (Biomechanics of Bodies) has been written in m-code within the MATLAB environment. BoB inherits much of the analysis capability of MATLAB and will be familiar to existing MATLAB users resulting in a minimal learning curve and rapid productivity. BoB can calculate joint torques, muscle load distribution and joint contact forces. BoB can acquire motion capture data from any system which produce files in the industry standard format C3D or MVNX formats. BoB can be used as an analysis tool in a variety of disciplines i.e. sports, ergonomics, product development and health sciences. In this example BoB was used to analyse the action of horticulturalists and it was found that professional horticulturalists adopted a posture and action which resulted in significantly lower joint contact forces between the sacrum and L5 vertebra than observed in the amateurs.

BoB can be downloaded from http://www.marlbrook.com/download.

References

[1] Pandy, M. 2001. Computer modeling and simulation of human movement, *Annual Review of Biomedical Engineering* 3: 245–273. http://dx.doi.org/10.1146/annurev.bioeng.3.1.245

[2] *OpenSim* [online]. 2010. Stanford University [cited 22 February 2016]. Available from Internet: http://opensim.stanford.edu/

[3] *LifeMOD* [online]. 2016. LifeModeler, Inc. [cited 22 February 2016]. Available from Internet: http://www.lifemodeler.com/

[4] *AnyBody Technology* [online]. 2016. Aalborg University [cited 22 February 2016]. Available from Internet: http://www.anybodytech.com/

[5] An, K. N., *et al.* 1984. Determination of muscle and joint forces: a new technique to solve the indeterminate problem, *Journal of Biomechanical Engineering* 106(4): 364–367. http://dx.doi.org/10.1115/1.3138507

[6] Coleman, T. F.; Li, Y. 1996. A reflective Newton method for minimizing a quadratic function Subject to bounds on some of the variables, *SIAM Journal on Optimization* 6(4): 1040–1058. http://dx.doi.org/10.1137/S1052623494240456

[7] Byrd, R. H.; Gilbert, J. C.; Nocedal, J. 2000. A trust region method based on interior point techniques for nonlinear programming, *Mathematical Programming* 89(1): 149–185. http://dx.doi.org/10.1007/PL00011391

11TH INTERNATIONAL CONFERENCE
BIOMDLORE 2016
OCTOBER 20–22, 2016, DRUSKININKAI, LITHUANIA
BIOMDLORE.VGTU.LT

eISSN 2345-0630
ISBN 978-609-457-959-2
eISBN 978-609-457-958-5
DOI: 10.3846/biomdlore.2016.03

Peculiarities of the supervision of vascular catheters

Zyta Kuzborska[1], Zita Gierasimovič[2]
[1] Vilnius Gediminas Technical University, Lithuania
[2] Vilnius University, Lithuania
E-mails: [1] *zyta.kuzborska@vgtu.lt (corresponding author)*, [2] *zitagieras@gmail.com*

(Received 22 February 2016; accepted 22 April 2016)

Abstract. The article analyses the supervision of vascular catheters, as well as the factors influencing the complications that occur. The method of observation was applied to assess the supervision of catheters, sample size target. The patients were assessed by gender, age, changes in their state of health, the type of vascular catheters and the assessment of dressing. It was established that the following physical (the condition of skin and the dressing, place and duration of the insertion of a catheter) and mechanical (catheter displacement of vascular injection local tissue stretching for biological fluids stay) factors were of great significant.

Keywords: supervision of vascular catheters, risk factors, complications.

Introduction

Through a catheter medication gets directly into the central circulation of the blood where it dissolves quickly and spreads all over the organism [1]. Complications that occur due to a vascular catheter insertion depend on the following factors; anatomical deformation of the body in the place of a catheter insertion; the condition of the patient; the skills and knowledge of the staff [2]. The early complications are bleeding, haematoma, the improper position of the catheter [3]. Catheter-related sepsis, thrombosis, tissue extravasations and infection are the cause of late complications. [4]. The improper localisation of the catheter with respect to vein projection is the course of health problems of the patient and his/her heart rhythm disorders (arrhythmia) [5]. In case the rules of aseptic are not observed, the patients with involuntary bowel movement and urination problems are subject to a greater risk of infection [6]. Other authors state that the course of infection is artificial lung ventilation, the patient's old age, the use of immunosuppressive medication [7, 8]; practical training of the staff decreases the incidence of vascular catheter-related infections in from 3.29 to 2.36 cases [9]. The incidence of vascular catheter-related infections established in Lithuania is from 9.3 to 2.7 cases [10]. According to the data presented in literature, places of the insertion of vascular catheters are complicated with respect to infection, the place of catheter insertion projection is inconvenient on account of possible injury of the surrounding tissues [2, 10], and the group of the patients who are old and have adjacent diseases are particularly prone to complications [12].

Swelling and reddening of the place of the vascular catheter insertion, as well as pain in it, is a local complication [11, 12].

The aim of this work is to assess the peculiarities of the supervision of vascular catheters in the reanimation and intensive care units.

Methods

A total of 104 patients were under observation in one of the hospitals in Vilnius who underwent treatment in the reanimation and intensive care units in 2014. The method of observation was used to assess the supervision of vascular catheters, sample size target. The research data were encoded and analysed by means of the programme IBM SPSS Statistics 19.0. Methods of descriptive statistics were applied, and the characteristics of the samples were calculated: the average, the median and the percentage. Differences between non-parametric indicators were established by

means of the Fisher's χ^2 (chi square) criterion. The relationship between the independent variable and the dependent variable was considered to be statistically significant when $p \leq 0,05$.

Results

53.8% (56) of males and 46.5% (48) of females between the ages of 30 and 71 years and older underwent treatment at the intensive care units in 2014. The average age of the patients was as follows: 63.1 years ± 12.9 years. The duration of the patient's treatment is as follows: 5.25 days ± 7.5 days, minimum one day, maximum 50 days, the median is three days. From that number 57.7% (60) of the patients had a peripheral vascular catheter inserted, and 91.3% (95) of the patients had a central vascular catheter. In assessing the condition of the patients' skin the place of the insertion of a vascular catheter, it was established that a change in the patient's skin condition depended on the patient's behaviour, that is, if the patient was self-contained, did not toss, was quiet, did not try to take out the inserted catheter by himself/herself, no cases of complications were observed ($p < 0.05$) (Table 1). The risk factors which influence changes in the skin in the place of the insertion of a vascular catheter have been established ($p < 0.05$) (Table 2).

Table 1. Skin condition in the placers of the insertion of catheters

Vascular catheter	Assessment of skin condition	Patient is self-contained	Patient is partly self-contained	Patient is not self-contained	Total	χ^2	df	p
		Abs. number (%)	Abs. number (%)	Abs. number (%)	Abs. number (%)			
	Skin is injured	3 (17.6)	18 (41.9)	22 (62.9)	43 (45.3)	9.807	2	0.007* 0.007*
	Skin is not injured	14 (82.4)	25 (58.1)	13 (37.1)	52 (54.7)			

Note: * – statistically significant figure $p \leq 0.05$

Two types of dressing are used in supervising vascular catheters, which protect the place of the insertion of a catheter: breathable, adhesive coated polyurethane film dressing Tegaderm and cloth dressing Mesoft. It was established by investigations that Tegaderm dressing remains unsoiled by biological liquid 1.5 times longer, and Mesoft dressing has to be changed 5 times more often than the polyurethane dressing. The cloth dressing when soaked with blood/biological liquid came off 6 times more often than flexible polyurethane dressings which become adjusted in places which are difficult to dress and protect them from external pollution.

Table 2. Risk factors influencing the patient's skin condition in the places of the insertion of a vascular catheter

Adjacent diseases of the patient	Lesions exist Abs. number (%)	No lesions Abs. number (%)	Total Abs. number (%)	OR (PI)	χ^2	df	p
Lesions (exist)	3 (7.0)	1 (1.9)	4 (4.2)	3.86 (0.38–38.18)	1.490	1	0.222 0.325*
(No) lesions	40 (93.0)	51 (98.1)	91 (95.8)				
CD (exist)	14 (32.6)	9 (17.3)	23 (24.2)	2.31 (0.88–6.03)	2.98	1	0.084 0.097*
CD (no)	29 (67.4)	43 (82.7)	72 (75.8)				

Note: * – statistically significant figure $p \leq 0.05$

Discussion and acknowledgements

When analysing the results obtained it was established that nursing actions for the supervision of central catheters 45.3% (43) and the supervision of peripheral catheters 57.1% (12) were applied. To avoid cases of complications skin around the place of the insertion of catheters was

watched and catheters were held in carrying out treatment or nursing interventions, as well as in changing the dressing.

The following nursing measures were applied in the supervision of vascular catheters in the reanimation and intensive care units: the condition of the skin and dressing, around the place of the insertion of a vascular catheter was assessed; such mechanical actions as pushing the permanent place of the insertion of a vascular catheter, the presence of infection in the place of the insertion of catheters, soaking of the bandage with blood and biological liquid increase the number of cases of complications.

References

[1] Budginaitė, R.; Sinkevič, V.; Zagrebnevienė, G. 2013. *Infekcijų, susijusių su kraujagyslių kateterių naudojimu, profilaktikos metodinės rekomendacijos* [online]. Užkrečiamųjų ligų ir AIDS centras [cited 22 February 2016]. Available from Internet: http://www.ulac.lt/uploads/downloads/leidiniai/m_r_%20kateteriai.pdf

[2] Strainys, T., *et al.* 2012. Evaluation of the main pathogens and risk factors for catheter associated sepsis in chronic hemodialysis patients, *Theory and Practice in Medicine* 18(4.2): 534–538.

[3] Valintėlienė, R.; Gailienė, G.; Beržanskytė, A. 2012. Prevalence of healthcare-associated infections in Lithuania, *Journal of Hospital Infection* 80(1): 25–30. http://dx.doi.org/10.1016/j.jhin.2011.09.006

[4] Kalibatienė, D.; Černiauskaitė, I. 2011. Centrinių venos kateterių naudojimas ir priežiūra reanimacijos ir intensyviosios terapijos skyriuose, *Slauga. Mokslas ir praktika* 170: 14–18.

[5] Schweickert, W. D., *et al.* 2009. A randomized, controlled trial evaluating postinsertion neck ultrasound in peripherally inserted central catheter procedures, *Critical Care Medicine* 37(4): 1217–1221. http://dx.doi.org/10.1097/CCM.0b013e31819cee7f

[6] Froehlich, C. D., *et al.* 2009. Ultrasound-guided central venous catheter placement decreases complications and decreases placement attempts compared with the landmark technique in patients in a pediatric intensive care unit, *Critical Care Medicine* 37(3): 1090–1096. http://dx.doi.org/10.1097/CCM.0b013e31819b570e

[7] Zarb, P., *et al.* 2012. The European Centre for Disease Prevention and Control (ECDC) pilot point prevalence survey of healthcare-associated infections and antimicrobial use, *Eurosurveillance* 17(46): 20316.

[8] Galpern, D., *et al.* 2008. Effectiveness of a central line bundle campaign on line-associated infections in the intensive care unit, *Surgery* 144(4): 492–495. http://dx.doi.org/10.1016/j.surg.2008.06.004

[9] O'Grady, N. P., *et al.* 2011. Guidelines for the prevention of intravascular catheter-related infections, *Clinical Infectious Diseases* 52(9): e162–e193. http://dx.doi.org/10.1093/cid/cir257

[10] Ašembergienė, J., *et al.* 2013. Nosocomial infections in the intensive care units in Lithuania: results of the national nosocomial surveillance system, 2009–2011, *Visuomenės sveikata* 60: 58–66.

[11] Berezhanski, B. V.; Zhevnerev, A. A. 2006. Catheter-associated bloodstream infections, *Diseases and Pathogens* 8(2): 130–144.

[12] Gulbinas, A.; Barauskas, G. 2007. Central venous catheters in the prevalence of nosocomial infection study, *Lithuanian Surgery* 5(2): 181.

11TH INTERNATIONAL CONFERENCE
BIOMDLORE 2016
OCTOBER 20–22, 2016, DRUSKININKAI, LITHUANIA
BIOMDLORE.VGTU.LT

eISSN 2345-0630
ISBN 978-609-457-959-2
eISBN 978-609-457-958-5
DOI: 10.3846/biomdlore.2016.04

Assessment of the effectiveness of pressure ulcer care

Zita Gierasimovič[1], Zyta Kuzborska[2]
[1] Vilnius University, Lithuania
[2] Vilnius Gediminas Technical University, Lithuania
E-mails: [1] *zitagieras@gmail.com (corresponding author)*, [2] *zyta.kuzborska@vgtu.lt*

(Received 29 February 2016; accepted 22 April 2016)

Abstract. The article deals with the external and internal factors influencing development of pressure ulcers and the effectiveness of their care. The patients were assessed according to their age, gender and changes in their condition. The modified Norton Scale was used to assess the effectiveness of pressure ulcer care. It has been established that internal factors increase the risk of developing pressure ulcers. The effectiveness of pressure ulcer care is promoted by pressure ulcers preventative measures, medicines and skin hygiene.

Keywords: pressure ulcer care, risk factors, preventative measures.

Introduction

Pressure ulcers are necrosis of skin and tissues underlying skin [1], which occurs due to pressure over places where the bones are close to the skin (bone prominences), poor diet and other external and internal factors [1, 2]. Scientific sources [2, 3] state that pressure ulcers develop more often in elderly patients or the patients who are confined to a chair or a bed, especially moisture and enuresis, as one of etiological factors, which accelerates skin damage and the appearance of pressure ulcers [3]. In European countries, according to one-time research, the risk of development of Stage I-IV pressure ulcers among different age groups accounts for 18.1%. Sacrum and heels are most often affected areas of skin [3, 4], in Canada they constitute from 15.8% to 28.2% [5], prevalence of pressure ulcers in Lithuania ranges between 2.7% and 29.5% of all the hospitalized patients [6]. It is necessary to use pressure ulcer preventative measures during all the stages of providing nursing services because they reduce the risk of pressure ulcer development by more than fivefold [6]. The effectiveness of the preventative measures in treating pressure ulcers was noticed after carrying out clinical experiments. Recommendations with respect to avoidance of development of pressure ulcers have been put forward [7]. Sources of scientific literature state [8, 9] that the following actions taken by the nursing staff are conducive to development of pressure ulcers: a badly devised plan for watching development of pressure ulcers, a limited or improperly applied pressure ulcer preventative measures and a lack of knowledge, as well as forgetfulness. Though the scientific literature offers a lot of ways to solve the problems of pressure ulcer development [9] treatment of pressure ulcers is still one of the most complicated tasks, and it is especially urgent in nursing the immobile patients (those who are confined to a chair or a bed). The aim of this work is to determine the factors that influence development of pressure ulcers and the effectiveness of their care.

Methods

A retrospective data analysis of 655 patients suffering from pressure ulcers who underwent treatment in one of Vilnius hospitals between 2009 and 2014 was carried out. Samples of the respondents were selected objectively of the respondents was made. Patients who needed urgent care or were brought to hospital in a planned manner with bedsores; and patients who were already in hospital and had bedsores. The respondents' observation was done according to the number of the patients who arrived to hospital with pressure ulcers. The efficiency of bedsore care was assessed before the respondents were from hospital.

The modified Norton Scale was used to assess the effectiveness of pressure ulcer care.

The research data have been encoded and analysed by means of the programme IBM SPSS Statistics 19.0. Differences between non-parametric indicators were established by means of the Fisher's χ^2 (chi square) criterion. The Spearman's coefficient of rank correlation denoted by r_s was calculated to determine strengthening of the statistical relationship. Differences were considered to be statistically significant when the value of the error probability $p \leq 0,05$.

Results

In the course of carrying out the investigation between 2009 and 2014, a total of 423 (64.6%) patients suffering from pressure ulcers arrived at the hospital (the minimum number of pressure ulcers was one and their maximum number amounted to 11; the median accounted for 2 pressure ulcers). As many as 232 (35.4%) patients developed pressure ulcers while undergoing treatment in hospital (the minimum number of pressure ulcers was 8, the median accounted for one). The average age of the patients was 61.7 years. The patients who underwent treatment at the in-patient department developed pressure ulcers within the following time period: the minimum number of pressure ulcers took one day to develop, the maximum number developed within the period of 50 days; the average was ±9,55 days and the median took 6 days to develop. Both females and males have the same possibilities for pressure ulcers to develop (p = 0.001) (Table 1).

Table 1. Number of pressure ulcers in the patients who arrived and those who underwent treatment by gender

Variables		Number of pressure ulcers upon arrival Abs. number (%) (n = 423)	Number of pressure ulcers in hospital Abs. Number (%) (n = 232)	OR 95 % PI	$\chi 2$	P
Gender	Male	215 (50.8)	163 (70.3)	0.44 [0.31–0.62]	23.18	0.001*
	Female	208 (49.2)	69 (29.7)	2.29 [1.63–3.21]	23.18	0.001*

Note: * – statistically significant number $p \leq 0.05$

Speaking about the age groups of the patients, symptoms of acute inflammation of epidermis and lesions of epidermis and dermis are eight times more frequent in the group of the patients between the ages of 41 and 50 than in the patients belonging to the age group under the age of 30. Pressure ulcers are as much as 2.8 times more frequent in the group of patients over 61 years than those in the age group of the patients between the ages 41 and 50 (Fig. 1).

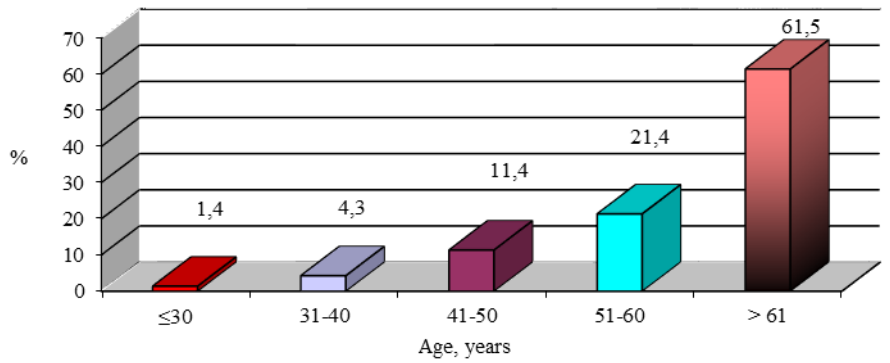

Fig. 1. Patients who developed pressure ulcers in hospital by age groups

With the duration of pressure ulcer treatment becoming longer, stage III of pressure ulcers with lesions of the deeper layers of the tissues (p = 0.001) was most often diagnosed in the patients, and stage IV was most often diagnosed in a group of the patients older than 61 years, as compared

with the patients whose length of treatment was shorter (p = 0.003). Places of localisation of pressure ulcers in the long-stay patients were assessed (Fig. 2).

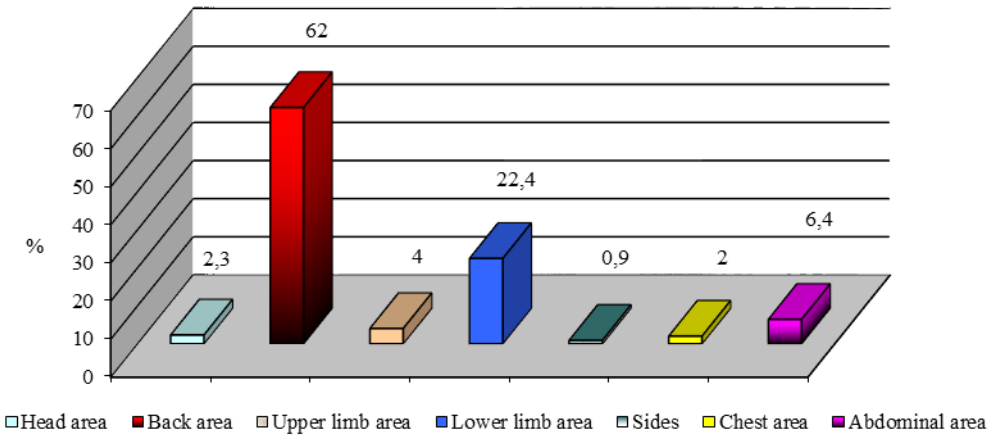

Fig. 2. Most common areas of localisation of pressure ulcers

The statistically significant difference was established in comparing the places of the localisation of pressure ulcers in the occipital lobe areas and in the region of large tubercles of the femur (p = 0,001). With the physical condition of the patients deteriorating, the places of the localisation of pressure ulcer development increase (r_s = –0.130; p = 0.016). An involuntary bowel movement and urination also contribute greatly to an increase in the number of pressure ulcers (r_s = –0.108; p = 0.047).

Discussion

The research data obtained confirmed the supposition that the majority of the patients belonging to the age group of 41–50 years and older and whose physical condition was poor developed pressure ulcers 3.5 times more often that other patients. The researchers in foreign countries present similar data [10, 11].

Under the influence of external factors, turning the patients every two hours and more often, the probability of development of skin lesions in the back area is slight. It was established during the investigation that prolonged reddening and minor skin ulceration determine lesions in skin integrity and the localisation of a pressure ulcer of stage I in the back area in 60% of cases. It was thought that on account of external factors the frequency of turning the patient failed to meet the nursing plan devised individually for the patient. The researchers Lapsley and Vogels established that the patients' stay in hospital that was extended up to on average 11 days additionally increased the volume of nursing services by as much as 25% and that of the use of nursing facilities by 7% [12]. It was established that the patients suffering from pressure ulcers underwent treatment in hospital on average for 9.5 days and it is thought that this increases the volume of nursing services by as much as 21.6% and that of the use of nursing facility by 2.3 times.

Acknowledgments

The risk of pressure ulcer development is increased by the following external factors: the patient's age, his/her poor physical condition. Pressure ulcer preventative measures, medicines (the use of mono and combined anti-bacterial measures) and skin hygiene promote the effectiveness of pressure ulcer care.

References

[1] Doughty, D. 2012. Differential assessment of trunk wounds: pressure ulceration versus incontinence associated dermatitis versus intertriginous dermatitis, *Ostomy Wound Management* 58(4): 20–22.

[2] Meesterberends, E., *et al.* 2011. Pressure ulcer incidence in Dutch and German nursing homes: design of a prospective multicenter cohort study, *BMC Nursing* 10: 8. http://dx.doi.org/10.1186/1472-6955-10-8

[3] Beeckman, D., *et al.* 2014. A systematic review and meta-analysis of incontinence-associated dermatitis, incontinence, and moisture as risk factors for pressure ulcer development, *Research in Nursing & Health* 37(3): 204–218. http://dx.doi.org/10.1002/nur.21593

[4] Vanderwee, K., *et al.* 2007. Pressure ulcer prevalence in Europe: a pilot study, *Journal of Evaluation in Clinical Practice* 13(2) 227–235. http://dx.doi.org/10.1111/j.1365-2753.2006.00684.x

[5] Denny, K.; Lavand, C.; Perry, S. D. 2014. Compromised Wounds in Canada, *Healthcare Quarterly* 17(1): 7–10. http://dx.doi.org/10.12927/hcq.2014.23787

[6] Pečeliūnienė, R. 2012. Tinkamai parinktos priemonės – slaugomų pacientų kokybiško gyvenimo garantas, *Lietuvos gydytojo žurnalas* 9: 17.

[7] Gunningberg, L.; Stotts, N. A. 2008. Tracking quality over time: what do pressure ulcer data show?, *International Journal for Quality in Health Care* 20(4): 246–253. http://dx.doi.org/10.1093/intqhc/mzn009

[8] Baharestani, M. M., *et al.* 2009. Dilemmas in measuring and using pressure ulcer prevalence and incidence: an international consensus, *International Wound Journal* 6(2): 97–104. http://dx.doi.org/10.1111/j.1742-481X.2009.00593.x

[9] Gunningberg, L.; Brudin, L.; Idvall, E. 2010. Nurse Managers' prerequisite for nursing development: a survey on pressure ulcers and contextual factors in hospital organizations, *Journal of Nursing Management* 18(6): 757–766. http://dx.doi.org/10.1111/j.1365-2834.2010.01149.x

[10] Hill-Brown, S. 2011. Reduction of pressure ulcer incidence in the home healthcare setting: a pressure-relief seating cushion project to reduce the number of community-acquired pressure ulcers, *Home Healthcare Nurse* 29(9) 575–579. http://dx.doi.org/10.1097/NHH.0b013e31822eb830

[11] Moore, Z. E., Webster, J.; Samuriwo, R. 2014. Wound-care teams for preventing and treating pressure ulcers, *Cochrane database of systematic reviews* 9: CD011011. http://dx.doi.org/10.1002/14651858.CD011011

[12] Dumville, J. C., *et al.* 2015. Alginate dressings for treating pressure ulcers, *Sao Paulo Medical Journal* 133(5): 455. http://dx.doi.org/10.1002/14651858.cd011277.pub2

11TH INTERNATIONAL CONFERENCE
BIOMDLORE 2016
OCTOBER 20–22, 2016, DRUSKININKAI, LITHUANIA
BIOMDLORE.VGTU.LT

eISSN 2345-0630
ISBN 978-609-457-959-2
eISBN 978-609-457-958-5
DOI: 10.3846/biomdlore.2016.05

Propagation of measurement uncertainty for balance platform model involving two output quantities

Adam Idźkowski[1], Wojciech Walendziuk[2], Aleksander Sawicki[3]
[1, 2, 3] Bialystok University of Technology, Poland
E-mails: [1] *a.idzkowski@pb.edu.pl (corresponding author)*, [2] *w.walendziuk@pb.edu.pl*,
[3] *aleksander.sawicki.91@gmail.com*

(Received 1 March 2016; accepted 22 June 2016)

Abstract. The paper topic is about the propagation of uncertainty in a multivariate measurement. The Law of Propagation of Uncertainty defined in the Guide to the Expression of Uncertainty in Measurement is used to calculate the standard uncertainties, covariance matrix and correlation coefficient. The procedure is presented for a set of samples, acquired from a balance platform, which are used to calculate the centre of pressure (*COP*) coordinates. The possibility of evaluating the uncertainty of *COP* results in different way is also discussed.

Keywords: balance platforms, centre of pressure, multivariate measurements, uncertainty.

Introduction

Multivariate measurements are present in many disciplines. Balance platforms are very popular devices and they are applied in rehabilitation or sport training. A training on a platform aims to stimulate parts of the human musculoskeletal system and the nervous system which are responsible i.a. for controlling the balance.

The ways of reliability and validity tests as well as accuracy calculations of the results obtained by using balance platforms are presented in many publications. The tests are performed in the following manner. The experimental method involves the use of additional testing devices intended to produce a concentrated force at a point of reference or force distributed over a specified area of the platform. In order to check the reliability, the arithmetic mean and standard deviation are calculated [1] as well as, among other parameters, the repeatability of series of measurements. A validation is performed by using another device with higher accuracy, which leads to determine the mean difference of results and the interclass correlation coefficient (*ICC*) [2], [3]. The authors of above mentioned publications did not assume that the coordinates of the *COP* were correlated. These parameters were determined for both coordinates COP_X, COP_Y separately. But they were, since they depended on the same input quantities. The aim of this paper is to present a bivariate measurement model and another way of uncertainty calculations basing on the data samples recorded by a balance platform.

Methods

It will be used a method for determining the uncertainty of measured values of *COP* components presented in the Guide ISO GUM [4]. This document assumes that the Law of Propagation of Uncertainty (LPU) should be used [5]. Output quantities *f* of a balance platform are two coordinates COP_X, COP_Y. Then the multivariate measurement model is

$$COP_X = \frac{L_X}{2}\frac{(TR+BR)-(TL+BL)}{TR+BR+TL+BL},\ COP_Y = \frac{L_Y}{2}\frac{(TR+TL)-(BR+BL)}{TR+BR+TL+BL}, \quad (1)$$

where: L_X, L_Y – dimensions of platform, weight values from four load sensors: *TL* – Top Right, *BL* – Bottom Right, *TR* – Top Right, *BR* – Bottom Right.

Input quantities x (*TR*, *BR*, *TL* and *BL*) and the equivalent sensors of a platform are independent what causes that covariance matrix V (*TR*, *BR*, *TL*, *BL*) is diagonal. A covariance matrix V (COP_X, COP_Y) is:

$$V(COP_X, COP_Y) \cong \left[\frac{\partial f}{\partial x}\right] \times V(TR, BR, TL, BL) \times \left[\frac{\partial f}{\partial x}\right]^T = \\ = \begin{bmatrix} V_{11} & V_{12} \\ V_{21} & V_{22} \end{bmatrix} = \begin{bmatrix} \sigma^2_{COP_X} & \text{cov}(COP_X, COP_Y) \\ \text{cov}(COP_Y, COP_X) & \sigma^2_{COP_Y} \end{bmatrix}. \quad (2)$$

Jacobian matrix contains the partial derivatives of the scalar components of f with respect to the scalar elements of x. Then correlation coefficient is:

$$\rho_{xy} = \frac{\text{cov}(COP_X, COP_Y)}{\sigma_{COP_X} \times \sigma_{COP_Y}} = \frac{V_{12}}{\sqrt{V_{11}} \times \sqrt{V_{22}}}. \quad (3)$$

Results

The sample results in Tables 1 and 2 were acquired by putting a load on the Wii Balance Board (WBB). The WBB contains four transducers which are used to assess force distribution and the resultant movements in *COP* [3]. The platform was calibrated in the range 0–100 kg. The calculated parameters on the basis of covariance matrix are presented in Table 3.

Table 1. The experimental results of weight obtained for four sensors

Sample	*BL*[kg]	*BR* [kg]	*TL* [kg]	*TR* [kg]
1	3.3590	3.1680	4.0774	3.0436
….	…	…	…	…
300	3.3781	3.1302	4.0678	2.9465

Table 2. Standard deviations for 10, 100, 300 samples of the acquired *TR*, *BR*, *TL* and *BL*

Number of samples	σ_{BL} [kg]	σ_{BR} [kg]	σ_{TL} [kg]	σ_{TR} [kg]
10	0.0327	0.0205	0.0130	0.0344
100	0.0326	0.0294	0.0294	0.0281
300	0.0309	0.0299	0.0296	0.0305

Table 3. Combined uncertainties calculated for 10, 100, 300 samples (square roots from variances), their covariance coefficient (2) and correlation coefficient (3)

Number of samples	σ_{COPX} [cm]	σ_{COPY} [cm]	cov (COP_X, COP_Y)	Correlation coefficient
10	0.0061	0.0033	0.00001103	0.536
100	0.0068	0.0038	0.00000036	0.014
300	0.0069	0.0038	0.00000029	0.011

The result of measurement (i.e. 300 measured samples) can be presented as the mean and the surrounded area (ellipse) with 95% level of confidence (Fig. 1):

COP_X = (0.2979±0.0138) cm, COP_Y = (0.1073±0.0076) cm. (4)

The results were verified by NIST Uncertainty Machine [6] which applies a univariate Monte Carlo Method.

After assuming Gaussian distributions of four input quantities it was created the summary statistics for 100000 realizations of the output quantity. The result was similar:

COP_X = (0.2952±0.0134) cm, COP_Y = (0.1100 ± 0.0070) cm for k = 2 and p = 0.95. (5)

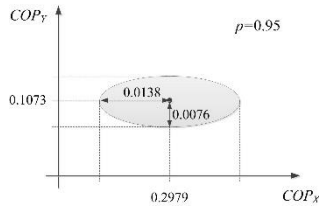

Fig. 1. Bivariate normal density contour (the result of COP with probability 95%)

The probability density functions (PDF) for both output quantities generated by NIST UM are presented in Fig. 2 and Fig. 3.

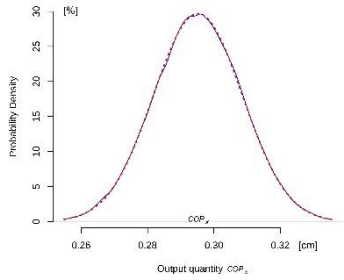

Fig. 2. Univariate PDF of COP_X

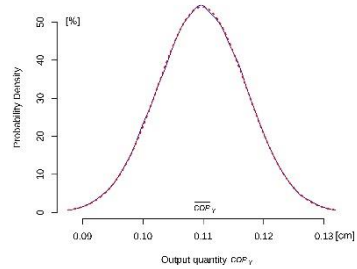

Fig. 3. Univariate PDF of COP_Y

Conclusions

The result (4) was obtained by using Law of Propagation of Uncertainty (LPU). The central region of a bivariate normal distribution is presented. For a condition $V_{11} > V_{22}$ and correlation coefficient near zero in (2) the axes of the ellipse are parallel to the coordinate axes, with the major axis parallel to the horizontal axis. For different conditions and correlation greater than 0 the ellipse can have a slope and can be elongated. The results (5) of simulation obtained by univariate Monte Carlo Method were convergent (for the same p = 0.95).

Acknowledgements

The paper was prepared at Bialystok University of Technology within a framework of the S/WE/1/2013 project sponsored by Ministry of Science and Higher Education.

References

[1] Dias, J. A., *et al.* 2011. Validity of a new stabilometric force platform for postural balance evaluation, *Brazilian Journal of Kinanthropometry and Human Performance* 13(5): 367–372. http://dx.doi.org/10.5007/1980-0037.2011v13n5p367

[2] Mauch, M.; Rist, H. J.; Kaelin, X. 2014. Reliability and validity of two measurement systems in the quantification of jump performance, *Schweizerische Zeitschrift für Sportmedizin und Sporttraumatologie* 62(1): 57–63.

[3] Clark, R. A., *et al.* 2010. Validity and reliability of the Nintendo Wii Balance Board for assessment of standing balance, *Gait & Posture* 31(3): 307–310. http://dx.doi.org/10.1016/j.gaitpost.2009.11.012

[4] *Evaluation of measurement data – supplement 2 to the "Guide to the expression of uncertainty in measurement" – Extension to any number of output quantities* [online]. 2011. Bureau International des Poids et Mesures [cited 1 March 2016]. Available from Internet: http://www.bipm.org/en/publications/guides/gum.html

[5] Hall, B. D. 2004. On the propagation of uncertainty in complex-valued quantities, *Metrologia* 41(3): 173–177. http://dx.doi.org/10.1088/0026-1394/41/3/010

[6] Lafarge, T.; Possolo, A. 2013. *NIST Uncertainty Machine – User's Manual* [online]. National Institute of Standards and Technology [cited 1 March 2016]. Available from Internet: http://uncertainty.nist.gov/NISTUncertaintyMachine-UserManual.pdf

11TH INTERNATIONAL CONFERENCE
BIOMDLORE 2016
OCTOBER 20–22, 2016, DRUSKININKAI, LITHUANIA
BIOMDLORE.VGTU.LT

eISSN 2345-0630
ISBN 978-609-457-959-2
eISBN 978-609-457-958-5
DOI: 10.3846/biomdlore.2016.06

3D microfabrication of complex structures for biomedical applications via combination of subtractive/additive direct laser writing and 3D printing

Linas Jonušauskas[1], Sima Rekštytė[2], Edvinas Skliutas[3], Simas Butkus[4], Mangirdas Malinauskas[5]
[1, 2, 3, 4, 5] Vilnius University, Lithuania
E-mails: [1] *linas.jon@gmail.com (corresponding author)*, [2] *sima.rekstyte@gmail.com*, [3] *edvinas.skliutas@gmail.com*, [4] *simas.butkus@ff.vu.lt*, [5] *mangirdas.malinauskas@ff.vu.lt*

(Received 1 March 2016; accepted 19 May 2016)

Abstract. In this work we present current progress on employing direct laser writing (DLW) for creation of 3D microstructures for biomedical applications. Both subtractive and additive variations of DLW allow fabricating structures for *in vitro* bioanalysis and *in vivo* tissue engineering. Furthermore, we show that efficiency of 3D microstructure manufacturing can be enhanced by combining femtosecond laser material processing with commercial 3D printers.

Keywords: laser microfabrication, biocompatible polymers, 3D biomedical structures.

Introduction

The prospect of manufacturing 3D microstructures that could be used in regenerative medicine and bioanalysis always generated high interest in the field of biomedicine. However, requirements for such objects are highly nontrivial. Materials have to be biocompatible, produced structures must have desired functional properties and high-throughput high-precision 3D fabrication technologies should be used.

An answer for such requirements could be direct laser writing (DLW). By applying ultrashort (from picosecond to femtosecond) laser pulses both subtractive and additive manufacturing is possible (Fig. 1) [1]. This enables combining a wide array of materials as well as freeform 3D geometry best suited for any given task. What is more, efficiency can be further enhanced by coupling laser fabrication with conventional 3D printing (3DP) technologies [2]. In such case fast 3DP is employed for the creation of the base structure, while the laser is used to further decorate it with fine features (from tens of μm to hundreds of nm [1]) that cannot be produced using 3D printing [2].

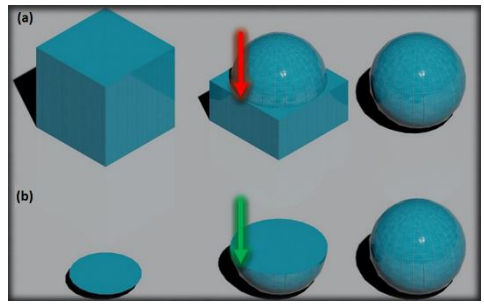

Fig. 1. Schematic representation of (a) subtractive and (b) additive fabrication [3]

Here we will discuss current progress on the aforementioned approach of combining subtractive and additive DLW with 3DP for the creation of structures that could be used in biomedical applications. Capabilities and problems arising when combining these technologies in

practice will be explained. Examples of produced 3D microstructures such as scaffolds with defined pores/porosity or intertwined channels will be given.

Methods

Two high precision femtosecond laser "Pharos" (Light Conversion Ltd.) based fabrication systems were used. The first setup was tuned for subtractive sample processing by using higher light intensities (~hundreds of TW/cm^2) and first laser harmonic (1030 nm). Both cutting via sharp focusing or light filamentation can be realized with it (Fig. 2. (a)). The second one was applied in additive fashion for 3D microfabrication of the polymers and was based on the multiphoton light-matter interaction (Fig. 2. (b)) [1]. Much lower light intensities (~TW/cm^2) as well as II laser harmonic (515 nm) was applied in it. Details on these systems can be found in [4] and [5] respectively. Polymers used for the creation of the structures include but are not limited to hybrid organic-inorganic photopolymers (namely SZ2080), polylactic acid (PLA) and PEG-DA [2], including their formulation doped with metallic nanoparticles.

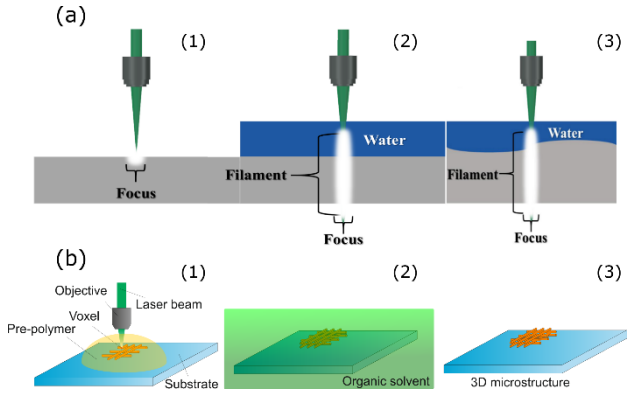

Fig. 2. (a) Schematics of cutting via sharp focusing (1) and via light filamentation (2) [2]. (3) – usage of light filaments also allows cutting when the sample surface is uneven [6]. (b) Multiphoton polymerization based 3D manufacturing: (1) fabrication, (2) development and (3) finished 3D microstructure [5]

Additionally two types of 3DP were tested. Applying either fused filament fabrication or stereolithography they offered different fabrication speeds (from mm/s to cm/s), resolutions (from tens of μm to tens of cm) and processable materials (thermocurable and photocurable).

Results

Microfluidical systems that could be used in bioanalysis or scaffolds for tissue engineering can be produced via the combination of 3DP and laser cutting. 3DP guarantees relatively high throughput fabrication of low spatial resolution structures. Cm/s linear translation speeds result in fabrication durations in the range of minutes for cm sized microchannel systems and scaffolds. Laser cutting allows further functionalization of such objects by providing them with required shape and/or surface topography that cannot be produced with only 3DP (Fig. 3).

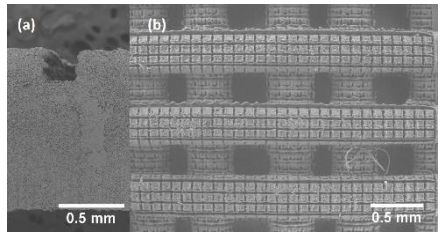

Fig. 3. Cross section of 3DP created microchannel that was afterwards cut via laser filamentation (a) [5]. (b) – enhanced topography of a 3DP scaffold via sharp focusing cutting [2]. Material – PLA

Additive fabrication via multiphoton absorption opens the possibility to produce complex true 3D microstructures with feature size as small as hundreds of nm [1]. Furthermore, composite manufacturing combining different materials in distinct parts of the structure can be realized this way [2]. Here we show that these capabilities can be used for the creation of 3D biomedical microobjects complex both in their architecture (Fig. 4 (a)) and materials used (Fig. 4. (b)). This is crucial for precise tunability needed in biomedical applications. Size of these structures can be from µm to mm in size with hundred nm resolution internal features. Shown objects can be manufactured in times ranging from minutes to hours depending on the complexity of internal geometry and overall volume (filling ratio) of the structure.

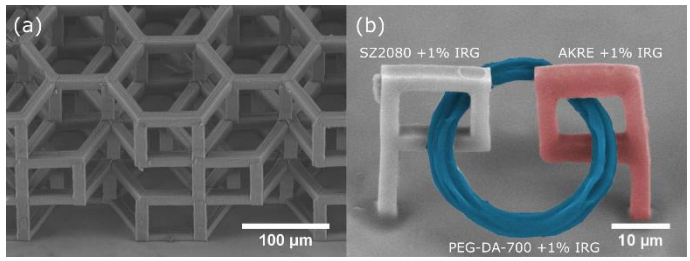

Fig. 4. (a) Complex shaped 3D scaffold for stem cell growth with hexagonal structure and poor size in range of tens of µm. (b) Composite 3D microstructure created out of three different materials [2]

Conclusions

The presented results show how combination of sub-micrometre precision femtosecond laser material processing and rapid 3DP offers an efficient fabrication of complex 3D structures of biocompatible materials for applications in the fields of micro-analysis and tissue engineering.

Acknowledgements

We acknowledge ECs Seventh Framework Programme Laserlab-Europe VI JRA support BIOAPP (EC-GA 654148).

References

[1] Sugioka, K.; Cheng, Y. 2014. Femtosecond laser three-dimensional micro- and nanofabrication, *Applied Physics Reviews* 1(4): 041303. http://dx.doi.org/10.1063/1.4904320

[2] Malinauskas, M., *et al.* 2014. 3D microporous scaffolds manufactured via combination of fused filament fabrication and direct laser writing ablation, *Micromachines* 5(4): 839–858. http://dx.doi.org/10.3390/mi5040839

[3] Malinauskas, M., *et al.* 2014. Multiscale 3D manufacturing: combining thermal extrusion printing with additive and subtractive direct laser writing, in *Proceedings of SPIE Vol. 9135: Laser Sources and Applications II*. April 14, 2014, Brussels, Belgium. Bellingham: SPIE, 91350T. http://dx.doi.org/10.1117/12.2051520

[4] Jonušauskas, L., *et al.* 2015. Custom on demand 3D printing of functional microstructures, *Lithuanian Journal of Physics* 55(3): 227–236. http://dx.doi.org/10.3952/physics.v55i3.3151

[5] Jonušauskas, L.; Rekštytė, S.; Malinauskas, M. 2014. Augmentation of direct laser writing fabrication throughput for three-dimensional structures by varying focusing conditions, *Optical Engineering*, 53(12): 125102. http://dx.doi.org/10.1117/1.OE.53.12.125102

[6] Malinauskas, M., *et al.* 2016. Ultrafast laser processing of materials: from science to industry, *Light: Science & Applications* 5: e16133. http://dx.doi.org/10.1038/lsa.2016.133

11TH INTERNATIONAL CONFERENCE
BIOMDLORE 2016
OCTOBER 20–22, 2016, DRUSKININKAI, LITHUANIA
BIOMDLORE.VGTU.LT

eISSN 2345-0630
ISBN 978-609-457-959-2
eISBN 978-609-457-958-5
DOI: 10.3846/biomdlore.2016.07

Smart textile gloves for luge athletes paddling monitoring

Katrina Dimitre[1], Alexei Katashev[2], Alexander Okss[3]
[1, 2, 3] Riga Technical University, Latvia
E-mails: [1] *katrina.dimitre@gmail.com*, [2] *katashev@latnet.lv (corresponding author)*, [3] *siaesta@gmail.com*

(Received 1 March 2016; accepted 28 April 2016)

Abstract. Results of the luge athletes strongly depend on the successful start. While number of methods successfully analysed movements around start handles, still there is lack of methods to monitor paddling strokes. Present paper demonstrates smart textile gloves, designed for such a purpose. Developed gloves allow to measure timing of the arms strokes as well as easily distinguish between good stroke, when athlete's palms are in full contact with ice, and insufficient one, when fingers just slide over ice without providing good push.

Keywords: luge start, paddling, athlete performance, wearables, smart textile.

Introduction

Although the first documented sled races took place in mid-15th century, the first modern luge competitions were organised in 1883 [1]. From 1964, luge is included in the Winter Olympic Games program. Despite of long history and high technical progress in sled design, the biomechanical performance of luge athletes – "sliders" found rather limited interest of researchers. Still, it was demonstrated [2] that high starting speed is one of the key points in achieving better results in luge. Number of researchers paid their attention exactly to the analysis of luge start [3, 4, 5].

The starting phase includes three major steps: pulling and pushing starting handles to thrust luge into the track, paddling with special spiked glow for a first 7 meters of track, changing position to the one of the best aerodynamics [6]. The majority of papers concentrated mainly on propulsion form the handles. For this, the number of techniques, such as use of tensometric handles [3], high speed cinematographic [3, 5], simulation stands [4], motion capture technique [5] were applied. Besides, the second phase of the start, i.e. paddling, was studied in a less extent. One could mention the work of Lembert *et al*. [7], where special conveyor belts were installed on the simulation start stage to measure the force of the arm strokes. This technique obviously is not suitable for the evaluation of the paddling strokes during training at the real luge track.

The aim of the present work is development of the sensing gloves, applicable for the recording and analysis of the paddling efforts.

Methods

Figure 1 demonstrates design of the sensing glow. Velostat® based piesoresistive sandwich type sensors (Fig. 1a) were attached to the tips of index, middle and ring fingers as well as to the fingers' base (Fig. 1b). Metallic spiked pads cover the fingertips sensors, being attached to the gloves in a manner, usual for the luge athletes. Resistivity of the sensors were measured using wireless data registration unit BioRadio® (manufacturer Great Lake Neurotechnologies, formerly Clevemed Inc). The unit was equipped with custom – made resistivity – voltage transducer.

Paddling arm strokes were recorded with the kind assistance of the Latvian luge team member Arturs Darznieks. The sportsman was instructed to perform paddling on his best, providing firm contact of the palms with ice, as well as simulate insufficient strokes, when fingers are sliding over the ice surface, and poor hands synchronization, when right and left hands contacts ice at

slightly different instants. All tests were performed at the luge start training stage at the luge and bobsleigh track in Sigulda, Latvia.

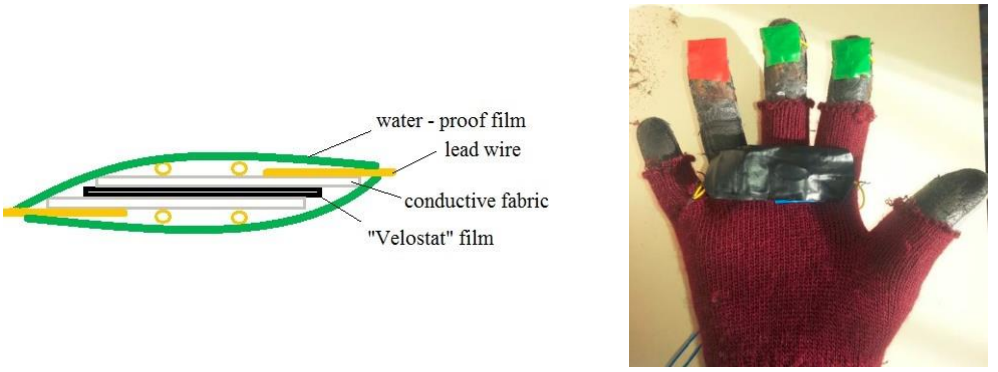

a b

Fig. 1. Cross-section of the Velostat® pressure sensor (a) and design of the sensing glove (b)

Results

Figure 2 demonstrates typical recording, obtained during puddling stroke from the right hand index finger. The pattern, obtained at firm contact between ice and athlete's palm has noticeably longer duration and amplitude, comparing with "poor" stroke. The patterns, obtained from other fingers, as well as from the left hand fingers, are similar to one at the Fig. 2. Time shifts due to poor synchronization of left and right hands are easily observable, as well.

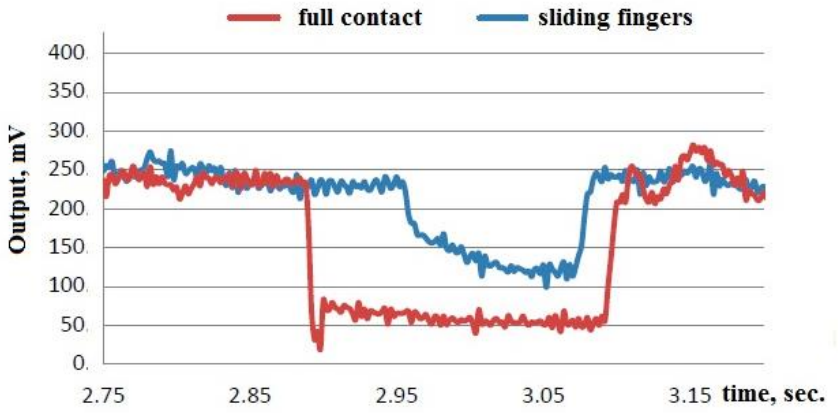

Fig. 2. Typical paddling stroke patterns for the right hand index finger

Conclusions

Developed smart textile gloves demonstrated ability to monitor luge start paddling strokes, measure time intervals between left and right arms strokes and distinguish between good stroke, when athlete's palms are in full contact with ice, and poor stroke, when fingers slides over ice.

Acknowledgements

This research was carried out in the framework of RTU project "Smart textile equipment for effective athlete training" under sponsorship of the Latvian luge federation.

References

[1] *USA Luge Association* [online]. 2016. United States Olympic Committee [cited 29 February 2016]. Available from Internet: http://www.teamusa.org/usa-luge/history-and-fast-facts

[2] Bruggemann, G. P.; Morlock, M.; Zatsiorsky, V. M. 1997. Analysis of the bobsled men's luge events at the XVII Olympic Winter Games in Lillehammer, *Journal of Applied Biomechanics* 13(1): 98–108. http://dx.doi.org/10.1123/jab.13.1.98

[3] Young, K., *et al.* 1986. Biomechanical analysis of the luge start, *American Society of Mechanical Engineers, Design Engineering Division* 1: 81.

[4] Platzer, H.-P.; Raschner, C.; Patterson, C. 2009. Performance-determining physiological factors in the luge start, *Journal of Sports Sciences* 27(3): 221–226. http://dx.doi.org/10.1080/02640410802400799

[5] Fedotova, V.; Pilipivs, V. 2010. Biomechanical patterns of starting technique during training and competitive events for junior lugers, in *IFMBE Proceedings of 6th World Congress of Biomechanics*, August 1–6, 2010, Singapore. Berlin Heidelberg: Springer, 282–285. http://dx.doi.org/10.1007/978-3-642-14515-5_73

[6] Layton, J. 2006. *How luge works* [online]. HowStuffWorks [cited 7 February 2016]. Available from Internet: http://adventure.howstuffworks.com/outdoor-activities/snow-sports/luge.htm

[7] Lembert, S.; Schachner, O.; Raschner, C. 2011. Development of a measurement and feedback training tool for the arm strokes of high-performance luge athletes, *Journal of Sports Sciences*, 29(15): 1593–1601. http://dx.doi.org/10.1080/02640414.2011.608433

11TH INTERNATIONAL CONFERENCE
BIOMDLORE 2016
OCTOBER 20–22, 2016, DRUSKININKAI, LITHUANIA
BIOMDLORE.VGTU.LT

eISSN 2345-0630
ISBN 978-609-457-959-2
eISBN 978-609-457-958-5
DOI: 10.3846/biomdlore.2016.08

Comparison of different microstructure scaffolds for tissue regeneration

Andžela Šešok[1], Deividas Mizeras[2], Algirdas Vaclovas Valiulis[3], Julius Griškevičius[4], Mangirdas Malinauskas[5]
[1, 2, 3, 4] Vilnius Gediminas Technical University, Lithuania
[5] Vilnius University, Lithuania
E-mails: [1] *andzela.sesok@vgtu.lt (corresponding author),* [2] *deividas.mizeras@vgtu.lt,*
[3] *algirdas.valiulis@vgtu.lt,* [4] *julius.griskevicius@vgtu.lt,* [5] *mangirdas.malinauskas@ff.vu.lt*

(Received 9 March 2016; accepted 22 April 2016)

Abstract. In this work we aim to determine the mechanical properties of 3D printed PLA objects having various orientation woodpile microarchitectures. In this work we chose three different 3D microarchitectures: woodpile BCC (each layer consists of parallel logs which are rotated 90 deg every next layer), woodpile FCC (every layer is additionally shifted half of the period in respect to the previous parallel log layer) and a rotating woodpile 60 deg (each layer is rotated 60 deg in respect to the previous one). Compressive and bending tests were carried out TIRAtest2300 universal testing machine. We found that 60 deg rotating woodpile geometry had the highest values which was approximately 3 times than the BCC or FCC log arrangements. Thus we prove that employing low-cost equipment and applying the same raw material one can create objects of desired rigidity.

Keywords: scaffolds, polylactic acid (PLA), microstructure.

Introduction

Three-dimensional (3D) scaffolds are used with the intention to repair, replace, or regenerate injured tissues and organs (for example bone, cartilage, skin, liver, heart, lung and other). Ideally, a tissue engineering scaffold should be biocompatible, biodegradable, highly porous and interconnected, and mechanically reliable. Scaffolds mechanical properties are one of the main aspects to take into account for the development of 3D matrices: stiffness and strength, microstructure changes (resulting from the mechanical deformation of the surface), orientation. The exact control of these factors have a significant influence on the mechanical properties [1, 2].

In this work we applied polylactic acid (PLA) material and used it as supplied by the manufacturer. PLA is one of the most widely used synthetic polymers in biomedical products for drug delivery, orthopaedics, sutures, and scaffolds for tissue engineering [3].

3D printing based on fused filament fabrication (FFF) is emerging as a tool for rapid prototyping as well as additive manufacturing [4]. It offers production of complex shaped micro-objects with high feature spatial definition. Mechanical properties of such printed objects will depend dramatically on the applied material, geometry and filling factor.

In this work we aim to determine the mechanical properties of 3D printed PLA objects having various orientation woodpile microarchitectures.

Methods

Structures were created out of polylactic acid (PLA) using fabrication speed of 15 mm/s and layer height – 50 μm. This allowed us to reach good compromise between fabrication throughput and quality of finished structure. We employ FFF 3D printer "Ultimaker" for the manufacturing of woodpile structures having 1.2 mm lattice period and ~50% fill factor.

Mechanical tests for plastics must be carried strictly on equal terms as set out in the relevant standards. In this work we analysed mechanical testing standards for plastics [5, 6] were formed

3D microporous structures of PLA mechanical properties experimental testing methodology adapted to such samples. Most of the existing research attention was focused on the assessment of behavioural scaffolds during compression. Also equally important of scaffolds is tensile and bending properties. Are used standardized mechanical testing methods. Compressive and bending tests were carried out TIRAtest2300 universal testing machine (Germany) with the computer power and displacement measurement system. The methods and equipment have been chosen for their versatility, accuracy and accessibility. Machine used to test the samples suitable for testing of polymers. Load measurement error is less than ±1%. Step displacement measuring device accuracy ±0.5%. The specimens for compressive tests are prepared according to ISO 604 recommendations. The measurements of the specimens and measurement process correspond to this standard recommendation. Initial scaffolds height was measured by a micrometre 0.01 mm. The specimens were placed between two standard solid clamping plates in test machine. The testing speed was 1 mm/min. Mechanical compression test was repeated for all specimens and recorded graphs of the load/displacement.

Bending tests are performed according to ISO 178. The measurements of the specimens and measurement process correspond to this standard recommendation. Initial samples height was measured by a micrometre 0.01 mm. The distance between supports is 64 mm. The supports are rounded, rounded radius is 5 mm. The testing speed was 1 mm/min.

In this work we chose three different 3D microarchitectures: woodpile BCC (each layer consists of parallel logs which are rotated 90 deg every next layer), woodpile FCC (every layer is additionally shifted half of the period in respect to the previous parallel log layer) and a rotating woodpile 60 deg (each layer is rotated 60 deg in respect to the previous one). The 3D microarchitectures are shown in Fig. 1.

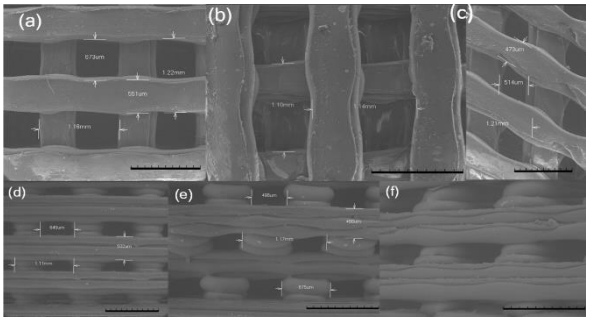

Fig. 1. SEM micrographs of 3D microarchitectures: woodpile (BCC), woodpile (FCC) and a rotating woodpile (60 deg); top and oblique views, (a-c) and (d-f), respectively

Results

Compression test results. Stress-strain curves are shown in Fig. 2. The maximum compressive strength limit, the elastic modulus and stiffness were characterized specimens of 60 deg geometry. This shows that printing orientation (3D architecture) has an influence on the mechanical properties.

Bending test results. Stress/deflection curve is presented in Fig. 3.

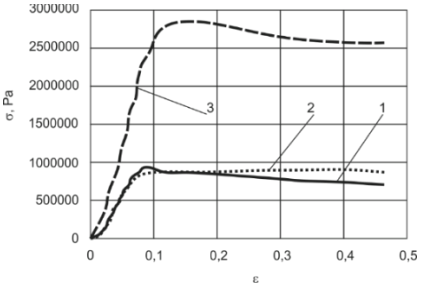

Fig. 2. Stress-strain curves: 1 – woodpile BCC; 2 – woodpile FCC; 3 – woodpile 60 deg

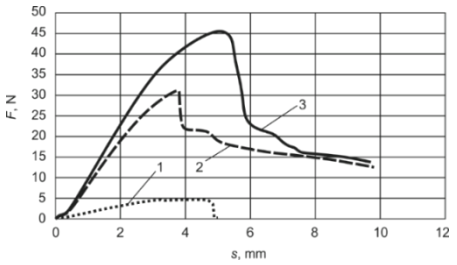

Fig. 3. A graph of stress/deflection curve: 1 – woodpile BCC; 2 – woodpile FCC; 3 – woodpile 60 deg

The lowest values of strength limit by bending had woodpile BCC. 60 deg rotating woodpile geometry had the highest values.

Conclusions

In this work we 3D printed objects having internal woodpile geometries and experimentally measured stress-strain and load/displacement curves of such specimens. 3 different geometries varying woodpile arrangement were examined by means of compression and bending enabling to experimentally determine elastic modulus, strength limit and stiffness. Within the limitation of the study we show that micro-architecture (variation of log orientation in respect to each other) can significantly modify the mechanical properties. We found that 60 deg rotating woodpile geometry had the highest values which was approximately 3 times than the BCC or FCC log arrangements. Thus we prove that employing low-cost equipment and applying the same raw material one can create objects of desired rigidity. By means of additive manufacturing one can produce objects with specific micro-architectures which allows exploitation the structural advantages of stretching and compression constructions as well as size dependent strengthening effects. Future work is focused on modeling mechanical properties of 3D printed objects dependence on internal microarchitecture and experimentally measuring more specimens in order to evaluate the repeatability.

References

[1] Malinauskas, M., *et al.* 2015. Tailoring bulk mechanical properties of 3D printed objects of polylactic acid varying internal micro-architecture, in *Proceedings of SPIE Vol. 9505: Quantum Optics and Quantum Information Transfer and Processing*, April 13, 2015, Prague, Czech Republic. Bellingham: SPIE, 95050P. http://dx.doi.org/10.1117/12.2178515

[2] Wolfe, P. S., *et al*. 2011. Natural and synthetic scaffolds, in *Tissue engineering*. Ed. by N. Pallua, C. V. Suschek. Berlin Heidelberg: Springer, 41–67. http://dx.doi.org/10.1007/978-3-642-02824-3_3

[3] Nair, L.; Laurencin, S. I. 2007. Biodegradable polymers as biomaterials, *Progress in Polymer Science* 32(8–9): 762–798. http://dx.doi.org/10.1016/j.progpolymsci.2007.05.017

[4] Malinauskas, M., *et al.* 2014. 3D microporous scaffolds manufactured via combination of fused filament fabrication and direct laser writing ablation, *Micromachines* 5(4): 839–858. http://dx.doi.org/10.3390/mi5040839

[5] *EN ISO 178:2003 Plastics – determination of flexural properties*. Brussels, 2003. 28 p.

[6] *EN ISO 604:2002 Plastics – determination of compressive properties.* Brussels, 2002. 21 p.

11TH INTERNATIONAL CONFERENCE
BIOMDLORE 2016
OCTOBER 20–22, 2016, DRUSKININKAI, LITHUANIA
BIOMDLORE.VGTU.LT

eISSN 2345-0630
ISBN 978-609-457-959-2
eISBN 978-609-457-958-5
DOI: 10.3846/biomdlore.2016.09

Numerical modelling of the forklift tip-over to test effectiveness of the safety components

Marcin Milanowicz[1], Paweł Budziszewski[2], Krzysztof Kędzior[3]
[1, 2, 3] Central Institute for Labour Protection – National Research Institute, Poland
E-mails: [1] *marmi@ciop.pl (corresponding author),* [2] *pabud@ciop.pl,* [3] *krked@ciop.pl*

(Received 22 March 2016; accepted 17 May 2016)

Abstract. Forklift overturning with its operator is the most common and dangerous type of an accident involving internal transport. The forklifts are equipped with safety components to avoid, or reduce the effects of forklift tip-over. However, there is very few information on the effectiveness of such systems. The aim of the research was to evaluate their effectiveness with the use of numerical simulation. The study relied on carrying out numerical simulations of forklift overturning with its operator. Active human body model was used in the research. Human body output parameters, e.g. forces and accelerations of the head and neck were used to estimate injuries sustained by an operator. The effectiveness of the safety components was assessed on the basis of estimated injuries.

Keywords: numerical simulation, injuries criteria, Madymo, accident analysis, multibody dynamics, numerical human body model.

Introduction

About 100 000 forklifts is registered in Poland. According to the data of the National Labour Inspectorate, Poland, every year there is an average of 90 accidents involving them. As a result of these accidents nearly 100 people are injured (out of which approx. 10–15 deaths) [1]. The most common and dangerous type of an accident involving internal transport is forklift overturning with its operator inside. This might be caused by turning a corner too fast, having an unbalanced load, driving onto a curb, or transport the load raised too high. New forklifts are equipped with an active or passive safety systems to avoid, or reduce the effects of forklift tip-over. Older forklifts (without safety systems) must be retrofitted with the safety components available on the market. However, there is very few information on the effectiveness of such systems. Studies on the safety components effectiveness, with the use of numerical modelling, were conducted in Central Institute for Labour Protection – National Research Institute (CIOP-PIB), Poland. The effectiveness was assessed on the basis of estimated injuries. The methodology and results of the research are described in the article.

Methods

The study relied on carrying out numerical simulations of the forklift overturning with its operator inside. Study was carried out with the use of the Madymo package [2]. A model of the accident site, consisting of the numerical models of: forklift; human body; ground and safety components, was developed (Fig. 1). The simulation was performed for several different configurations include three speeds: 0 km/h; 13.5 km/h and 23 km/h. The overturning forklift model was validated based on experimental results [3] for 0 km/h, [4] for 13.5 km/h and based on real-life accident reconstruction [5] for 23 km/h.

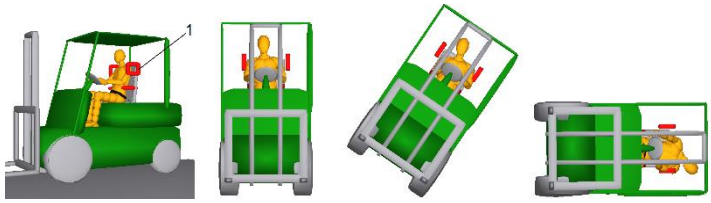

Fig. 1. Simulation model. 1 – example of safety component: seat wings model

For each test configuration forklift model was equipped with the following safety components: two-, three-, four-point seatbelts (2B, 3B, 4B), support structure to maintain the operator in the seat so-called seat wings (SW) (Fig. 1), seat armrest (SA) structure to prevent falling out of the forklift cab, in the form of additional door bar (D) and safety helmet for operator (H). Models of 2B, 3B, 4B were taken from Madymo database; models of SW, SA, D were developed as rigid bodies; H model was developed as multibody one and validated; described in [6]. Active human body model, based on Pedestrian model available in the Madymo database [7], was used in the research (model retains the position recommended by forklifts producers and responds to external forces acting on it by mapping the human reaction and behaviour). To activate human model a kinematic excitation is used. In the Madymo package, it is possible to pre-set motion (in this case – rotational motion in joints simulating human joints) in a kinematic joints by introducing a function defining the behaviour of the angle over time [8]. Model was developed and validated based on experimental results described in [4]. The effectiveness of the safety components was evaluated on the basis of the potential injuries of the head and neck sustained by a forklift operator (the more protection, the less severity of injuries).

Results

Results of the simulation, each time contain the following data: animation showing kinematics of an overturning forklift; injury criteria for head and neck. For head HIC 15 ms (Head Injury Criterion) was used and for neck shear/axial forces, measured in upper cervical spine, were used to evaluate potential injuries. Evaluated injuries of head and neck were transfer to Abbreviated Injury Scale (AIS) using tables from [9] (tables 13, 14 for head; 15, 22 for neck). Where for AIS: 1 – minor injuries; 2 – moderate injuries; 3 – serious injuries; 4 – severe injuries; 5 – critical injuries; 6 – maximum injuries; 9 – not further specified [10].

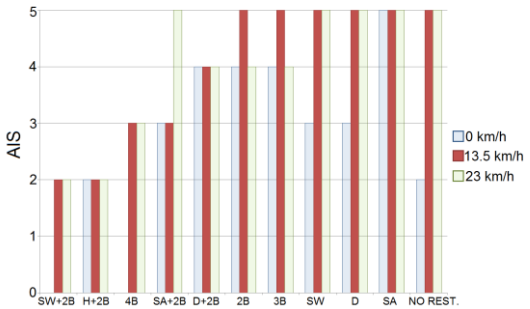

Fig. 2. The AIS results for different safety components and velocities

Results in AIS scale in order from most to less effective safety components are shown in Figure 2. Results are shown for each safety components configuration and for three forklift velocities. The last results labelled NO REST are for forklift without safety components.

Conclusions and discussion

As the results show, in most cases, the effectiveness of the safety components decreases with increasing velocity. A two-point seatbelt (2B, Fig. 2), uses as only safety component, does not fully protect the operator from life-threatening injuries. However, 2B significantly reduce the probability of serious injuries in connection with other safety components, e.g. SW+2B; H+2B. The most effective safety component are seat wings while lap seatbelt is fastened (SW+2B). In the case when the seatbelt is not fastened (SW) there is a high probability of hitting operator's head on the forklift ceiling. A very effective solution is to use four-point seatbelt (4B). However, this solution is impractical because the belt limits the movement of the operator during manoeuvring. Three-point belt is a solution as effective as four-point belt only if the forklift overturns the side on which shoulder belt attachment is fixed. Otherwise, the operator will not be maintained by a shoulder belt and there is a high probability of hitting his head on the ground (3B). Structures to prevent falling out of the forklift cab, in the form of additional door bar (D and D + 2B), effectively protect the operator from falling out when, e.g. cornering at high speed but only in cases when do not come to overturn. However, if it comes to overturn, there is a high probability of suffering severe life-threatening injuries.

Similar studies are conducted in different research centres all over the world. Usually these are experimental studies using ATD (anthropomorphic test device) crash test dummies, e.g. [4] using numerical simulation, e.g. [3]. The use of numerical simulation has many advantages, among others it enables testing of many different safety components and scenarios. Thereby, selection of optimal safety solution is possible. Furthermore, knowledge of the course of this type of accidents can be used to train forklift operators in the field of Occupational Safety and Health procedures. Moreover, the use of an active model of the human body enabled the modelling of the human responses - in this case the behaviour recommended by the forklift producers and operators training centres. The human response taking into account in this type of research is an innovation. Based on the French Institute for Research and Security (INRS, France) results [4] an active human body model was developed by CIOP-PIB. The use of active models is another step to improve the accuracy of simulation results.

Acknowledgements

This paper has been based on the results of a research task carried out within the scope of the third stage of the National Programme "Improvement of safety and working conditions" partly supported in 2014–2016 – within the scope of state services – by the Ministry of Labour and Social Policy (Poland). The Central Institute for Labour Protection – National Research Institute (Poland) is the Programme's main co-ordinator.

References

[1] *Informacja Państwowej Inspekcji Pracy* [online]. 2013. Rada Ochrony Pracy [cited 20 March 2016]. Available from Internet: http://rop.sejm.gov.pl/1_0ld/opracowania/pdf/material60.pdf

[2] *Madymo Theory Manual Release 7.5*. 2013. Helmond: TASS International.

[3] Rebelle, J.; Mistrot, P.; Poirot, R. 2009. Development and validation of a numerical model for predicting forklift truck tip-over. Vehicle system dynamics, *International Journal of Vehicle Mechanics and Mobility* 47(7): 771–804. http://dx.doi.org/10.1080/00423110802381216

[4] Rebelle, J. 2015. Use of a modified HYBRID III 50th dummy to estimate the effectiveness of market restraint systems for forklift truck drivers, *International Journal of Crashworthiness* 20(4): 348–369. http://dx.doi.org/10.1080/13588265.2015.1015362

[5] Milanowicz, M.; Budziszewski, P. 2013. Numerical reconstruction of the real-life fatal accident at work: a case study, in *Lecture Notes in Computer Science*. Vol. 8026. Ed. by V. G. Duffy. Berlin Heidelberg: Springer-Verlag, 101–110. http://dx.doi.org/10.1007/978-3-642-39182-8_12

[6] Milanowicz, M. 2012. Development of the numerical safety helmet model for reconstruction and prevention of the accidents in the work place, *Mechanik* 7: 537–545.
[7] *Madymo Human Body Models Manual Release 7.5*. 2013. Helmond: TASS International.
[8] Milanowicz, M. 2015. *Numerical modelling of occupational accidents caused by falls from a height. PhD Thesis*. Warsaw: Central Institute for Labour Protection – National Research Institute.
[9] *Occupant protection & egress in rail systems* [online]. 2006. EURailSafe [cited 1 May 2016]. Available from Internet: http://www.eurailsafe.net/subsites/operas/HTML/appendix
[10] *Abbreviated Injury Scale (AIS) 2005 – update 2008*[online]. 2008. Association of the Advancement of Automotive Medicine [cited 1 May 2016]. Available from Internet: http://www.aaam.org/

11TH INTERNATIONAL CONFERENCE
BIOMDLORE 2016
OCTOBER 20–22, 2016, DRUSKININKAI, LITHUANIA
BIOMDLORE.VGTU.LT

eISSN 2345-0630
ISBN 978-609-457-959-2
eISBN 978-609-457-958-5
DOI: 10.3846/biomdlore.2016.10

Stress analysis of osteoporotic femur

Oleg Ardatov[1], Vladimir Barsukov[2], Dmitriy Karev[3]
[1] Vilnius Gediminas Technical University, Lithuania
[2] Yanka Kupala State University of Grodno, Belarus
[3] Grodno Medical State University, Belarus
E-mails: [1] *oleg.ardatov@vgtu.lt (corresponding author)*, [2] *v.g.barsukov@grsu.by*,
[3] *dmitriy.karev@gmail.com*

(Received 24 March 2016; accepted 28 April 2016)

Abstract. Osteoporosis and degenerative diseases cause low bone mass that increases fracture risks. This study presents the modelling of osteoporotic femur by employing finite element method (FEM). The loading of femur using FEM tools was performed. The level of degradation was modelled by changing the thickness of cortical shell and using power-law equations, which determine the dependence between apparent density of cancellous bone and its mechanical properties. Obtained results could be useful for both medical diagnosis and bone health check.

Keywords: osteoporosis, finite element method, bone mechanics, femur.

Introduction

Osteoporosis is a disease characterized by low bone mass and micro-architectural deterioration of bone tissue, with a consequent increase in bone fragility and susceptibility to fracture [1]. Osteoporosis is one of the most common health problems affecting both men and women, and it is becoming increasingly prevalent in our aging society. Osteoporosis affects over 200 million people worldwide [2] with an estimated 1.5 million fractures annually in the United States alone [3] and attendant costs exceeding $10 billion per annum [4]. Although osteoporosis affects the entire skeleton, many osteoporotic fractures occur in the femur [5]. It has a high mortality rate: survival is 72% in the first year and only 28% after five years [5].

Due to the complex anatomy of the femur body, the difficulties associated with obtaining bones for in vitro experiments, and the limitations on the control of the experimental parameters, finite element models have been developed in order to analyse the biomechanical properties of bone tissue.

The present study is aimed to determine the stress distribution on cortical shell of femur with verification of various grades of osteoporosis.

Methods

A three-dimensional continuum boundary problem is raised. In order to define the mechanical behaviour of femur model under the compression load, theory of elasticity was applied. Main equations are presented in tensor form:

$$\frac{\partial \sigma_{ij}}{\partial x_j} + f_i = 0, \tag{1}$$

$$\varepsilon_{ij} = \frac{1}{2}\left(\frac{\partial U_i}{\partial x_j} + \frac{\partial U_j}{\partial x_i}\right), \tag{2}$$

$$\sigma_{ij} = C_{ijkl} \times \varepsilon_{kl}, \tag{3}$$

where σ_{ij} is a tensor of stress, ε_{ij} is a strain tensor, U is a displacement tensor, f_i corresponds to volume forces and C_{ijkl} is a fourth-order tensor of elasticity.

The von Mises-Hencky criterion is chosen to analyse the stressed state of the model. The selection of this criterion is based on mechanical properties of the bone, which seems to behave as a ductile material [6]. Also, the model is continuous and isotropic, so the von Mises stress criterion is applied to the research of stresses, which occur on cortical shell of the model.

The von Mises stress is defined in Eq. (4) below, where σ_1, σ_2 and σ_3 are the maximum, intermediate, and minimum principal stresses respectively; σ_{eq} is a von Mises equivalent stress:

$$\sqrt{\frac{(\sigma_1-\sigma_2)^2+(\sigma_2-\sigma_3)^2+(\sigma_3-\sigma_1)^2}{2}}=\sigma_{eq}. \quad (4)$$

The initial geometry of the model was derived from DICOM data files and converted into the numerical body using *SolidWorks* software. The model consists of two basic components – cortical shell and cancellous bone, both modelled as isotropic and elastic. Section view of the model is presented in Fig. 1. Elasticity constants of healthy model were calculated using power-law equations [7]. They are presented in Table 1.

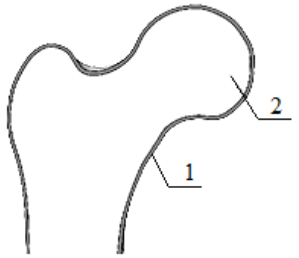

Fig. 1. Section view of numerical femur model: 1 – cortical shell; 2 – cancellous bone

Table 1. Elasticity constants of the healthy model

Component of the model	*E*, MPa	ν
Cortical shell	18000	0.300
Cancellous bone	3260	0.200

The impact of osteoporosis is modelled by decreasing the elasticity modulus of the cancellous bone and thickness of cortical shell, as it is pointed out in Table 2.

Table 2. Varying of parameters of the model

Parameters of the osteoporotic model	Range
Cortical shell thickness, mm	0.5–1.5
Elasticity modulus of cancellous bone	260–3260

The model was rigidly constrained through distal part of femur, and static compressive load collinear to axis of femoral neck in the range of 1000–2000 N was applied. The meshing of the model was performed with volume finite elements due to its curvature. The number of elements and nodes is presented in Table 3.

Table 3. Finite element model

Model component	Number of finite elements	Number of nodes
Cortical shell	4157	7351
Cancellous bone	20560	45139

Results

The stress distribution on the cortical shell of the model was obtained for various grades of osteoporotic degradation and model with 0.5 mm thickness of cortical shell is presented in Fig. 2.

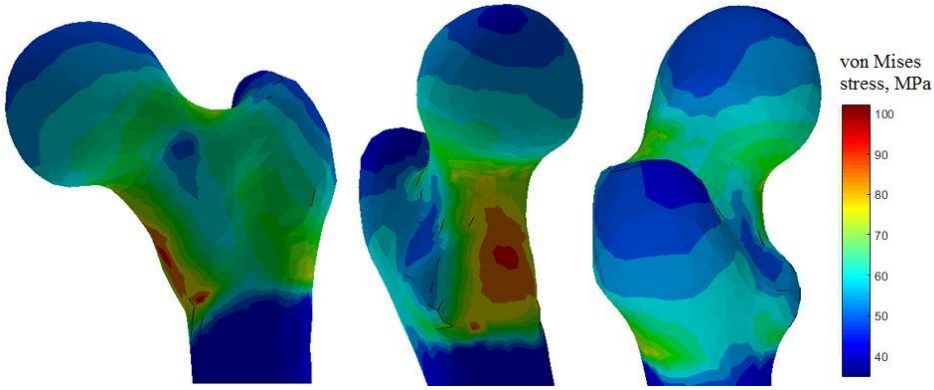

Fig. 2. Stress distribution on the cortical shell of femur model with 0.5 mm cortical shell

As it shown in Fig. 2, the highest von Mises stress appears along the inner area of the neck, near the intertrochanteric line. The difference between the maximal values of stresses in the healthy and osteoporotic model (with 0.5 mm cortical shell thickness) reaches 350%.

Conclusions

We developed the finite element model of human femur, which consisted of the cortical shell and cancellous bone. The model was treated for various grades of degenerative diseases. The distribution of von Mises stress was obtained on the cortical shell of the model. It was found, that value of von Mises stress depends both on quality of cancellous bone and thickness of cortical shell, while the thickness of cortical shell remains critical.

References

[1] Anon. 1993. Consensus development conference: Diagnosis, prophylaxis and treatment of osteoporosis, *American Journal of Medicine* 94(6): 50–56. http://dx.doi.org/10.1016/0002-9343(93)90218-E

[2] Lin, J. T.; Lane, J. M. 2004. Osteoporosis: a review, *Clinical Orthopaedics and Related Research* 425: 34–42. http://dx.doi.org/10.1097/01.blo.0000132404.30139.f2

[3] Nevitt, M. C., *et al.* 1999. Association of prevalent vertebral fractures, bone density, and alendronate treatment with incident vertebral fractures: effect of number and spinal location of fractures, *Bone* 25(5): 9–13. http://dx.doi.org/10.1016/S8756-3282(99)00202-1

[4] Johnell, O., *et al.* 2004. Mortality after osteoporotic fractures, *Osteoporosis International* 15(1): 38–42. http://dx.doi.org/10.1007/s00198-003-1490-4

[5] Riggs, B. L.; Melton 3rd, L. J. 1995. The worldwide problem of osteoporosis: Insights afforded by epidemiology, *Bone* 17(5): 501S–505S. http://dx.doi.org/10.1016/8756-3282(95)00258-4

[6] Doblaré, M.; García, J. M.; Gómez M. J. 2004. Modelling bone tissue fracture and healing: a review, *Engineering Fracture Mechanics* 71(13–14): 1809–1840. http://dx.doi.org/10.1016/j.engfracmech.2003.08.003

[7] Helgason, B., *et al.* 2008. Mathematical relationships between bone density and mechanical properties: a literature review, *Clinical Biomechanics* 23(2): 135–146. http://dx.doi.org/10.1016/j.clinbiomech.2007.08.024

11TH INTERNATIONAL CONFERENCE
BIOMDLORE 2016
OCTOBER 20–22, 2016, DRUSKININKAI, LITHUANIA
BIOMDLORE.VGTU.LT

eISSN 2345-0630
ISBN 978-609-457-959-2
eISBN 978-609-457-958-5
DOI: 10.3846/biomdlore.2016.11

Myotonometry as a tool for determination of fatigue in the upper extremities of garment industry workers

Viive Pille[1], Piia Tint[2]
[1, 2] Tallinn University of Technology, Estonia
E-mails: [1] *viive.pille@regionaalhaigla.ee*, [2] *piia.tint@ttu.ee (corresponding author)*

(Received 29 March 2016; accepted 5 May 2016)

Abstract. The myotonometric measurements of upper limb muscles of garment workers working in a static posture are presented. The workers' pain intensity was followed on the pain Visual Analogue Scale. The results show that *M trapezius* and other spine muscles differ at the beginning and the end of the workweek. In hand muscles, the difference is not so significant. The load accumulates in the hands over the years, and the spine and neck get tired more quickly; therefore, there are more complaints of pain in the neck and back. The values of measured stiffness of the muscles was between 156–278 N/m and for the own frequency of muscles 11.2–16.5 Hz.

Keywords: myotonometry, fatigue, musculoskeletal disorders, garment workers.

Introduction

The majority of occupational diseases (OD) in Estonia and in the world [1, 2] pertain to musculoskeletal disorders (MSDs) caused by long-term monotonous work or a static working posture. This is a great problem in the garment industry [3]. The ODs in Estonia are diagnosed in a late stage when the worker is already disabled. In this last stage, it is difficult to find proper rehabilitation methods for total recovery [4]. Therefore, rehabilitation has to begin sooner. The present investigation is dedicated to determination of fatigue of the hand, shoulder and higher-back muscles after work in a static posture, using the advanced measuring method – "myotonometry" [5]. The parameters that show changes in the muscles are as follows: (a) Frequency which characterizes muscle tension. The own frequency of muscle describes the muscle tone in the relaxed state of the muscle. The value of the parameter is usually 11–16 Hz, depending on the muscle. In a normal state, the muscle tension at rest is insignificant, but the frequency increases when the muscle is energized. Increased muscle tone at rest may reduce blood flow to the muscles; (b) Decrement characterizes muscle elasticity i.e. a muscle's ability to recover its original shape after contraction. Values of the decrement are normally less than 1.0–1.2, depending on the type of the muscle. The changed elasticity may affect blood flow in muscles when working movements are performed. There may be greater wear, and the speed of movement may be limited [5]; (c) Stiffness characterizes a muscle's ability to resist its shape-shifting power. The values of stiffness are in the range of 150 N/m to 300 N/m, depending on the type of the muscle. The results of "myotonometric" measurement of workers in different occupations can be found in [6–8]. The aim of the study is to determine the fatigue of muscles during the work process in the garment industry.

Methods and Contingent

The MYOTON-3 myotonometer was used to evaluate the functional state of the skeletal muscles of garment industry workers (N = 32, all female). The workers of gore machine (N = 4) and universal sewing machines (N = 28) were the most ergonomically not well-designed workstations. Completing and ironing workers were excluded from the study group. The myotonometer is a handheld device (Fig. 1, 2) developed at the University of Tartu, Estonia, by Dr. Arved Vain. The myotonometer exerts a local impact on the biological tissue by means of a brief mechanical impulse. The impact force is small enough so that it causes no changes in the

neurological reaction of the biological tissue. The tissue responds to the mechanical impact with damping or oscillation, which is registered by an acceleration sensor located on the measuring tip of the device. The workers' musculoskeletal pain intensity was assessed by using the pain Visual Analogue Scale (VAS, a scale from one to ten). The workers filled in the questionnaire forms. The arithmetic mean and standard deviation (SD) were calculated. To ascertain the relationships between the characteristics, *Spearman's rank correlation coefficient* (Spearman's Rho) was applied, the differences between the groups were tested by means of *Student's t-test*. The difference $p<0.05$ was considered to be statistically significant.

Fig. 1. Myotonometer "MYOTON-3"

Fig. 2. Measurement of muscles stiffness

Results

The following muscles were measured myotonometrically: *M abductor pollicis brevis, M adductor pollicis brevis* (hand muscles), *M trapezius med and M erector spinae* (spine muscles). The results show that various *M trapezius* and other spine muscles differ at the beginning and at the end of a workweek. In the hand muscles, the difference is not so significant. The load is accumulated in the hands over the years, and the spine and the neck get tired more quickly, therefore there are more complaints of pain in the neck and in the spine. The stiffness (S), decrement (D) and frequency (F) of various muscles at the beginning (BEGIN) and at the end (END) of the workweek are presented in Table 1.

Table 1. The myotonometric measurements of hand and spine muscles at the beginning and at the end of the workweek

Adductor poll left BEGIN			*Adductor poll left* END			*Adductor poll right* BEGIN			*Adductor poll right* END		
F	S	D	F	S	D	F	S	D	F	S	D
16.5	**278.9**	2.35	15.8	**277.4**	2.33	15.9	**268.7**	2.6	15.8	**277.2**	2.3
*3.0	31.5	0.3	2.01	29.77	0.44	2.38	31.29	0.3	2.2	33.44	0.4
Trapezius med left BEGIN			*Trapezius med left* END			*Trapezius med left* BEGIN			*Trapezius med right* END		
F	S	D	F	S	D	F	S	D	F	S	D
11.8	**156.0**	1.24	11.2	**175.5**	1.43	12.0	**161.3**	1.3	11.5	**186.5**	1,6
*2.7	37.78	0.46	3.13	72.1	0.33	2.6	42.8	0.5	3.51	81.2	0.5
Er spinae left BEGIN			*Er spinae left* END			*Er spinae right* RIGHT			*Er spinae right* END		
F	S	D	F	S	D	F	S	D	F	S	D
15.0	**265.0**	2.0	15.0	**272.2**	1.9	14.9	**242.6**	2.0	15.4	**259.7**	2.1
*2.3	57.85	0.37	2.9	58.50	0.33	2.52	49.9	0.4	3.0	51.2	0.4

Note: * – SD

The correlation between the myotonometric measurement values (F, S, D) of garment workers at the beginning and at the end of the workweek were calculated (R^2 = 0.92–0.97) and the p-value (Anova) was between 0.01 and 0.03.

The stiffness of muscles is higher (except of M *add poll left*) at the end of the workweek. The stiffness of different muscles is marked in bold in Table 1. Muscle tiredness increases during the workweek; the left hand is less loaded than the right hand, therefore the stiffness values are more constant.

Discussion

The results of the present study of garment workers correspond to the previous data regarding back pain (59.1%). The frequency of pain occurrence in the neck area (71.4% of all GW), in the shoulders (67.3% of all GW), the wrist/hand region (53.1% of all GW) is higher when compared to the study of Reinhold et al. [9]. In the study of Friedrich et al. [3], the proportion of garment industry workers suffering from neck, upper back and lower back pain was much higher: 52.4%, 54.8% and 72.8% respectively of all the workers studied, which is in better conformity with the results of the present study. Comparing the results of the myotonometry (stiffness) acquired in the current study with the data on office workers and sportsmen of other researchers [6, 8], it could be concluded, that the values are comparable (stiffness *M erector spinae* right Pille (present study) = 242.6–259.7 N m^{-1}; Oha et al. [6] = 325.1–332.1 N m^{-1}; left Pille (present study) = 265.0–272.2 N m^{-1}, Oha et al. [6] = 330.6–320.5 N m^{-1}; stiffness of lower limbs acquired by Pruyn et al. [8]: = 293.8–393.2 N m^{-1}.

Conclusion

There are persistent muscle tone changes in garment workers' muscles. Increased decrement results indicate a slight muscle overload rather than a persistent condition. The stiffness of the investigated muscles increased and the frequency decreased during the workday as a rule; the decrement changes depend on the side of the body. The patented myotonometrical technology [5] – non-invasive, quick and easy measurement of superficial skeletal muscles – can be used in occupational health for diagnostics of work-related musculoskeletal disorders.

References

[1] *Annual Report of Work Environment 2014* [online]. 2015. Labour Inspectorate [cited 29 March 2016]. Available from Internet: http://www.ti.ee/fileadmin/user_upload/failid/dokumendid/Meedia_ja_statistika/Toeoekeskkonna_uelevaated/2014/TKY_2014_ik.pdf

[2] Hoy, D. G., *et al.* 2015. Reflecting on the global burden of musculoskeletal conditions: lessons learnt from the Global Burden of Disease 2010 Study and the next steps forward, *Annals of the Rheumatic Diseases Journal* 74(1): 4–7. http://dx.doi.org/10.1136/annrheumdis-2014-205393

[3] Friedrich, M.; Cermak, T.; Heller, I. 2000. Spinal troubles in sewage workers: epidemiological data and work disability due to low back pain, *International Archives of Environmental Health* 73(4): 245–254. http://dx.doi.org/10.1007/s004200050424

[4] Pille, V., *et al.* 2015. Work-related musculoskeletal symptoms in industrial workers and the effect of balneotherapy, *Agronomy Research* 13(3): 820–828.

[5] Vain, A. 2002. *Myotonometry*. Tartu.

[6] Oha, K.; Viljasoo, V.; Merisalu, E. 2010. Prevalence of musculoskeletal disorders, assessment of parameters of muscle tone and health status among office workers, *Agronomy Research* 8(special issue): 192–200.

[7] Roja, Z., *et al.* 2006. Assessment of skeletal fatigue of skeletal fatigue of road maintenance workers based on heart rate monitoring and myotonometry, *Journal of Occupational Medicine and Toxicology* July: 1–9. http://dx.doi.org/10.1186/1745-6673-1-20

[8] Pruyn, E. C.; Watsford, M. L.; Murphy, A. J. 2015. Validity and reliability of three methods of stiffness assessment, *Journal of Sports and Health Science* 1–8. http://dx.doi.org/10.1016/j.jshs.2015.12.001

[9] Reinhold, K., *et al.* 2008. Innovations at workplace: improvement of ergonomics, *Engineering Economics* 60(1): 85–94.

11TH INTERNATIONAL CONFERENCE
BIOMDLORE 2016
OCTOBER 20–22, 2016, DRUSKININKAI, LITHUANIA
BIOMDLORE.VGTU.LT

eISSN 2345-0630
ISBN 978-609-457-959-2
eISBN 978-609-457-958-5
DOI: 10.3846/biomdlore.2016.12

The use of DTW method as an effective way of uroflowmetry data screening analysis

Wojciech Walendziuk[1], Aleksander Sawicki[2], Adam Idźkowski[3]
[1, 2, 3] Bialystok University of Technology, Poland
E-mails: [1] *w.walendziuk@pb.edu.pl (corresponding author)*, [2] *aleksander.sawicki.91@gmail.com*, [3] *a.idzkowski@pb.edu.pl*

(Received 29 March 2016; accepted 29 June 2016)

Abstract. The aim of this work is to present an application of the Dynamic Time Warping (DTW) method for the preliminary classification of data obtained during uroflowmetric tests. This enables determining whether the recorded data from the urine flow speed measurements is accurate or not. Example urine flow characteristics obtained from a uroflowmeter based on a strain gauge transducer were used in the research. The analysis of the algorithm performance was done on the basis of real tests results of patients with the risk of the prostate hyperplasia occurrence. Moreover, the results of example experiments are presented in this paper.

Keywords: uroflowmeter, uroflowmetry, urine flow, dynamic time warping.

Introduction

The benign prostatic hyperplasia is one of most frequent diseases occurring at men over 50 years old. The enlargement of the prostate gland (> 30ml) is the reason of lesions within the urinary system, called the acute urinary retention (AUR) [1]. One of the ways of patient examination is uroflowmetry which can be treated as a non-invasive preliminary diagnostic method. Currently the devices used to measure the urine flow are usually based on strain gauge sensors [2–5]. It is possible to determine the urine mass by the voltage analysis in bridge circuits (e.g. Wheatstone's bridge). Additionally, recording data with a defined sampling frequency, it is possible to determine the urine mass increase in time. A flowmeter equipped with a rotating disc on which the patient's urine drops is another solution [2]. The disc rotates with constant speed due to an electric engine. In a measurement system of this type, the values such as current voltage supplying the engine, which is proportional to the urine flow intensity, are measured. The urine flow speed measurement by analyzing the hydrostatic pressure read by a pressure transducer is another solution. Such system uses the pressure measurement in a container closed at one side, e.g. at the top, where a pressure sensor is placed. The open side is situated in a container with fluid, therefore, raising its level causes the pressure increase. The pressure is, then, proportional to the urine flow [5]. All systems enable estimating the urine flow through the urethra on the basis of the measurements of the excreted urine volume and its flow speed [6–8]. In tests of this type, micturition parameters are usually presented in the form of a graph. Evaluation of the parameters helps the urologist to plan the therapy and monitor the conservative treatment.

Unfortunately, the lack of possibility of automatic data analysis in order to identify the abnormalities in the urine flow is a disadvantage of this solution. There are, however, devices that analyze the urine flow characteristics by applying the neural network, but they require appropriate computing performance. For all those reasons, the main aim of this work is to create an algorithm of the measurement data analysis which could be helpful with the BPH (benign prostatic hyperplasia) preliminary diagnosis. This algorithm could be implemented in a mobile uroflowmeter which would draw the urine flow characteristics, whose analysis would be used to classify patients to further diagnostic tests. The idea could also be used in a device permanently installed in the patient's house. The tests concerning the benign prostatic hyperplasia could be

carried out constantly, and the device could inform the patient about the necessity of consulting the doctor immediately after detecting the urine flow disorder.

DTW algorithm as a method of uroflowmetric data analysis

The principle of the DTW algorithm is to compare a series of measurement results that have common features but are different in terms of time and amplitude [9].

The algorithm of comparing the flows in time uses two signals: the model one – X_p, and the measured one – X_m, whose individual samples are recorded in the data board. During the first stage of the algorithm work, Euclidean distances between all samples of the compared signals are determined (1):

$$Y(n_p, n_m) = \sqrt{\sum_{i=1}^{N_p \times N_m} \left(X_p(i) - X_m(i)\right)^2}, \; n_p = 1...N_p, \; n_m = 1...N_m. \tag{1}$$

Next, the Y_{ac} cumulative cost on the matrix boundary elements towards X_p and X_m is calculated. Searching the path of the least cumulative cost of transition will be the next step of the process (2). In order to do it, the backtracking procedure is used. It consists in transition from the (N_p, N_m) point to (1, 1). Minimizing the transition function, e.g. finding the path in the matrix that has the least cumulative cost, is an important element of this stage of the process. The function that describes this issue can be presented as:

$$Y_c = \sum_{i=N_p}^{1} \sum_{j=N_m}^{1} \min \{Y_{ac}(i-1, j-1); Y_{ac}(i, j-1); Y_{ac}(i-1, j) \tag{2}$$

After finding the shortest path, the elements qualified as the least are summed up.

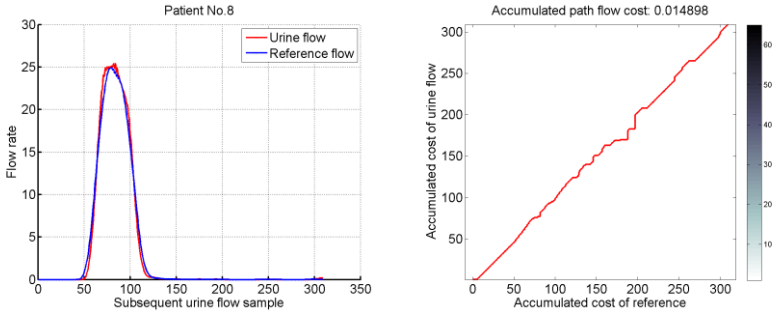

Fig. 1. Proper urine flow and the DTW least cost path (0.01489)

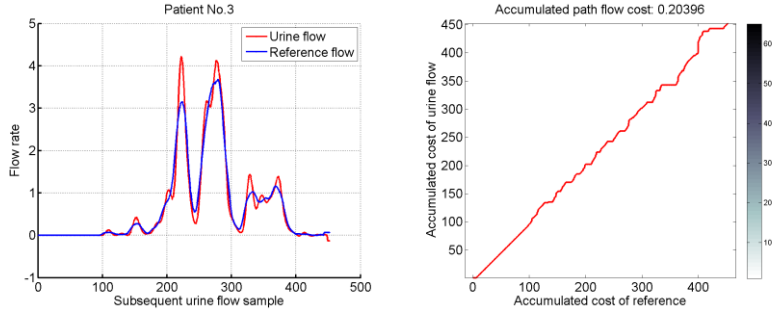

Fig. 2. Improper urine flow and the DTW least cost path (0.20396)

Those summed up numerical values can be then used as a classifier of the measurement data analysis, indicating the degree of the signals similarity. It is worth stressing that in the carried out experiments, the average value of the urine flow obtained during the measurement was used as the reference model. Due to this fact, the algorithm employing the DTW method was not sensitive to the urination time, the urine flow amplitude or the urination initiation time until the moment of the maximum value of the urine flow. An example of the accurate urine flow and the characteristics of the transition path with the accumulative cost are presented in Fig. 1. Whereas, the inaccurate urine flow can be seen in Fig. 2.

In order to test the algorithm, an original uroflowmeter based on a strain gauge was used [4]. The device was equipped with a microcontroller that acquired the measurement data and recorded it in the local memory. After the tests had been done, their analysis was conducted with the use of the previously mentioned DTW algorithm in the MATLAB environment. A group of randomly chosen 20 patients aged 45–82 with hypothetic prostate hyperplasia were tested for the purpose of this research. The obtained results were consulted with a urologist in terms of the correctness of their medical interpretation.

As a result of implementing the presented algorithm, satisfying data analysis results were obtained. In the tested cases, the following cost coefficients were applied: less than 0.3 for the accurate flows and more than 0.31 for the inaccurate flows. The efficiency of detecting the accurate urine flows equaled 97%.

Conclusions

The present work contains the implementation of the DTW method in the urine flow characteristics analysis. Real results of the uroflowmetric tests of a group of men aged 45–82 with hypothetic prostate hyperplasia were used in the research. The tests of the algorithm proved its correctness of 97%, which can be treated as a very satisfactory result. Such a great efficiency caused the authors to implement the worked out algorithm in a microcontroller-based measurement system which will acquire data from a strain gauge transducer. Further research will be therefore focused on an algorithm of the reference flow automatic generating, as well as on constructing a new version of the device aiming at measuring the urine flow speed.

Acknowledgements

The paper was prepared at Bialystok University of Technology within a framework of the S/WE/1/2013 and the MB/WE/4/2016 projects sponsored by Ministry of Science and Higher Education.

References

[1] Marks, L. S.; Roehrborn, C. G.; Andriole, G. L. 2006. Prevention of benign prostatic hyperplasia disease, *Journal of Urology* 176(4): 1299–1306. http://dx.doi.org/10.1016/j.juro.2006.06.022

[2] Dejhan, R. B. K.; Yimman, S. 2014. Uroflowmetry recording design, in *Proceedings of TENCON 2014 – IEEE Region 10 Conference*, 22–25 October 2014, Bangkok, Thailand. Piscataway: IEEE. http://dx.doi.org/10.1109/TENCON.2014.7022392

[3] Makal, J.; Idźkowski, A.; Walendziuk, W. 2006. Computer assisted uroflowmetry diagnostic system, *Proceedings of SPIE* 6347: 63472B. http://dx.doi.org/10.1117/12.714637

[4] Walendziuk, W.; Idzkowski, A. 2009. Portable acquisition system for domiciliary uroflowmetry, *Journal of Vibroengineering* 11(3): 592–596.

[5] Suryawanshi, A.; Joshi, A. 2012. Urine flow rate measurement based on volumetric pressure measurement principle, in *1st International Symposium on Physics and Technology of Sensors*, 7–10 March 2012, Pune, India. http://dx.doi.org/10.1109/ISPTS.2012.6260961

[6] Altunay, S., *et al.* 2006. Interpretation of uroflow graphs with artificial neural networks, in *Proceedings of IEEE Signal Processing and Communications Applications*, 16–19 April 2006, Antalya, Turkey. Piscataway: IEEE. http://dx.doi.org/10.1109/SIU.2006.1659698

[7] Chapple, C. R.; Mangera, A. 2011. Overview of the evaluation of lower urinary tract dysfunction, in *Practical Urology: Essential Principles and Practice*. Ed. by C. R. Chapple, W. D. Steers. London: Springer, 261–282. http://dx.doi.org/10.1007/978-1-84882-034-0_20

[8] Bray, A., *et al.* 2012. Methods and value of home uroflowmetry in the assessment of men with lower urinary tract symptoms: a literature review, *Neurourology and Urodynamics* 31(1): 7–12. http://dx.doi.org/10.1002/nau.21197

[9] Müller, M. 2007. *Information Retrieval for Music and Motion*. Berlin Heidelberg: Springer-Verlag. 318 p. http://dx.doi.org/10.1007/978-3-540-74048-3

11TH INTERNATIONAL CONFERENCE
BIOMDLORE 2016
OCTOBER 20–22, 2016, DRUSKININKAI, LITHUANIA
BIOMDLORE.VGTU.LT

eISSN 2345-0630
ISBN 978-609-457-959-2
eISBN 978-609-457-958-5
DOI: 10.3846/biomdlore.2016.13

The supporting method for automatic diagnosis of prostatic hypertrophy

Wojciech Walendziuk[1], Aleksander Sawicki[2], Adam Idźkowski[3]
[1, 2, 3] Bialystok University of Technology, Poland
E-mails: [1] *w.walendziuk@pb.edu.pl (corresponding author)*, [2] *aleksander.sawicki.91@gmail.com*, [3] *a.idzkowski@pb.edu.pl*

(Received 29 March 2016; accepted 14 June 2016)

Abstract. In the paper numerical algorithms used in the automatic diagnosis of prostatic hypertrophy are presented. The liquid flow during urination was applied as a signal that describes the condition of prostate. In order to register the signal, the uroflowmeter was used. Patients were included in a two-step procedure. In the first step, an analysis of signal characteristics, such as maximum and the mean value with the use of Liverpool Nomogram, were performed. Then, the signal was tested for the presence of oscillation. For this purpose, an algorithm that generates the reference signal was created. Moreover, the similarity waveform was investigated with the help of the integral index. The diversity of signals indicated the presence of anomalies and had an impact on the final classification of the patient.

Keywords: uroflowmetry, urine flow, BPH diagnosis.

Introduction

The aim of this paper is to work out a numerical algorithm that realizes automatic classification of the urine flow speed characteristics. Such solution enables detecting oscillation in the urine flow, which may be a sign of the urinary tract disorders, e.g. benign prostatic hyperplasia (in the case of significant flow oscillations or the lack of the continuity of the characteristics). The methods which have been applied so far, e.g. Nomogram Liverpool, do not exploit information related to the urine flow characteristics. They are based on the analysis of the volume, average and maximum value of urination. The final diagnosis is formed by a doctor who analyses the shapes of time characteristics individually. The worked out algorithm will enable automate the screening tests process with the use of simple devices based on force transducers, such as uroflowmeters. They enable doing tests at a patient's home, and if the anomalies of the characteristics shape occur, the device will inform the user about the necessity of consulting the doctor. On the basis of the characteristics obtained from the machine, the doctor will be able to take decisions concerning further treatment. It should be stressed that the authors have never found any record of another solution concerning the urine flow curves classification with the use of a similar method. However, there are other solutions in terms of the urine flow charts identification based on neural networks [1].

Algorithm of the dynamic urine flow analysis

The urination is characterized by: the maximum and average flow rate, the urine volume, the time to maximum flow, the flow time and the time of urination [2–5]. Examples of the accurate and the impaired urination are shown in Fig. 1.

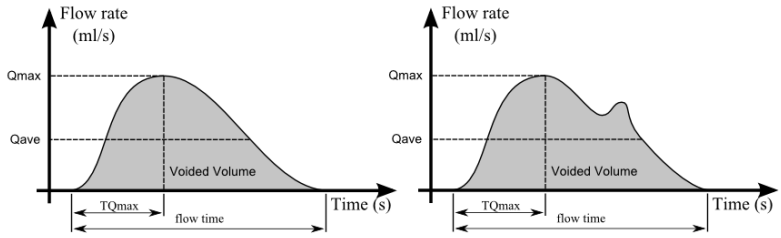

Fig. 1. The examples of urination patterns [6]

Nomograms considering the signal features such as maximum and average values are widely available in literature [7]. However, some anomalies of the flow (oscillations), not detected through the described parameters, can occur. They may indicate the occurrence of the disease and should be detected. In the further part of the study, a set of algorithms using nomograms, as well as the original idea for oscillations detection in the curve of the urination, are presented.

The described diagnostic algorithm worked in two steps. In the first one, the analysis of parameters such as the maximum and mean value, with the use of Liverpool Nomogram, was performed. The particular waveforms were replaced by the third and fourth order approximating polynomial and expressed by the following equation:

$$\begin{cases} \text{Average}_{90th} = -1.87\times10^{-10}\times V_v^4 + 2.92\times10^{-7}\times V_v^3 + 0.072\times V_v + 4.656 \\ \text{Average}_{10th} = 1.66\times10^{-8}\times V_v^4 - 1.77\times10^{-5}\times V_v^2 + 0.029\times V_v + 0.765 \end{cases}, \tag{1}$$

where: V_v – voided volume.

If the determined average flow rate was between Average_{90th} and Average_{10th}, the patient was considered to be within the normal range. An example of the nomogram is shown in Fig. 2.

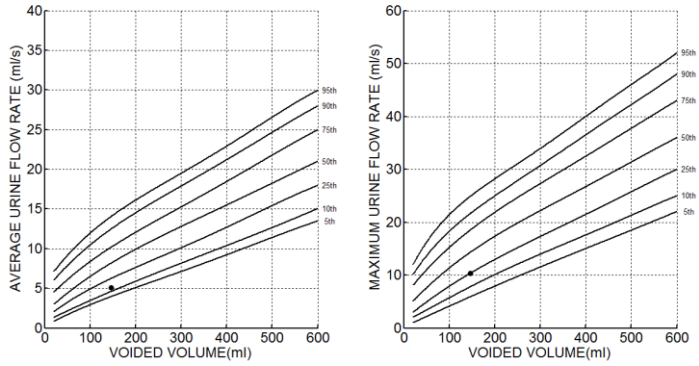

Fig. 2. Examples of generated nomograms

Then, a comparison between the generated reference signal with the urination signal was performed. The integral indicator described the similarity of signals and is expressed by the following equation:

$$J = \int_{t_0}^{t_k} |Y - Y_w|, \tag{2}$$

where: t_0 – the initial time, t_k – the final time, Y – signal value, Y_w – value pattern.

In order to generate the reference waveform, two third order Bézier curves [8] were used. The Bezier curve is generated dynamically for individual cases. It has the same time of achieving the maximum value, the same area under the curve, average and maximum value as the characteristics obtained during the urine flow tests.

The waveforms of the generated curves are presented in Fig. 3. On the left side, the Bézier curve is superimposed on the inaccurate waveform, while on the right side – the Bézier curve is within the normal range. For the first one, the coefficient value equalled $J = 79.55$, while for the second one – $J = 27.78$. The boundary coefficient value $J = 70.00$ was empirically established as considered to be abnormal.

Achieved results

The application of the first of the described methods resulted in classifying 18 of the 50 available waveforms of urination within the normal range. However, in this group of waveforms, oscillations occurred in 8 cases. The second of the described methods was characterized by high numerical cost and was used in 18 selected waveforms of urination. Furthermore, in this case, the application of the algorithm enabled detection 6 of 8 irregularities.

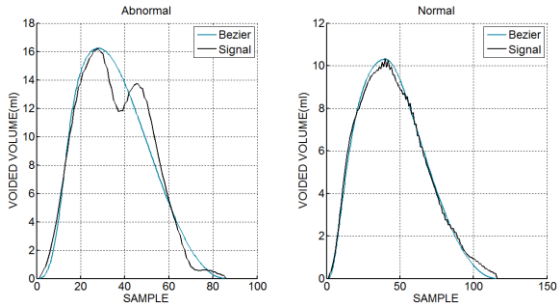

Fig. 3. The Bézier curves imposed on inaccurate and accurate waveforms

Conclusions

The aim of this paper was to present a method that can be applied in preliminary classification of the urine flow curves. It may be used in early diagnosis of e.g. prostatic hyperplasia. The worked out procedure of analyzing data from a uroflowmeter enables conducting an automatized classification of data that may indicate a urinary tract disorder.

It is worth underlying that application of the first method is insufficient for a definite diagnosis. In the group of patients considered to be healthy, waveforms with oscillations occurred as frequently as in 8 cases. Therefore, this method was not able to detect local anomalies. However, the application of the second method was characterized by high numerical cost, which considerably increased the efficiency of the algorithm in the detection of 6 inaccurate results out of 8 tests.

Undoubtedly, a diagnostic system should include at least two methods. In further study it is planned to replace the second method by a method using the wavelet transform.

Acknowledgements

The paper was prepared at Bialystok University of Technology within a framework of the S/WE/1/2013 and the MB/WE/4/2016 projects sponsored by Ministry of Science and Higher Education.

References

[1] Altunay, S., *et al*. 2006. Interpretation of uroflow graphs with artificial neural networks, in *Proceedings of IEEE Signal Processing and Communications Applications*, 16–19 April 2006, Antalya, Turkey. Piscataway: IEEE. http://dx.doi.org/10.1109/SIU.2006.1659698

[2] Marks, L. S.; Roehrborn, C. G.; Andriole, G. L. 2006. Prevention of benign prostatic hyperplasia disease, *Journal of Urology* 176(4): 1299–1306. http://dx.doi.org/10.1016/j.juro.2006.06.022

[3] Abrams, P. 1997. *Urodynamics*. London: Springer-Verlag. 339 p. http://dx.doi.org/10.1007/978-1-4471-3598-2

[4] Chapple, C. R.; Steers, W. D. [eds.] 2011. *Practical urology: essential principles and practice*, London: Springer. 569 p. http://dx.doi.org/10.1007/978-1-84882-034-0

[5] Walendziuk, W.; Idzkowski, A. 2009. Portable acquisition system for domiciliary uroflowmetry, *Journal of Vibroengineering* 11(3): 592–596.

[6] Suryawanshi, A.; Joshi, A. 2012. Urine flow rate measurement based on volumetric pressure measurement principle, in *Proceedings of 1st International Symposium on Physics and Technology of Sensors (ISPTS)*, March 7–10, 2012, Pune, India. Piscataway: IEEE, 334–337. http://dx.doi.org/10.1109/ispts.2012.6260961

[7] Haylen, B. T., *et al.* 1989. Maximum and average urine flow rates in normal male and female populations – the Liverpool nomograms, *British Journal of Urology* 64(1): 30–38. http://dx.doi.org/10.1111/j.1464-410X.1989.tb05518.x

[8] Prautzsch, H.; Boehm, W.; Paluszny, M. 2002. *Bézier and B-spline techniques*. Berlin Heidelberg: Springer-Verlag. 304 p. http://dx.doi.org/10.1007/978-3-662-04919-8

11TH INTERNATIONAL CONFERENCE
BIOMDLORE 2016
OCTOBER 20–22, 2016, DRUSKININKAI, LITHUANIA
BIOMDLORE.VGTU.LT

eISSN 2345-0630
ISBN 978-609-457-959-2
eISBN 978-609-457-958-5
DOI: 10.3846/biomdlore.2016.14

Relation between treatment duration and temperature factors in rheumatoid arthritis

Jolanta Pauk[1], Agnieszka Wasilewska[2], Justyna Chwiećko[3], Izabela Domysławska[4], Stanisław Sierakowski[5], Adam Idźkowski[6], Kristina Daunoravičienė[7], Julius Griškevičius[8]
[1, 2, 6] Bialystok University of Technology, Poland
[3, 4, 5] Bialystok Medical University, Poland
[7, 8] Vilnius Gediminas Technical University, Lithuania
E-mails: [1] *j.pauk@pb.edu.pl (corresponding author)*, [2] *a.wasilewska@doktoranci.pb.edu.pl*, [3] *chwiecko6@wp.pl*, [4] *izadomyslawska@o2.pl*, [5] *stanislaw.sierakowski@interia.pl*, [6] *a.idzkowski@pb.edu.pl*, [7] *kristina.daunoraviciene@vgtu.lt*, [8] *julius.griskevicius@vgtu.lt*

(Received 30 March 2016; accepted 28 April 2016)

Abstract. Introduction: Rheumatoid arthritis (RA) is a chronic autoimmune disease which results in the loss of joint function and several deformities. The aim of the study was to evaluate the influence of duration of the disease and prescribed treatment on the temperature of RA joints.
Methods: The evaluation was carried out on 30 patients with rheumatoid arthritis and 30 typical subjects as a control group. Thermograms were taken using thermograph camera.
Results: Statistically significant difference was found for ankle joint temperature between the group of patients treated for more than 10 years and healthy subjects.
Conclusions: The observations indicate that mean temperature of the skin above the ankle joint tends to decrease with rising duration of disease course. Progression of a RA leads to an erosive destruction in ankle joint in late stages of a disease.

Keywords: rheumatoid arthritis, thermovision, skin temperature.

Introduction

Rheumatoid arthritis is a chronic autoimmune disease which results in the loss of joint function and several deformities [1]. The duration of disease activity in RA patients is an important factor impacting joint destruction and functional disability [2]. Joint damage often begins within weeks or months after the onset of symptoms and is detectable on radiographs within 2 years [3]. There are now three main combinations that play substantial role: MTX+sulfasalazine (SSZ)+hydroxychloroquine, MTX+leflunomide (LEF), and MTX+biologics. Landewe et al. [4] administered the treatment combined of SSZ, MTX, prednisolone or SSZ monotherapy. Combination treatment during the 4–5 years presented greater decrease of sharp progression rate. Hetland et al. [5] described the therapy which include: MTX + cyclosporine + intra-articular glucocorticoid betamethasone. The authors report a delay to progression of erosions in patients at 2 years. Mottonen et al. [6] used a combination of DMARDs (SSZ, MTX, HCQ), and prednisolone or a single DMARD with or without prednisolone. Combination of 3 DMARDs for the first 2 years limits peripheral joint damage (Larsen scores) for at least 5 years. Smolen et al [7] estimated the effectiveness of the combination of INF + MTX and observed significant benefit with regard to the destructive process, clinically relevant improvement in physical function and quality of life. However, currently available techniques used for assessing treatment efficacy present limitations. For example, ultrasound is a highly user- dependent method and MRI requires administration of contrast agent and sedation in case of children [8]. Progressing inflammatory process in joints result in rise of the warmth of skin surfaces covering the joint and its temperature may be measured by non-invasive technique called thermovision. Thus, the aim of the study was to evaluate the influence of duration of the disease and administered treatment on the temperature of RA joints.

Methods

The evaluation was carried out on 15 patients of up to 10 years duration of RA, 15 patients with RA lasting more than 10 years and 30 typical subjects as a control group, aged between 44–80 years old. All the patients had RA diagnosis according to the standards of the American College of Rheumatology [9] and were free from any coexistent disease that could influence the outcome. None of the participants in the control group had a known health problem that would interfere with their performance. The patients were identified and selected at Medical University of Bialystok Hospital's Rheumatology Clinic, Poland. At the beginning of the procedure, one medical doctor conducted a questionnaire to gain basic data (age, height, weight) and DAS28 (disease activity score). Inclusion criteria for patients recruited for the study included: age above 18 years old, the duration of treatment above 1 year. Patients were excluded if they were under the age of 18 years, the duration of treatment under 1 year, rheumatoid factor below 50 IU/mL. The patients participated in the study with their consent, according to the declaration of Helsinki and the approval of the Ethical Committee. Thermograms were taken in a sitting subject position in room temperature of 23 deg. Centigrade. The thermographic camera (Thermo GEAR G100, NEC Avio) was used. Camera was placed perpendicularly to the scanned surface. Measurements were taken at the distance of 1.5 m from the subject. Pictures of both hands and feet were taken simultaneously. Computer software Statistica 12.5 (StatSoft, Tulsa, OK, USA)) was used for analysis.

Results

Comparison between patients undergoing biological treatment, patients without biologicals and typical subjects did not reveal any substantial difference ($p > 0.05$). However, the authors observed different joint temperatures for various durations of treatment. Statistically significant difference was found for ankle joint ($p < 0.05$). According to the observations the mean ankle joint temperature is significantly lower in RA > 10 years group compared with typical subjects (Tab. 1).

Table 1. The temperature [˚C] of selected parts of lower limbs

Joint	Group	Mean (SD)	Difference RA < 10 years vs. typical subjects	Difference RA > 10 years vs. typical subjects	Difference RA < 10 years vs. RA > 10 years
Metatarsophalangeal joints	RA < 10 years	30.3 (2.7)	0.4	–1.5	1.9
	RA > 10 years	28.4 (2.9)			
	Typical subjects	29.9 (1.7)			
Ankle joint	RA < 10 years	31.3 (1.7)	–0.2	–0.9*	0.7
	RA > 10 years	30.6 (0.6)			
	Typical subjects	31.5 (0.8)			

Note: * – statistically significance ($p < 0.05$)

Conclusions and discussion

Rheumatoid arthritis in its early stages tends to affect smaller joints, mostly the joints of hand, toes and feet. Progression of the disease may lead to the involvement of bigger joints: wrists, knees, ankles, elbows, hips and shoulders. Belt [10] used radiographs to estimate the relation between RA timing and destruction process of the ankle and subtalar joints. At the 15-year follow-

up the authors detected a total of 17 ankles with minor changes in 15 patients. At the 20-year follow-up nine ankles of seven patients presented major changes, and 12 ankles of 11 patients' minor changes. Major changes were described as ankles with marked erosions and/or destroyed joints with no joint space left. In current study the authors observed significantly lower joint temperatures in late stages of a disease (> 10 years duration) compared with healthy subjects. Rasmussen et al. demonstrate that degenerative process in joints can result in hypothermia [11]. Supporting this theory means we can consider our results consistent with observations made by Belt [10]. We provide two possible explanations of the results obtained in this study. Our theories assume that lower ankle joint temperature in late stages of RA can either be a result of long-term anti-rheumatic treatment or an advanced bone degeneration in the area of ankle joint. Joint temperature changes in different stages of RA can be observed with thermovision camera. Thus, apart from prevalent available methods such as radiography, thermovision should also be considered as diagnostic tool for assessing bone erosions.

References

[1] Cojocaru, M., *et al.* 2010. Extra-articular Manifestations in Rheumatoid Arthritis, *Maedica (Buchar)* 5(4): 286–291.

[2] Aletaha, D., *et al.* 2009. Rheumatoid arthritis joint progression in sustained remission is determined by disease activity levels preceding the period of radiographic assessment, *Arthritis & Rheumatology* 60(5): 1242–1249. http://dx.doi.org/10.1002/art.24433

[3] Plant, M. J., *et al.* 1998. Patterns of radiological progression in early rheumatoid arthritis: results of an 8 year prospective study, *Journal of Rheumatology* 25(3): 417–426.

[4] Landewe, R. B., *et al.* 2002. COBRA combination therapy in patients with early rheumatoid arthritis: long-term structural benefits of a brief intervention, *Arthritis & Rheumatology* 46(2): 347–356. http://dx.doi.org/10.1002/art.10083

[5] Hetland, M. L., *et al.* 2006. Combination treatment with methotrexate, cyclosporine, and intraarticular betamethasone compared with methotrexate and intraarticular betamethasone in early active rheumatoid arthritis: an investigator-initiated, multicenter, randomized, double-blind, parallel-group, placebo-controlled study, *Arthritis & Rheumatology* 54(5): 1401–1409. http://dx.doi.org/10.1002/art.21796

[6] Mottonen, T., *et al.* 1999. Comparison of combination therapy with single-drug therapy in early rheumatoid arthritis: a randomised trial. FIN-RACo trial group, *Lancet* 353(9164): 1568–1573. http://dx.doi.org/10.1016/S0140-6736(98)08513-4

[7] Smolen, J. S.; Han, C.; Bala, M. 2005. Evidence of radiographic benefit of treatment with infliximab plus methotrexate in rheumatoid arthritis patients who had no clinical improvement: a detailed subanalysis of data from the anti-tumor necrosis factor trial in rheumatoid arthritis with concomitant therapy study, *Arthritis & Rheumatology* 52(4): 1020–1030. http://dx.doi.org/10.1002/art.20982

[8] Spalding, S., *et al.* 2008. Three-dimensional and thermal surface imaging produces reliable measures of joint shape and temperature: a potential tool for quantifying arthritis, *Arthritis Research & Therapy* 10(1): 1–9. http://dx.doi.org/10.1186/ar2360

[9] Tepperman, S. P., Delvin, M. 1986. The therapeutic use of local heat and cold, *Canadian Family Physician* 32: 1110–1114.

[10] Belt, E. A.; Kaarela, K.; Lehto, M. U. K. 1998. Destruction and reconstruction of hand joints in rheumatoid arthritis. A 20-year follow-up study, *Journal of Rheumatology* 25(3): 459–461.

[11] Rasmussen, L. K.; Mercer, J. B. 2004. A comparison of thermal responses in hands and feet of young and elderly subjects in response to local cooling as determined by infrared imaging, *Thermology International* 14(2): 71–76.

11TH INTERNATIONAL CONFERENCE
BIOMDLORE 2016
OCTOBER 20–22, 2016, DRUSKININKAI, LITHUANIA
BIOMDLORE.VGTU.LT

eISSN 2345-0630
ISBN 978-609-457-959-2
eISBN 978-609-457-958-5
DOI: 10.3846/biomdlore.2016.15

AFM investigation of hyaline cartilage's surface destruction

Mikhail Ihnatouski[1], Dmitriy Karev[2], Boris Karev[3], Jolanta Pauk[4], Kristina Daunoravičienė[5]
[1] Yanka Kupala State University of Grodno, Belarus
[2] Grodno State Medical University, Belarus
[3] Grodno City Emergency Hospital, Belarus
[4] Bialystok University of Technology, Poland
[5] Vilnius Gediminas Technical University, Lithuania
E-mails: [1] *mii_by@mail.ru (corresponding author),* [2] *dmitriy.karev@gmail.com,* [3] *bkarev@gmail.com,* [4] *j.pauk@pb.edu.pl,* [5] *kristina.daunoraviciene@vgtu.lt*

(Received 30 March 2016; accepted 22 April 2016)

Abstract. Introduction: Osteoarthritis is a chronic, progressive disease. The aim of this paper is presenting the AFM investigation of cartilage in relation to the assessment of degenerative changes in the surface of hyaline cartilage. It can be useful in choosing the most effective methods of therapy.
Methods: Samples were taken from the cartilage surface of the femoral head after its removal during total hip arthroplasty. Images of the surface of the sample were obtained using an optical microscope equipped with a digital video camera, in the reflected light and by atomic force microscopy.
Results: The longitudinal orientation of the collagen fibers and sub-fibers beams on the surface, up to a diameter of 50 nm are identified in non-destroyed area sites.
Conclusions: Images of the destroyed areas displaying separately passing collagen fibers, strongly exposed to the surface: the size measured and found substructure.

Keywords: osteoarthritis, atomic force microscopy, hyaline cartilage.

Introduction

Osteoarthritis is a chronic, progressive disease which is characterized by an imbalance between the anabolic and catabolic processes in joint tissue [1]. Symptoms of osteoarthritis include the following: deep, achy joint pain exacerbated by extensive use, reduced range of motion and crepitus, frequently present, stiffness during rest [2]. The disease occurs in every third patient aged between 45 and 64 years and in 60–70% patients over 65 years. Osteoarthritis primarily affects weight-bearing joints, which considerably impairs the quality of life of patients during the initial stages of its development, and ultimately leads to a disablement. A wide range of drugs' classes are used to treat osteoarthritis, although there is a lack of detailed guidance because of the variable nature of the condition. Despite the large amount of experimental and clinical data, no single scheme in the treatment and prevention of osteoarthritis is provided. Atomic force microscopy (AFM) has been widely used in studying nanostructure and nanomechanical properties of cartilage [3, 4]. The aim of this paper is presenting the AFM of cartilage in relation to the assessment of degenerative changes in the surface of hyaline cartilage. It can be useful in choosing the most effective methods of therapy.

Methods

Tissue samples were taken from the cartilage surface of the femoral head after its removal during total hip arthroplasty were taken for nanostructure studies (Fig. 1a, b). Producing cartilage sample selection was based on initial visual inspection and evaluation of the degree of deformation of its surface was made. A sample intended for measurement was cut into a rectangular plate

having a size of ~ 10 × 5 mm^2. We tried to achieve flatness of platinum parties, protecting its edges so that they do not rise above its average level. The plate was fixed on a metal substrate. Images of the surface of the sample were obtained using an optical microscope "Micro 200 T-01", equipped with a digital video camera, in the reflected light. Study of examples surface morphology was performed using an AFM NT-206 (©ALC "Microtestmachines") in the static mode scan by a silicon cantilever 38 CSC. The processing and visualization was carried out by experimental software Surface Explorer (©ALC "Microtestmachines") and nanoImages (©RCRSP of A. V. Luikov HMTI of the NPreliminary studies of the cartilage, which allow to determine the extent of the fracture surface, the presence of large parts of the morphology and the presence of artefacts were performed using an optical microscope at a magnification 100×, 200×, 500× 1000×. These optical images are shown in Fig.1b-e. The picture has no significant damage to the cartilage area (Fig. 1e, f) obtained at magnifications 200× and 500×, you can find a variety of morphological objects, including rounded depressions ("gaps") in diameter from 3 to 16 microns; folds ("fibers") in width from 3 to 30 micrometers, laying in different directions; large surface protrusions. The area of the destroyed cartilage (Fig. 1d, f) obtained by increasing 200× and 1000×, morphology more monotonous. In addition to large surface protrusions, it is possible to consider displayed essentially in one-direction fibers. The fiber width is about 5 microns. The dry substance of cartilage should contain from 50 to 70% collagen and orientation of fibers is determined by the direction of lines of force arising from the deformation of the cartilage in the operation.

Results

Preliminary studies of the cartilage, which allow to determine the extent of the fracture surface, the presence of large parts of the morphology and the presence of artefacts were performed using an optical microscope at a magnification 100×, 200×, 500× 1000×. These optical images are shown in Fig. 1b–e. The picture has no significant damage to the cartilage area (Fig. 1e, f) obtained at magnifications 200× and 500×, you can find a variety of morphological objects, including rounded depressions ("gaps") in diameter from 3 to 16 microns; folds ("fibers") in width from 3 to 30 micrometers, laying in different directions; large surface protrusions. The area of the destroyed cartilage (Fig. 1d, f) obtained by increasing 200× and 1000×, morphology more monotonous. In addition to large surface protrusions, it is possible to consider displayed essentially in one-direction fibers. The fiber width is about 5 microns. The dry substance of cartilage should contain from 50 to 70% collagen and orientation of fibers is determined by the direction of lines of force arising from the deformation of the cartilage in the operation.

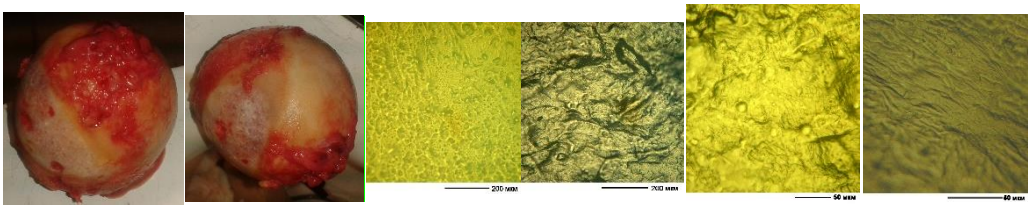

a) b) c) d) e) f)

Fig. 1. Optical image: a) and b) of the femoral head with strong destructions and with whole cartilaginous surfaces; c) and d) of the surface is not destroyed cartilage with increasing 200× and 500×; d) and e) of the surface is destroyed – 200× and 1000×

The AFM images of the surface of the cartilage not destroyed are presented in Fig. 2. Thus, it can be assumed that Fig. 2f displays a layer of one direction orientated fibers, exposed as a result of wear of the cartilage of the outer layers. Fig. 2b shows the three-dimensional AFM image obtained with a relatively small magnification, the size of the surface area of the cartilage

15×15 μm^2 with a maximum height difference of up to 1 micron. Irregularities of three cylindrical shapes are detected on the surface, which can be regarded as fiber. Cylinder axes are approximately parallel. The diameters of the fibers – about 4 microns. The complex structure of each fiber can be clearly observed. However, Fig. 2d shows a two-dimensional AFM images obtained at high magnification, the surface of the cartilage portion size 2×2 μm^2 with a maximum height difference of up to 300 nm.

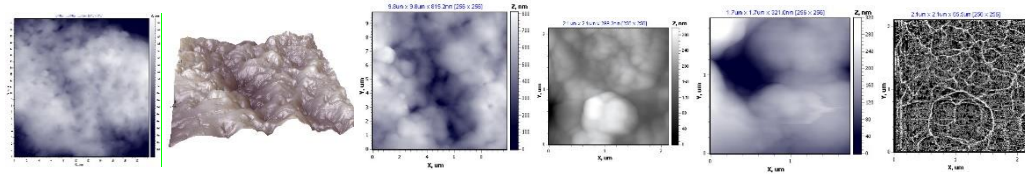

a) b) c) d) e) f)

Fig. 2. AFM images of the surface of the cartilage not destroyed: a) 21×21; b) 15×15; c) 10×10; d) 2,1×2,1; e) 1,5×1,5 and f) filtered images 2,1×2,1 μm^2

It can be achieved a digital resolution up to 8 nm/pix with such aperture in the lateral plane. In the AFM image can be considered a complex fiber structure in detail. Laplace filter 3×3 has been applied for AFM images processing, contrasting gradient "gray" (Fig. 2f). Due to apply filters on a segmented AFM image clearly visible boundaries between the individual "sub-fibers" typical diameters range from 50 to 350 nm. Interposition of sub-fibers and the presence of gaps between them are shown in Figure 2e with aperture 1.5×1.5 μm^2. The AFM images of the surface of the cartilage destruction are presented in Fig. 3. A two-dimensional AFM image obtained by increasing the average, the size of the surface area of the cartilage in 7×7 μm^2 with a maximum height difference of up to 2.5 microns is presented in Fig 3a. On the current image, scanning line intersecting the separate fiber lies about 3 microns wide. Likewise, the Fig. 3c shows three-dimensional AFM image of the surface of the heavily damaged area of cartilage the size 18×18 μm^2 with a maximum height difference of more than 2 microns. Almost half of the image (right end) has a level lower than the attitude of the measuring sensitivity of the device and presented at the AFM image in a monochromatic black field. The left edge in the image is occupied by two fibers having a developed surface structure (roughness). Fibers are directed along the diagonal of the image. Fig. 3b, e, f show profilograms' attitude measured along the scan line. On the left side in the Fig. 3d, e fiber's deformation can be seen, indicated by the arrow.

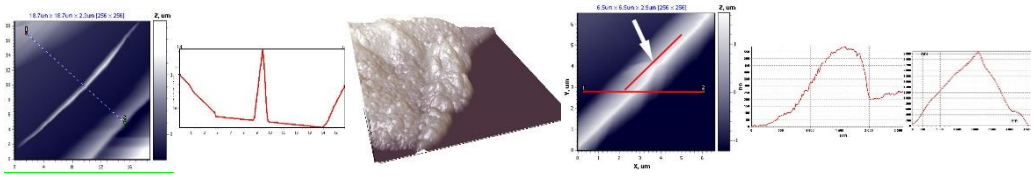

a) b) c) d) e) f)

Fig. 3. AFM images of the surface of the cartilage destruction: a) 18,2×18,2 mm^2; b) the profile of 13 microns, 1.8 nm; c) 16×16 μm^2; d) 6,4×6,4 μm^2; e) profile of 2.2 μm, 580 nm, and f) the profile of 3.5 μm, 2500 nm

Conclusions

Tissue samples during total hip arthroplasty were taken for elements of degradation of hyaline cartilage studies. Surface cartilage structures were detected by AFM. It is shown that the

pathological destruction of cartilage leads to the impoverishment of a set of morphological elements its surface.

References

[1] Loeser, R. F. 2010. Age-related changes in the musculoskeletal system and the development of osteoarthritis, *Clinics in Geriatric Medicine* 26(3): 371–386. http://dx.doi.org/10.1016/j.cger.2010.03.002

[2] Dieppe, P. 2010. Development in osteoarthritis, *Rheumatology* 50(2): 245–247. http://dx.doi.org/10.1093/rheumatology/keq373

[3] Wilusz, R. E. 2012. Immunofluorescence-guided atomic force microscopy to measure the micromechanical properties of the pericellular matrix of porcine articular cartilage, *Journal of The Royal Society Interface* 9(76): 2997–3007. http://dx.doi.org/10.1098/rsif.2012.0314

[4] Zhu, P.; Fang, M. 2012. Nano-morphology of cartilage in hydrated and dehydrated conditions revealed by atomic force microscopy, *Journal of Physical Chemistry & Biophysics* 2: 106. http://dx.doi.org/10.4172/2161-0398.1000106

11TH INTERNATIONAL CONFERENCE
BIOMDLORE 2016
OCTOBER 20–22, 2016, DRUSKININKAI, LITHUANIA
BIOMDLORE.VGTU.LT

eISSN 2345-0630
ISBN 978-609-457-959-2
eISBN 978-609-457-958-5
DOI: 10.3846/biomdlore.2016.16

Biomechanical analysis of the cancellous screws implantation schemes in surgical treatment of flexible flatfoot in children

Gennadiy Koshman[1], Vladimir Barsukov[2], Viktor Anosov[3], Jolanta Pauk[4]
[1, 3] Grodno State Medical University, Belarus
[2] Yanka Kupala State University of Grodno, Belarus
[4] Bialystok University of Technology, Poland
E-mails: [1] *genkoshman@gmail.com*, [2] *v.g.barsukov@grsu.by*, [3] *aviktor8@gmail.com (corresponding author)*, [4] *j.pauk@pb.edu.pl*

(Received 30 March 2016; accepted 22 April 2016)

Abstract. Carry out comparative biomechanical analysis of influence of the implantation scheme and characteristic sizes of cancellous screws on parameters of its strained condition, and elaborate guidelines for optimization of implantation parameters and decision for a material metalware choice. Performed mathematical modelling and comparative numerical analysis of the parameters of strained condition, slant and cantilevered schemes of implantation of cancellous screws, applied to a wide range of support loads variations acting on a screw. Made analysis of influence of size parameters (length of the overhanging part, angle with normal at supporting surface, core diameter) on the magnitude of the calculated stress that appear in compressed and extended zones of slant implanted screw. Carried out investigations reveal that short screws, installed on the hard circuit, from the standpoint of operational reliability according to the criteria of strength under static loading (occasional overload) and multicyclic loading have the highest capacity for work. Least favourable in application are slant and cantilevered implanted screws. With increasing length of cantilevered part and angle between axis of a screw and line of loading force calculated values of stress also increases. Screws of heat-treated stainless steel are preferred from the standpoint of saving bearing capacity with unit congestion due to increased plasticity in 4–5 times (residual strain at failure) compared with titanium alloys.

Keywords: cancellous screw, biomechanical analysis, strain, strength, flatfoot.

Introduction

Flatfoot is one of the most common reason orthopaedic consultation of children [1]. So far, the problem of conservative and surgical treatment of flexible flatfoot is not completely solved [2]. It offers a variety of methods of surgical correction, but none of them is not a panacea. Among commonly used in paediatric orthopaedics are methods based on blocking excessive pronation of the subtalar joint by setting foot in the tarsal sinus metal, plastic and biodegradable implants [3]. However, there is limitation of physiological motion of the subtalar joint and often develop post-operative complications in the form of avascular necrosis of the talus, fracture of the talus and calcaneus, tarsal sinus syndrome, the formation of cysts and migration of the implant [4]. The technically simplest in execution, more physiological and less dangerous from the standpoint of post-operative complications is biomechanical scheme based on the cancellous screws implanted in the lateral process of the talus body [5]. However, many questions related to the implantation and operation of the screws have not been studied. There are no clear scientific recommendations on the choice of material of screws (stainless steel or titanium alloy) and dimensional parameters of implant (length of the working part, the angle of cancellous screws to the supporting surface of the bone).

Methods

Surgical correction of deformation is generally carried out simultaneously on both feet. The intervention is made through approach of up to 1 cm for skin fold above the level of the tarsal sinus 1 cm anteriorly and downward from the outer ankle. Further by the awl (4 mm diameter) formed the channel in the distal part of anterior surface of the lateral process of the talus. The channel is formed in an oblique direction from bottom to top, front and back, outside-in at an angle of 40±5° in the coronal plane and 30±5° in the sagittal. The direction of the channel should be such that the screw head lay on the upper part of the anterior process of the calcaneus, thereby creating a restriction of excessive pronation of the subtalar joint. The foot during implantation of cancellous screw held in supination, then we estimated volume of supination-pronation movements in the subtalar joint. The degree of correction is determined by the value of immersion of the screw – if the working part of the screw is long, the longitudinal arch of the foot is more high. Final assessment of the screw position makes by X-ray examination [5].

A general view of the most commonly used screws is shown in Figure 1, the characteristic size – in Table 1, the mechanical properties in Table 2.

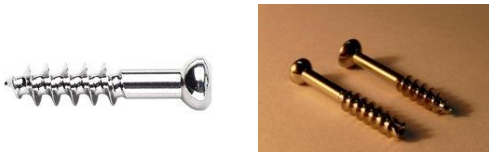

a b

Fig. 1. Steel (a) titanium and (b) a cancellous screws used to block excessive pronation of the subtalar joint

Table 1. The typical size of cancellous screws

Overall length of the screw, mm	Length of the thread part, mm	The diameter of the rod in the threaded part, mm	The diameter of the rod in the non-threaded part, mm	The diameter of the thread, mm
25	12	2.3	4.0	4.0
30	15	2.3	4.0	4.0
35	17	2.3	4.0	4.0
30	15	3.0	4.5	6.5
35	17	3.0	4.5	6.5

Table 2. The mechanical properties of the materials used for the manufacture of cancellous screws [6, 7]

The name and designation of the material	Strength limit, MPa	Yield point, MPa	Relative elongation at break, %
Corrosion-resistant steel (wrought stainless steel) heat-treated ISO 5832-1-2010*	490–690	190	40
Corrosion-resistant steel (wrought stainless steel) cold-deformed ISO 5832-1-2010	860–1100	690	12
Titanium alloy Ti6AL4V ISO 5832-3	860	780	8–10

Note: * – the heat treatment method selects a manufacturer to achieve the desired properties

Theoretically there are three possible installation schemes cancellous screws: thrust (Fig. 2a), inclined (Fig. 2b) and console (Fig. 2c).

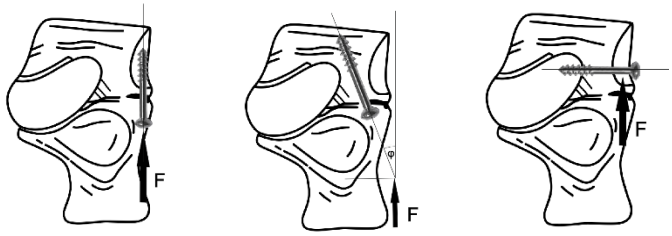

a b c

Fig. 2. Installation schemes of cancellous screws: a – thrust; b – inclined; c – console

When installing in the thrust scheme force F occurring in the reference area of contact with the bone screw directed along the screw axis, in console – perpendicular to the axis and inclined at – φ at an angle there to.

As a basis for calculations take inclined installation scheme screws because of it in the form of special cases you can get a thrust (φ = 0), and a console (φ = π/2) schemes. This takes into account that the supporting force F acts on the spherical bearing surface of the screw head (Fig. 3).

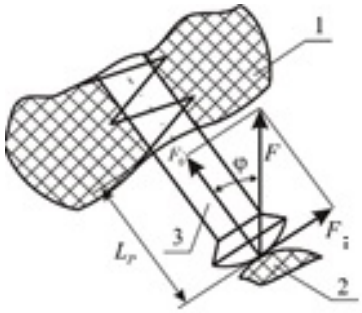

Fig. 3. Estimated biomechanical loading scheme obliquely set spongy screws: 1 – lateral process of the talus; 2 – calcaneus; 3 – cancellous screw

For ease of analysis we expand the force F into two components-compressive axial directed along F_0 screw axis and perpendicular to the axis of the bending force F_i. In this axial force F_0 may be expressed by the reference F_i, and the angle φ by using the following relationship

$$F_0 = F\cos\varphi. \tag{1a}$$

And bending force F_i as:

$$F_i = F\sin\varphi. \tag{1b}$$

Compression stress in the screw σ_c:

$$\sigma_c = \frac{4F_0}{\pi d^2} = \frac{4F\cos\varphi}{\pi d^2}, \tag{2}$$

where d – the diameter of the rod threaded part of the screw.

Bending moment M form force F_i:

$$M = F_i \cdot L_p = F \cdot L_p \sin\varphi, \tag{3}$$

where L_p – effective length of console part of the screw.

Bending stress σ_b:

$$\sigma_b = \frac{32M}{\pi d^3} = \frac{32FL_p \sin\varphi}{\pi d^3}. \tag{4}$$

Since the bending stresses are tensile in the same zone (the lower fiber) and compression in the other zone (upper fibers), then separately calculate the total tension in stretched and compressed parts as the sum or difference of bending stress and compression. The total compressive stress forces $\sigma_{c\Sigma}$ will be equal the sum of the stress of the longitudinal force F_0 and bending moment M:

$$\sigma_{c\Sigma} = \sigma_i + \sigma_c = \frac{4F}{\pi d^2}\left(8\frac{L_p}{d}\sin\varphi + \cos\varphi\right). \tag{5}$$

The maximum tensile stresses are the strain difference of the bending moment M and longitudinal force F_0:

$$\sigma_{p\Sigma} = \sigma_i - \sigma_c = \frac{4F}{\pi d^2}\left(8\frac{L_p}{d}\sin\varphi - \cos\varphi\right). \tag{6}$$

Formulae (5) – (6) are characteristic of the static loading of smooth rods. For estimating decrease strength properties of the screw when walking can act as a first approximation the stress concentration factor K_σ which shows how many times the limit of a smooth rod of endurance more than the endurance limit of the rod with the concentrator (in this case with the thread). Thereby perform a comparative biomechanical analysis of the impact of dimensional parameters of implanted screws on the indicators of the state of stress is possible in the form of a relative.

Results

Thrust scheme. Taking into (2), (4) and (6) $\varphi = 0$, receive $\sigma_i = 0$, $\sigma_c = \sigma_{c\Sigma}$. The range of change of the reference force F depends on the weight of a person, walking conditions and etc. Therefore, we will for the estimated settlement as a possible range F = 25–250 N.

Table 3. Estimated value of the nominal compressive stresses in the rod screw at the persistent installation diagram

Diameter of the rod in threaded part, mm	The value of stress σ_c (MPa) with force F (N)					
	25	50	100	150	200	250
Ø2,3	6,02	12,04	24,08	36,12	48,16	60,20
Ø3,0	3,53	7,06	14,16	21,25	28,33	35,41
Ø4,0	1,99	3,98	7,96	11,94	15,92	19,89
Ø4,5	1,57	3,14	6,29	9,43	12,58	15,72

From a comparison of the data with indicators of the strength of the used materials (Table 2) we can see that in considered range of loads in thrust scheme resulting stress loads is much less dangerous.

Console scheme. Taking into (2), (4) and (6) $\varphi = \pi/2$, receive $\sigma_c = 0$. Main result that in console scheme according cancellous screws to the calculated stress in the investigated range of sizes 45–62 times larger than the thrust scheme and do not provide the necessary high load strength.

Inclined scheme. Obtained data shows that with increasing angle φ from 0° to 90° values to compression and tensile stress increase many times, which is unfavourable from the standpoint of strength both in single overload and during multicyclic loading.

Conclusions

The complex of the research methods showed that from the standpoint of operational reliability according to the criteria of strength under static loading (occasional overload) and multicyclic loading highest workability characterized by short screws installed on the thrust scheme. The least favourable in the application are console and inclined set screws, and with an increase in the length of the arm portion and the angle between the line of action of the support efforts and screw axis of the calculated values of the stresses increase. Screws from heat-treated stainless steel are preferred from the standpoint of preserving the bearing capacity at single overload due to increased plasticity 4–5 times (residual strain at fracture) compared with titanium alloys.

References

[1] Jordan, K. P., *et al.* 2010. Annual consultation prevalence of regional musculoskeletal problems in primary care: an observational study, *BMC Musculoskeletal Disorders* 11(144): 1–10. http://dx.doi.org/10.1186/1471-2474-11-144

[2] Sviridenok, A. I.; Lashkovskij, V. V. 2009. *Biomechanics and correction dysfunctions of feet*. Grodno: GSMU. 279 p.

[3] Tamoev, S. K., et al. 2011. Subtalar arthroereisis in dysfunction posterior tibial tendon dysfunction, *Vestnik Travmatologii i Ortopedii im. N. N. Priorova*, 1: 54–58.

[4] Corpuz, M., et al. 2012. Fracture of the talus as a complication of subtalar arthroereisis, *Journal of Foot and Ankle Surgery* 51(1): 91–94. http://dx.doi.org/10.1053/j.jfas.2011.08.008

[5] Koshman, G. A., *et al.* 2011. *Corrective lateral arthrorisis of subtalar joint in treatment flexible flatfoot in children*. Grodno.

[6] *GOST R ISO 5832-1-2010 Implants for surgery. Metallic materials. Part 1: Wrought stainless steel*. Moscow, 2010. 12 p.

[7] *GOST R ISO 5832-3-2014 Implants for surgery. Metallic materials. Part 3: Wrought titanium 6-aluminium 4-vanadium alloy.* Moscow, 2014. 2 p.

11TH INTERNATIONAL CONFERENCE
BIOMDLORE 2016
OCTOBER 20–22, 2016, DRUSKININKAI, LITHUANIA
BIOMDLORE.VGTU.LT

eISSN 2345-0630
ISBN 978-609-457-959-2
eISBN 978-609-457-958-5
DOI: 10.3846/biomdlore.2016.17

Influence of dance therapy on the Parkinson's disease affected upper limb biomechanics

Donatas Lukšys[1], Dalius Jatužis[2], Rūta Kaladytė-Lokominienė[3], Ramunė Bunevičiūtė[4], Gabrielė Mickutė[5], Alvydas Juocevičius[6], Julius Griškevičius[7]
[1, 7] Vilnius Gediminas Technical University, Lithuania
[2, 3, 4] Clinics of Neurology and Neurosurgery of Vilnius University Hospital Santariškių Klinikos, Lithuania
[5, 6] Centre of Rehabilitation and Physiotherapy of Vilnius University Hospital Santariškių Klinikos, Lithuania
E-mails: [1] *donatas.luksys@vgtu.lt (corresponding author)*, [2] *dalius.jatuzis@santa.lt*, [3] *ruta.kaladyte-lokominiene@santa.lt*, [4] *ramune.buneviciute@santa.lt*, [5] *gabriele.mickute@santa.lt*, [6] *alvydas.juocevicius@santa.lt*, [7] *julius.griskevicius@vgtu.lt*

(Received 1 April 2016; accepted 18 May 2016)

Abstract. In this paper we investigate influence of the dance (lindy hop) therapy on the Parkinson's disease affected upper limb biomechanics. Wireless inertial sensors were used to measure acceleration and angular velocity during multi-joint movements of both upper limbs. In this research only wrist's pronation-supination movements in sagittal plane were analysed. Obtained results shows that dance therapy has a positive influence on improved biomechanics of upper limbs and general decrease of UPDRS score.

Keywords: Parkinson's disease, wireless inertial sensors, dance, upper limb.

Introduction

Parkinson's disease (PD) is neurodegenerative disorder, which affects part of central nervous system (CNS), which is responsible for the control of voluntary movements. It is second most common neurological disorder in Europe [1]. PD is characterized by resting tremor, bradykinesia, rigidity and postural instability. Patients with PD are applicable to various types of physical activity programs that improve motor function. Dance movement therapy is one of the possible activity programs and for patients with PD is among the most popular therapy programs [2], like tango dance, for example [3]. Dance therapy has a positive effect on psychologically and emotionally than regular exercise. Effect of dance therapy is usually evaluated using various scales. One of the most commonly applied is Unified Parkinson's Disease Rating scale (UPDRS), which allows estimate of motor and non – motor symptoms. For the quantitative assessment of the dance, various motion capture systems are used [4]. There are different temporal parameters that allow evaluating the movement. For example, acceleration zero crossing rate calculation performed for detecting the activities of daily living [5]. Average acceleration during the pronation-supination movement is calculated for UPDRS evaluation [6] or average movement time of rapid alternating movement [7].

Goal of this research is quantitatively evaluate therapeutic effect of dance therapy on the biomechanics of the upper limb using inertial sensors.

Methods

In cooperation with Vilnius University Hospital Santariškių Klinikos neurology and rehabilitation, physical and sports centres, 14 patients (mean age ± SD = 65.43±9.41, mean UPDRS score ± SD = 47.8571±17.6890) with PD (average stage of disease ± SD = 2.0714±0.6157) have been recruited for the modified lindy hop dance therapy. Comparing to other dance types, lindy hop dance was chosen, because this dance training is the simplest one. In total, subjects have had 22 dance lessons. Before each lesson 15 minutes of moderate exercise was performed and then 45 minutes of dancing.

Six wireless inertial sensors (Shimmer, Dublin) having nine degrees of freedom (acceleration, angular velocity and magnetic heading in 3D) were attached to each patient's hand, forearm and arm. Sensors recorded data at 51.2 Hz sampling rate, which is sufficient to measure the movement. Each subject was asked to perform pronation-supination motion task.

MATLAB software was used for the calculation and analysis of wrist pronation – supination movement using following metrics: acceleration zero crossing rate and average acceleration about *y-axis*, average movement time. Statistical analysis of the metrics was performed using IMB's SPSS v22 software. A paired-samples t-test with significance level of $\alpha = 0.05$ was used to compare calculation parameters before and after the dance therapy. The block diagram in figure 1 shows the general scheme of experiment and analysis.

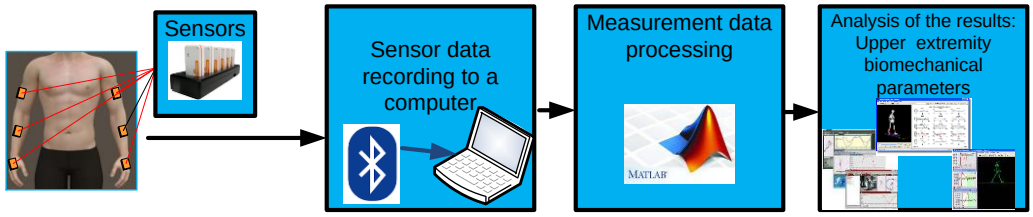

Fig. 1. Upper extremity motor biomechanics evaluation setup

Results

Calculation parameters are presented in Table 1. When analysing wrist pronation-supination movement, we found statistically significant difference of the right, left wrist average acceleration zero crossing rate, average movement time and average acceleration of the left wrist (bold values in the Table 1).

Table 1. Calculated parameters

Parameters / Joints	Acceleration zero crossing rate	Average acceleration (m/s^2)	Movement average time, s
Right shoulder	0.075±0.020*	0.412±0.411 *	0.897±0.209*
	0.076±0.012**	0.375±0.246 **	0.790±0.097**
Right elbow	0.057±0.013*	1.076±0.584 *	0.917±0.194*
	0.059±0.008**	0.743±0.536 **	0.791±0.133**
Right wrist	**0.064±0.013***	1.518±0.835 *	**0.903±0.188***
	0.070±0.010**	1.144±0.534 **	**0.792±0.131****
Left shoulder	0.083±0.014*	0.859±0.429 *	0.926±0.237*
	0.083±0.014**	0.315±0.211 **	0.756±0.119**
Left elbow	0.056±0.010*	0.859±0.611 *	0.912±0.226*
	0.064±0.008**	0.698±0.3564**	0.800±0.129 **
Left wrist	**0.061±0.016***	**1.703±1.104** *	**0.933±0.234***
	0.076±0.009**	**1.064±0.514****	**0.808±0.110** **

Note: * – before (mean ± SD), ** – after (mean ± SD)

Conclusions

Comparing data before and after therapy program can be noted that dance therapy affects the upper limb movements. Zero crossing rate of the right wrist increases (0.0636±0.0130 to 0.0701±0.0104), and left wrist (0.0608±0.0168 to 0.0766±0.0091). Average acceleration values decrease in the left wrist (1.7030±1.1043 to 1.0640±0.5141). Movement average time right wrist

decrease (of 0.9038±0.1884 to 0.7927±0.1310) and left wrist decrease (of 0.9331±0.2348 to 0.8082±0.1107). UPDRS score changed from 47.8571±17.6890 to 40±13.8119 after the dance therapy program. It can be said that the influence of dance for people with Parkinson's disease have a positive impact on upper limb biomechanics.

References

[1] de Dreu, M. J.; Kwakkel, G.; van Wegen, E. E. H. 2015. Partnered dancing to improve mobility for people with Parkinson's disease, *Frontiers in Neuroscience* 9: 444. http://dx.doi.org/10.3389/fnins.2015.00444

[2] Chase, M. 2004. *Marian Chace, her papers.* Columbia: American Dance Therapy Association. 261 p.

[3] Hackney, M. E.; Earhart, G. M. 2009. Effects of dance on movement control in Parkinson's disease: a comparison of Argentine tango and American ballroom, *Journal of Rehabilitation Medicine* 41(6): 475–481. http://dx.doi.org/10.2340/16501977-0362

[4] Hackney, M. E.; Earhart, G. M. 2010. Effects of dance on balance and gait in severe Parkinson disease: a case study, *Disability and Rehabilitation* 32(8): 679–684. http://dx.doi.org/10.3109/09638280903247905

[5] Olivares, A., *et al.* 2012. Detection of (in)activity periods in human body motion using inertial sensors: a comparative study, *Sensors 12*(5): 5791–5814. http://dx.doi.org/10.3390/s120505791

[6] Kaneko, M., *et al.* 2014. The comparison of pronation and supination between typically developing children and children with ADHD, *Proceedings of the International MultiConference of Engineers and Computer Scientists IMECS 2014*, March 12–14, 2014, Hong Kong, China. Hong Kong: Newswood Limited, 144–149.

[7] Soukoreff, R. W.; Zhao, J.; Ren, X. 2011. The entropy of a rapid aimed movement: Fitts' index of difficulty versus Shannon's entropy, in *Proceedings of 13th International Conference "Human Computer Interaction – INTERACT 2011"*. September 5–9, 2011, Lisbon, Portugal. Berlin Heidelberg: Springer, 222–239. http://dx.doi.org/10.1007/978-3-642-23768-3_19

11TH INTERNATIONAL CONFERENCE
BIOMDLORE 2016
OCTOBER 20–22, 2016, DRUSKININKAI, LITHUANIA
BIOMDLORE.VGTU.LT

eISSN 2345-0630
ISBN 978-609-457-959-2
eISBN 978-609-457-958-5
DOI: 10.3846/biomdlore.2016.18

Geometry and mechanical function of multijoint extremities from mammals to insects: towards biomimetic design of robotic arm

Oleg Denisov[1], Natalya Kizilova[2, 3]
[1] Kharkov National University, Ukraine
[2] Warsaw University of Technology, Poland
[3] Vilnius Gediminas Technical University, Lithuania
E-mails: [1] *biomech@bk.ru*, [2] *n.kizilova@gmail.com (corresponding author)*

(Received 26 April 2016; accepted 19 August 2016)

Abstract. Biomechanics of legs of different families of insects is studied. Geometry of different pairs of legs designed for walking, running, swimming, digging and other tasks has been measured on entomological collections. Relationships between the lengths of three main segments (femur, tibia, tarsus) as well as their smaller segments (if any) have been studied. It is shown the cursorial and fossorial legs satisfy the same nondimentional relationships in the insects of different size, habitat and evolutionary age, while the saltatorial, nanatorial and raptoridal legs possess different types of relations. Application of the nature inspired design to engineered macro and micro manipulators and robotic systems is discussed.

Keywords: movements of insects, biomechanics of leg, robotics, biomimetic design.

Introduction

Extremities of animals and human beings are designed as multijoint systems that allows their biomechanical functions like walking, running, jumping or crawling, digging, grasping, manipulation, etc. The number of joints vary from three (shoulder, forearm, hand or hip, shank, foot) in human beings, mammals, etc. to six segments in mites and some other insects. Relationships between the lengths of the segments of human arms, legs and palms have been described by Leonardo da Vinci. For instance, the relative lengths of the human palm segments correspond to the Fibonacci numbers 1, 2, 3, 5, 8 that provides optimal folding in fist according to the Archimedes spiral that allows holding and manipulating of tools.

Dimensionless relations between the segments of insect legs have been studied in connection with insect flight [2] and jumping of fleas, froghoppers and grasshoppers [3, 4], while comparative study of kinematics of the specialized and walking/running legs has not been carried out jet. In this paper the correspondence of design of the extremities (legs) of different families of insects to the optimal multijoint structures is studied accounting for different mechanical abilities of the legs. Such investigations are important for development of multipurpose nature inspired robotic arms.

Methods

Entomology collections of insects as well as high resolution photos collected in open source museums including the museums of fossils have been studied. The lengths of segments of 3 or 4 pairs of legs depending on the family (Fig. 1a, b) have been measured using freeware image measurement software (ImageJ 1.50i, National Institutes of Health USA ©). In total 21 families of 20 insects in each group have been studied. The measurement data have been used for numerical computations (Excel 2003) of the double ratio value:

$$W_j = \frac{\left(s_{j-1} + s_j\right)\left(s_j + s_{j+1}\right)}{s_j\left(s_{j-1} + s_j + s_{j+1}\right)}, \tag{1}$$

for each three consequent segments s_{j-1}, s_j, s_{j+1} of each leg. In that way, n-joint leg is characterized by n – 2 values W. The results have been compared to the double ratio value computed for the Fibonacci series $\{F_j\}_{j=1}^{\infty}$ [1]:

$$W_F = \lim_{j\to\infty} \frac{(F_{j-1}+F_j)(F_j+F_{j+1})}{F_j(F_{j-1}+F_j+F_{j+1})} \approx 1.31.$$

The results have been separated for different families as well as for the pairs of legs with different functions. Mostly one pair is specified on the function proper to the family while others are used for motion. The insects digging holes, catching preys, gathering food have the first (fore) pair of specialized legs; while the jumping insects and some gathering ones have the last (hind) pair specialized. Besides the fore/hind pairs are also used for eye/wings cleaning and, therefore, used as manipulators.

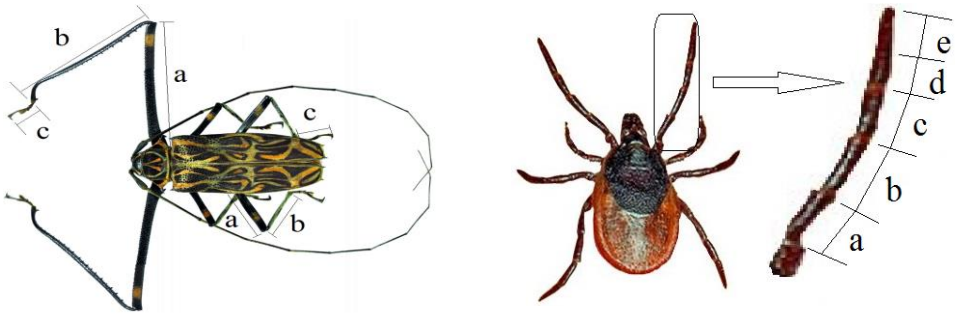

a b

Fig. 1. Three segment (a) and five segment (b) insect legs

Results

Some results summarized on different types of legs and families are presented in Fig. 2. The computed parameters have been averaged over each group. The upper and lower straight lines correspond to the Golden mean ratio 62/38 ~ 1.63 and W_F ~ 1.31.

Contrary to human and mammal arms and palms, the adjacent segments a–b–c (femur, tibia, tarsus) are not related as the Fibonacci numbers. The relations between a and b, as well as between b and c do not correspond to the Golden ratio which is proper to many optimal biomechanical systems. The only exception is the relation between the tibia and tarsus of the gathering hind legs of bees (Fig. 2). Nevertheless, most of the legs are characterized by $W \sim W_F$.

The most optimal in the meaning of the W criteria confirmed on the manipulating arms of mammals and humans, are the running and walking legs (deviations are 0.5% and 0.7% accordingly). The digging and gathering legs have the deviations of 2.8% and 4.4% that can be considered as minor differences. The grasping and jumping legs differ from the W_F design by 11% and 12.3% accordingly, which is also not large for the biological data. The swimming hands have special design defined by W values which are in 27% higher than the W_F value. In the most cases the segments are designed in the way allowing perfect folding of the leg into a chain (for the case presented in Fig. 1a) or spiral (Fig. 1b).

The lengths of the segments corresponded to the measurement data averaged over the family. The moments of forces m_j produced in the joints have been accepted to be proportional to the lengths l_j of the corresponding segments. Dynamics of folding of the leg when the beginning of the first segment a (shoulder) is fixed and the end of the last segment c or e (tips of the claws) reaches the shoulder. As optimization criteria, the energy E_m spent for the movement and the

operational time t_0 have been considered. The optimal Pareto solutions have been obtained for each case. The results are presented in Fig. 3 in dimensionless form. It was shown, the relations l_{j-1} / l_j and l_j / l_{j+1} are mostly far from 62/38 (red line in Fig. 2), but close to W_F value (blue line in Fig. 2).

The walking and running legs were found the most optimal in the meaning of the pair of criteria (E_m, t_0) (Fig. 3). The digging legs are the slowest in performance but optimal for energy consumption. The jumping legs are the fastest but energy consuming. In some areas the families of frontiers are located very close that means optimal performance for different types of action like digging and swimming and running, gathering and grasping (Fig. 3).

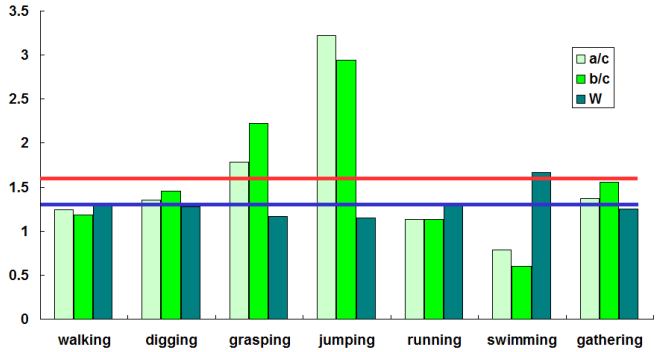

Fig. 2. Distribution of the a/c, b/c and W values for insect legs of different function

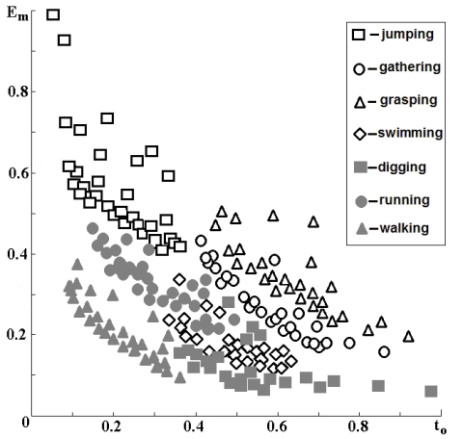

Fig. 3. Multi-objective Pareto frontiers for E_m and t_0

Conclusions

Geometry of insect legs as mechanical multi-link manipulators has been studied. The measurement data revealed high proximity of the running and walking legs, as well as digging and gathering legs to the double ratio W_F proper to upper extremities of humans and some animals, while the grasping, jumping and swimming legs are further from this value. Analysis of dynamics of the n-link leg revealed the relationships between the lengths of the links that are needed for optimal performance, namely the maximal force generation at the end of the leg at the same efficiency of the muscles rotating the joints. The perfect folding of the leg into a chain/spiral confirms the dynamical ability of the leg with the same lengths of the links. The obtained relationships are useful for designing multipurpose robotic arms and legs. Usually the robotic arms

are designed basing on one optimization criteria such as energy consumption, performance time, simplicity of the control [5], while the proposed approach allows multicriteria optimization for a pair of optimal criteria which are most suitable for the designed robotic system. The results for some other pair of the criteria will be presented in the full-text paper.

References

[1] Petukhov, S. V. 1981. *Biomechanics, bionics and symmetry*. Moscow: Nauka. 238 p.

[2] Dudley, R. 2000. *The biomechanics of insect flight: form, function, evolution*. Princeton: Princeton University Press. 476 p.

[3] Ritzmann, R. E.; Zill, S. N. 2009. Walking and jumping, in *Encyclopedia of insects*. Ed. by V. H. Resh, R. T. Cardé. San Diego: Academic Press, 1044–1048.

[4] Casas, J.; Simpson, S. J. [eds.]. 2008. *Advances in insect physiology, vol. 34: insect mechanics and control*. San Diego: Academic Press. 379 p.

[5] Corke, P. 2011. *Robotics, vision and control: fundamental algorithms in MATLAB*. Berlin Heidelberg: Springer-Verlag. 495 p. http://dx.doi.org/10.1007/978-3-642-20144-8

11TH INTERNATIONAL CONFERENCE
BIOMDLORE 2016
OCTOBER 20–22, 2016, DRUSKININKAI, LITHUANIA
BIOMDLORE.VGTU.LT

eISSN 2345-0630
ISBN 978-609-457-959-2
eISBN 978-609-457-958-5
DOI: 10.3846/biomdlore.2016.19

Characteristic upper extremity kinematic parameters of healthy people during defined motions

Artūras Linkel[1], Julius Griškevičius[2], James Shippen[3], Barbara May[4], Kristina Daunoravičienė[5]
[1, 2, 5] Vilnius Gediminas Technical University, Lithuania
[3, 4] Coventry University, United Kingdom
E-mails: [1] *arturas.linkel@vgtu.lt (corresponding author),* [2] *julius.griskevicius@vgtu.lt,*
[3] *j.shippen@coventry.ac.uk,* [4] *barbara.may@coventry.ac.uk,* [5] *kristina.daunoraviciene@vgtu.lt*

(Received 30 May 2016; accepted 20 June 2016)

Abstract. One of most common ways to examine the quality of the patient's upper extremity (UE) function is measuring the movement's kinematic parameters during the motion. However, is it reliable to compare a patient's UE motions data with healthy people's characteristic parameters? In this paper is shown that intrapersonal coefficient of variability (CV) in angles amplitudes differs from 3.2% during elbow flexion to 52.9% during wrist abduction and CV in angular velocity differs from 22.1% during shoulder abduction to 66.3% during wrist abduction.

Keywords: upper extremity, objective parameters, motion capturing system, biomechanics.

Introduction

The loss of UE function is one of the most common results after Central Nervous System (CNS) injuries [1] or musculoskeletal impairments [2]. A dysfunction in the UE can significantly limit a person's level of activity and participation in their social and physical environment [3]. The functional tests of UE are classified according to general clinical scales such as Jebsen-Taylor Hand function [4], Arm Research Assessment Test (ARAT) and Nine-Hole Peg Test and specific clinical scales applied to spinal cord injury (SCI) [5], stroke [6] or cerebral palsy (CP) [7]. The best-known ADL measures are Bartel Index [8] or Functional Independence Measure (FIM) [9]. It is clear that only functional and clinical subjective scales are not enough for accurate motion quality measurements and that objective methods are required. Quantitative measures of UE movement's quality can be valuable in the rehabilitation field for evaluating the quality of actual motion and recovery progress [10] which might help physicians to compare accurately healthy and pathological movement conditions in a clinical setting. The purpose of the research was to find if particular kinematic parameters of healthy participant's UE motions are reliable to compare with further experiments results with patients who have UE disability and trying to recover previous movement's conditions.

Methods

The study group included 23 adult participants (10 male and 13 female). The mean age was 29.2 years (range 19–63). Subjects' mean height was 1.71 m (range 1.55–1.85). The lengths of the arm segments were measured with a flexible measuring tape. All of the patients were right-handed. Inclusion criteria: none of the participants had any UE injuries that could influence kinematic results during the experiment. Experiments with all 23 participants were performed at the Coventry University laboratory in United Kingdom.

The three-dimensional motion analysis was performed with a Vicon Motion Capture System (Vicon, USA). Experimental data was transferred to windows-based data acquisition software (Vicon Nexus 1.7.1). Vicon system includes passive markers, sync box (or POE), 12 high resolution cameras with infrared illumination were located on tripods and positioned around the testing area (approx. volume dimensions, m: Height × Width × Length ≡ 2.5 × 1.8 × 1.8).

Measurements were performed at frequencies of 60–100 Hz. Overall system accuracy was 63±5μm and noise level of 15 μm, but during some cases because of dynamic calibration or arbitrary settings accuracy could be lower [11].

The UE experiment used a whole body Vicon system model and 39 passive retro-reflective spherical body markers were positioned at specific anatomical skeletal places [12] on the surface of a special suit.

All participants performed movements with their right and left arms. The subjects stood in a marked experiment area and have been asked to perform hand motions according to the created experiment methodology. Each subject performed 6 sessions during the experiment - three motions with the left side and three with the right side. Prepared hand joints motions chosen according to the possible biomechanical motions in human joints: flexion, extension, abduction, adduction, pronation and supination. During first session, wrist joint flexion, extension, adduction and abduction were examined. The second session investigated elbow joint motions: flexion, extension, pronation and supination. The third session examined shoulder motions: flexion, extension, adduction and abduction (pronation and supination were not tested). All motions were repeated three times.

Results

Mean (M) of measured amplitudes and calculated angular velocities with its standard deviations (SD) from all 23 participants data were used to determine intraperson coefficients of variability (CV=SD/M) outcome (Fig. 1).

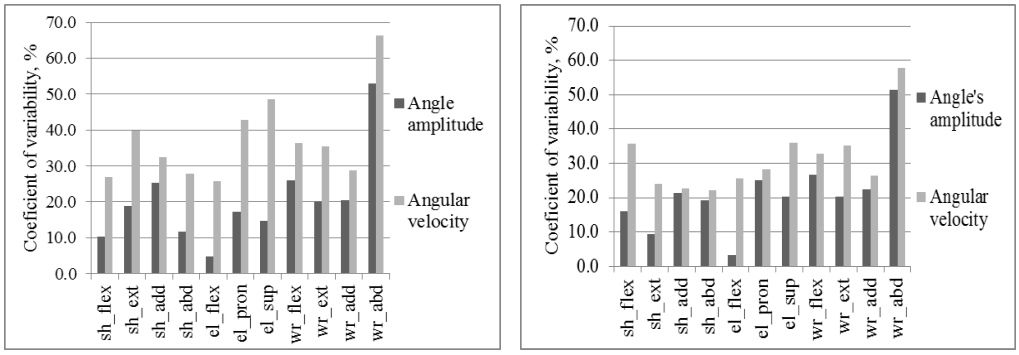

Fig. 1. Intraperson left-side (picture on the left) and right-side (picture on the right) coefficients of variability (CV) of angle's amplitudes and angular velocities of shoulder (sh), elbow (el) and wrist (wr) motions

Left-side motions showed that the lowest value of CV of angles amplitudes is at elbow flexion – 3.2% but highest is at wrist abduction 51.4% and the lowest/highest CV of angular velocities are 22.1% / 57.9% during elbow flexion/wrist abduction (Fig. 1). Right-side motions showed that the lowest value of CV of angles amplitudes is at elbow flexion – 4.7% but the highest at wrist abduction 52.9% and the lowest/highest CV of angular velocities are 25.7% / 66.3% during elbow flexion/wrist abduction (Fig. 1).

Comparing the right side motions of the left, intraperson CV of amplitudes of angles of both sides are very close but also differs from 1.5% during the elbow flexion to 10.3% during the wrist abduction and CV of angular velocity differs from 0% during the elbow flexion to 14.5% during the elbow pronation (Fig. 1).

Conclusions and discussion

There is a common way to examine human UE motions quality by evaluating of kinematic parameters such as angles amplitudes and angular velocities during specified motions methodology [13, 14]. Patient's upper extremity motions quality could be evaluated by comparing their kinematic motions parameters with healthy people parameters. However, from CV it is obvious that intrapersonal comparison could not be accurate during almost all UE motions. A different situation exists with interpersonal CV results because it is reliable for amplitude and angular velocity measurements and it means that the comparison of UE motions quality of the same person before and after the rehabilitation program should be available.

Acknowledgements

Special thanks for Coventry University (UK) professor dr. J. Shippen and dr. B. May for the support during the experiment with motion capturing system and the internship.

References

[1] Nakayama, H., *et al.* 1994. Compensation in recovery of upper extremity function after stroke: the Copenhagen stroke study, *Physical Medicine and Rehabilitation* 75(4): 394–398. http://dx.doi.org/10.1016/0003-9993(94)90108-2

[2] Jette, A. M.; Branch, M. G.; Berlin, J. 1990. Musculoskeletal impairments and physical disablement among the aged, *The Journals of Gerontology* 45(6): 203–208. http://dx.doi.org/10.1093/geronj/45.6.M203

[3] Broeks, J. G., *et al.* 1999. The long-term outcome of arm function after stroke: results of a follow-up study, *Disability and Rehabilitation* 21(8): 357–364. http://dx.doi.org/10.1080/096382899297459

[4] Jebsen, R. H., *et al.* 1969. An ojective and standardized test of hand function, *Physical Medicine and Rehabilitation* 50(6): 311–319.

[5] Van Tuijl, J.; Janssen-Potten, Y.; Seelen, H. 2002. Evaluation of upper extremity motor function tests in tetraplegics, *Spinal Cord* 40(2): 51–64. http://dx.doi.org/10.1038/sj.sc.3101261

[6] Fugl-Meyer, A. R., *et al.* 1974. The post-stroke hemiplegic patient. A method for evaluation of physical performance, *Scandinavian Journal of Rehabilitation Medicine* 7(1): 13–31.

[7] Boyce, W., *et al.* 1991. Measuring quality of movement in cerebral palsy: a review of instruments, *Physical therapy* 71(11): 813–819.

[8] Mahoney, F. I. 1965. Functional evaluation: the Bartel index, *Maryland State Medical Journal* 14: 61–65.

[9] Keith, R. A. 1987. The functional independence measure: a new tool for rehabilitation, *Advances in Clinical Rehabilitation* 1: 6–18.

[10] Murphy, M. A.; Sunnerhagen, K. S. 2013. Responsiveness of upper extremity kinematic measures and clinical improvement during the first three months after stroke, *Neurorehabilitation and Neural Repair* 27: 71–80. http://dx.doi.org/10.1177/1545968313491008

[11] Windolf, M.; Gotzen, N.; Morlock, M. 2008. Systematic accuracy and precision analysis of video motion capturing systems-exemplified on the Vicon-460 system, *Journal of Biomechanics* 41(12): 2776–2780. http://dx.doi.org/10.1016/j.jbiomech.2008.06.024

[12] Land, M. W., *et al.* 2013. From action representation to action execution: exploring the links between cognitive and biomechanical levels of motor control, *Frontiers in Computational Neuroscience* 7: 127. http://dx.doi.org/10.3389/fncom.2013.00127

[13] Murphy, M. A., *et al.* 2006. Three-dimensional kinematic motion analysis of a daily activity drinking from a glass: a pilot study, *Journal of Neuroengineering and Rehabilitation* 3: 18. http://dx.doi.org/10.1186/1743-0003-3-18

[14] Ozturk, A., *et al.* 2015. A clinically feasible kinematic assessment method of upper extremity motor function impairment after stroke, *Measurement* 80: 207–216. http://dx.doi.org/10.1016/j.measurement.2015.11.026

11TH INTERNATIONAL CONFERENCE
BIOMDLORE 2016
OCTOBER 20–22, 2016, DRUSKININKAI, LITHUANIA
BIOMDLORE.VGTU.LT

eISSN 2345-0630
ISBN 978-609-457-959-2
eISBN 978-609-457-958-5
DOI: 10.3846/biomdlore.2016.20

Posturographic study of human body sway before and after a work day for diagnosis of tiredness

Michail Karpinski[1], Natalya Kizilova[2, 3]
[1] N. I. Sytenko Institute of Spine and Joint Pathology, Ukraine
[2] Warsaw University of Technology, Poland
[3] Vilnius Gediminas Technical University, Lithuania
E-mails: [1] *medicine@online.kharkov.ua*, [2] *n.kizilova@gmail.com (corresponding author)*

(Received 11 June 2016; accepted 19 August 2016)

Abstract. Body sway measured by force platform is an excellent simple test for diagnostics of locomotory, balance, visual and neural disorders. In this study the body sway parameters have been measured on a group of healthy medical workers in the morning/evening time before/after their work day. The centre of pressure (CoP) trajectories in a series of different 2-leg stances and during a step forward off from the force platform have been recorded. It was found, in the morning the sway amplitudes were higher due to relaxed state of muscles, while after the work day the muscles were tired and the force platform test demanded more attention and body control which mostly lead to lower body sway amplitudes. The step off from the platform were executed faster in the evening, and the more elderly individuals exhibited more pronounced pathological signs in the CoP trajectory in the evening. Basing on the data analysis, new indices of tiredness and stress level are proposed for occupational medicine.

Keywords: body sway, posture balance, control, medical diagnostics, stress, tiredness.

Introduction

Postural stability is an important constituent of body health for it is based on the state of the skeletal, muscular, neural, visual, balance systems and their interactions. Computer-assisted posturography is widely used in medical diagnostics and sport medicine as fast, simple and reliable test of human locomotory system. Posturographic curves may be explained within accepted biomechanical models of different complexity, from the inverted pendulum discrete models to the 3D multibody finite element models [1]. The force platform allows measurements of the CoP coordinates ($X_C(t)$, $Y_C(t)$) and computations the CoP trajectory $Y_C(X_C)$ at different 2-leg and 1-leg stances [1–3]. Pattern of shifts in the CoP location when the body mass is transferred onto the left/right leg can be used for separation between the spine (osteochondrosis) and joint (coxarthrosis) problems in elderly patients [2]. Here the first experimental evidence of early diagnostics of tiredness and stress state from the posturographic data is presented. In the recent literature the sway parameters of the patients with different locomotory disorders only in the morning time [3] or after the sleepless night [4] could be found. Here the posturography data measured on the same volunteers before and after their 8-hour work day is analysed, that allows quantitative estimation of the normal daily tiredness for the persons of different age.

Methods

The force platform "Statograph-6' of the laboratory of biomechanics Kharkov Institute of Spine and Joint pathology has been used. Twenty healthy individuals (weight 71.4±12.1 kg, height 1.7±0.2 m, and age 45±17 years) without pronounced neuromuscular disorders have been asked to maintain upright stance on the force platform during 30 s. All the volunteers signed a written agreement on usage of their anonymous medical data for research purposes. The age, height, weight, gender and results of the standard series of 2-leg stances reported by authors in the previously published papers [2, 3] have been recorded and analysed (Fig. 1). It was a series of five

30-s tests included a quite symmetric 2-leg stance (Fig.1a), transfer of the body mass onto the left (Fig. 1b) and right (Fig. 1c) legs followed by a step off from the platform with left and right legs accordingly (Fig. 1d). The measured time series ($X_C(t)$, $Y_C(t)$) have been then amplified and the low ($f < 0.01$ Hz) and high ($f > 10$ Hz) frequency components have been subtracted using the second order Butterworth filter. Each of the trajectory $X_C(Y_C)$ were restricted by rectangle $\{X \in [-a, a], Y \in [-b, b]\}$, where $a = |\max(X_C) - \min(X_C)| / 2$, $b = |\max(Y_C) - \min(Y_C)| / 2$. The values 2a and 2b have been considered as sway amplitudes in the frontal and sagittal planes accordingly. The trajectories like presented in fig.1e and fig.1f were proper to the younger (age < 45, 10 persons) and the elderly (age > 45) subgroups of the volunteers accordingly.

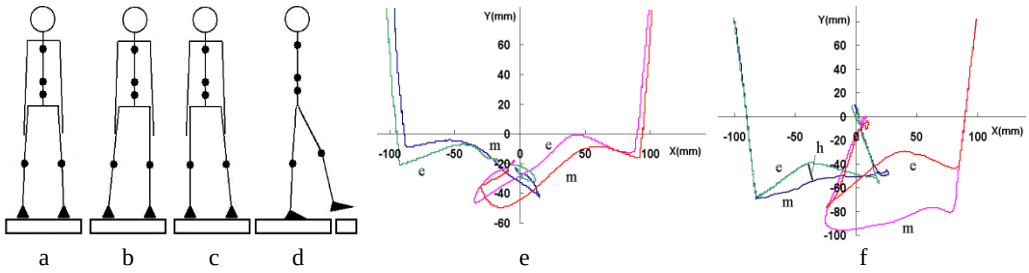

Fig. 1. 2-leg stances (a, b, c) and step off from the force platform (d) studied in experiments, and Y(X) trajectories of the first step off towards from the force platform with slight (e) and strong (f) morning-evening differences. The morning and evening trajectories are marked by *m* and *e*

Body sway can be efficiently described by the inverted n-link pendulum model described by Lagrange equations:

$$\frac{d}{dt}\frac{\partial T(t)}{\partial \dot{\Theta}_j} - \frac{\partial T(t)}{\partial \Theta_j} + \frac{\partial \Pi(t)}{\partial \Theta_j} = q_j(t-\tau), \qquad (1)$$

where T and Π are kinetic and potential energy, a dot over the symbol represents the time derivative, Θ_j is the angle between the *j*-th segment and vertical axis, q_j is the net moment of force in the j-th joint, τ is the time delay caused by reaction of the nervous system to information brought via receptors from the muscles and balance system. The time delay is bigger in elderly persons and at some neural diseases [1]. For each individual his/her body mass and height have been measured and the mass and moments of inertia of the segments of body have been computed from the tables [1]. Then the right-hand side of (1) was directly computed and the time delay in the control functions $q_j(t - \tau)$ was found by correlation analysis with the values $\Theta_j(t)$ computed from the measurement data.

As it was shown in different studies, generally $q_j(t) = F(\Theta_j, \dot{\Theta}_j)$, but usually the dependence $q_j(t) = k\,\Theta_j$ gives satisfactory results. Our correlation analysis revealed the time delay $\tau_{s,\,f}$ is slightly different for the sagittal (s) and frontal (f) plane models. The best correspondence to the measured data has been obtained for $q_j(t,\tau) = k_1\Theta_j(t-\tau) + k_2\dot{\Theta}_j(t-\tau)$.

Results

Analysis of the $X_C(Y_C)$ curves revealed two groups of individuals. The subjects of the first group have not demonstrated any qualitative differences in the trajectories of their CoP (Fig. 1e). Initial location of the CoP was the same and only slight quantitative differences between the curves have been found. The subjects of the second group demonstrated normal 'healthy' patterns in the

morning and clear signs of locomotory problems after the work day (Fig. 1f). According to our previous data [2, 3], young healthy volunteers transfer their body mass onto their support leg and make the step off with another leg, and the trajectories of their CoP are looking like left and right curves (*m*) in Fig. 1f. The elderly patients with spine and joint diseases demonstrate trajectories like those marked by (*e*) in Fig. 1f. During this step off the CoP moves forward, then backward and then again forward producing the 'hill' which 'height' h (Fig. 1f) is a confirmed characteristic of locomotory disorders [3]. It means the tiredness after the work day reveals hidden locomotory pathology that could be efficiently tested by posturographic test.

The tested individuals also demonstrated certain shift in the averaged CoP location in the morning and evening. The dependence dY(dX) between the shifts in X and Y coordinates in three corresponding 2-leg stance tests in the morning and evening is presented in Fig. 2a. Almost uniform shift in different directions (forward-backward, left-right) has been detected. The absolute value of the shift was bigger when in the morning tests the averaged CoP located further from the centre of coordinate system. It means, the body position was more stable when CoP was projected onto the (X0Y) plane closer to (0, 0).

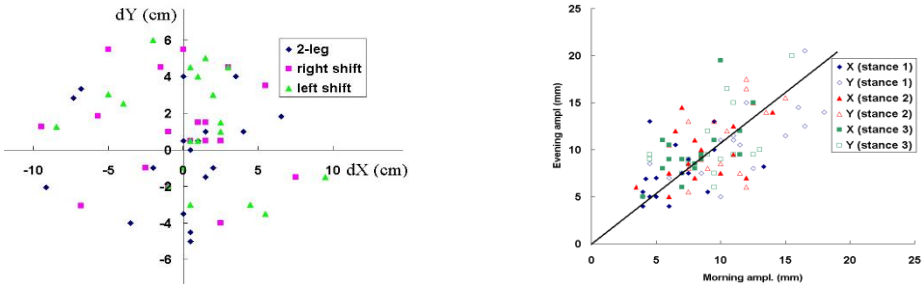

a b

Fig. 2. Shift (dX,dY) in location of the CoP (evening – morning) for different stances

The sway amplitudes could be either bigger (the marks over the straight line in Fig. 2b) or lower (the marks below the straight line in Fig. 2b), while the absolute variation in the amplitudes is smaller for the sway in the frontal plane (filled in marks in Fig. 2b) than the sway in the sagittal plane (empty marks in Fig. 2b). Since increase of the frontal sway is a good predictor of sudden fall in elderly persons [1], the test of tiredness could be a good diagnostic tool for early diagnostics of neural and other balance control systems.

Conclusions

It was shown the lower body sway amplitude and faster step off from the force platform are the important signs of tiredness after a work day which are proper to the elderly individuals. As it was shown before, those signs are also proper to the patients with locomotory disorders, independently on the hours of examination. The n-link model of the inverted pendulum with the delayed control function allows evaluation of the time delay τ between the generalized coordinates $\Theta_j(t)$ and the functions q_j controlling the body stability. The time delay may be proposed as a new index of daily tiredness and stress level in occupational medicine.

References

[1] Latash, M. L.; Zatsiorsky, V. M. [eds.] 2001. *Classics in Movement Sciences*. Champaign: Human Kinetics. 464 p.

[2] Kizilova, N., *et al.* 2009. Posturographic study of the human body vibrations for clinical diagnostics of the spine and joint pathology, *Mechanika* 6(60): 37–41.

[3] Sørensen, R. R., *et al.* 2014. Impaired postural balance in the morning in patients with knee osteoarthritis, *Gait & Posture* 39(4): 1040–1044. http://dx.doi.org/10.1016/j.gaitpost.2014.01.002
[4] Fabbri, M., *et al.* 2006. Postural control after a night without sleep, *Neuropsychologia* 44(12): 2520–2525. http://dx.doi.org/10.1016/j.neuropsychologia.2006.03.033

11TH INTERNATIONAL CONFERENCE
BIOMDLORE 2016
OCTOBER 20–22, 2016, DRUSKININKAI, LITHUANIA
BIOMDLORE.VGTU.LT

eISSN 2345-0630
ISBN 978-609-457-959-2
eISBN 978-609-457-958-5
DOI: 10.3846/biomdlore.2016.21

Estimation of temporal gait parameters of multiple sclerosis patients in clinical setting using inertial sensors

Julius Griškevičius[1], Vigita Apanskienė[2], Jurgita Žižienė[3], Kristina Daunoravičienė[4], Agnė Ovčinikova[5], Rasa Kizlaitienė[6], Ieva Sereikė[7], Gintaras Kaubrys[8], Jolanta Pauk[9], Adam Idźkowski[10]

[1, 2, 3, 4] Vilnius Gediminas Technical University, Lithuania
[5, 6, 7, 8] Clinics of Neurology and Neurosurgery of Vilnius University Hospital Santariškių Klinikos, Lithuania
[9, 10] Bialystok University of Technology, Poland
E-mails: [1] *julius.griskevicius@vgtu.lt (corresponding author)*, [2] *vigita.apanskiene@stud.vgtu.lt*, [3] *jurgita.ziziene@vgtu.lt*, [4] *kristina.daunoraviciene@vgtu.lt*, [5] *agne.ovcinikova@gmail.com*, [6] *rasa.kizlaitiene@santa.lt*, [7] *ieva.sereike@santa.lt*, [8] *gintaras.kaubrys@santa.lt*, [9] *j.pauk@pb.edu.pl*, [10] *a.idzkowski@pb.edu.pl*

(Received 21 June 2016; accepted 23 June 2016)

Abstract. Multiple sclerosis (MS) is the most frequent neurological disease causing permanent disability in young adults. Subtle walking difficulties, such as reduced walking speed, step length, cadence and increased step width can be detected at an early stage of the disease. Main goal of this research is by using non-invasive wireless inertial sensors measure gait of MS patients in clinical setting and extract temporal biomechanical parameters that would allow objectively evaluate level of disability in MS patients. Analysis of 25-Foot walk showed that the duration of stance phase is approximately 1.6 times greater in MS group than in healthy control group, while the duration of swing phase in MS group is 1.3 times longer. In general, the MS patients are walking approximately 1.6 times slower.

Keywords: multiple sclerosis, gait, inertial sensors, biomechanics.

Introduction

Multiple sclerosis is the most frequent neurological disease causing permanent disability in young adults [1]. However, the cause of MS remains unknown. The disease onset is often polysymptomatic. Common symptoms and signs of MS include sensory symptoms in limbs or face, visual loss, acute or subacute motor weakness, diplopia, gait disturbance and balance problems, vertigo, bladder problems, acute transverse myelitis and pain. People with MS frequently have neuromuscular deficits such as ataxia, early muscle fatigue, spasticity and sensory disturbances, which limit gait and considerably affect their everyday living activities [1]. Subtle walking difficulties, such as reduced walking speed, step length, cadence and increased step width can be detected at an early stage of the disease [2, 3, 4, 5]. Walking limitations have negative consequences in activities of daily living, quality of life, as well as employment etc. Like in many neurological disorders, such evaluations are typically approached by direct observation of the clinician supported by a timed analysis, functional scales and questionnaires. Information derived from neurological assessment is included in the expanded disability status scale (EDSS) and it is most widely used to evaluate disability in MS, in both daily clinical practice and trials [2, 3, 5]. However, it is essential to find new tools, complementary to the clinical scales, able to supply objective and quantitative data useful in supporting clinical assessment of the disability as well as its variations across time. In addition, it is very important to have available reliable and accurate techniques to assess the degree of deviation from a physiological gait pattern as well as to detect even small changes in it consequent to pharmacological or rehabilitative treatment. Many methods have been reported in the last decade objectively acquire quantitative data on gait alterations of MS patients. Quantitative gait observation has been collected using several of techniques: video

analysis, accelerometers [6, 7] and three-dimensional motion capture systems [8]. However specialized motion-analysis laboratories were required to capture sophisticated gait and balance data [6]. Portable technologies now that collect equivalent data rapidly and with instant analysis are being widely explored for use in MS. These include accelerometers, pedometers, and pressure mats for gait analysis [6].

Main goal of this research is by using non-invasive wireless inertial sensors measure gait of multiple sclerosis patients in clinical setting and extract temporal biomechanical parameters that would allow objectively evaluate level of disability in MS patients.

Methods

Research was carried out on volunteers who were divided into two groups – 11 control (CO) subjects (5 men, 6 women, aged: 31.5±4.7 (mean ± SD)), 14 multiple sclerosis (MS) subjects (6 men, 8 women, aged: 38.5±12.49 (mean ± SD)). None of the participants had any other injuries or disease affecting movement or coordination other than MS. All fourteen patients suffering from relapsing-remitting MS with EDSS score of ≤6 (range 2.5–6, mean EDSS 4.1±1.4 (mean ± SD)). The main inclusion criteria – the ability to walk independently without any assisting devices (i.e. crutches, working frames, foot supports and similar). Everyone provided informed consent prior to participating in the study. Neurological disability (EDSS score) was evaluated for each patient by a neurologist expert in MS.

Six, wireless inertial sensors (Shimmer Research, Dublin, Ireland), each able to measure linear acceleration, angular velocity and magnetic heading in three dimensions were attached to each patient's right and left thigh, shank and foot. The data from the sensors acquired via Bluetooth wireless connection at a sampling frequency of 51.2 Hz and stored on the computer for later processing. Each subject performed timed 25-Foot Walk (T25-FW) gait task at their selected pace as fast as possible. Each measurement was performed three times.

Following temporal parameters of gait have been selected for the analysis: stance phase duration (s), swing phase duration (s), average step time (s), approximate time of the whole gait task (s), velocity (m/s), cadence (steps × min^{-1}), stride length (m), coefficient of variability (CV, %). Statistical analysis of the metrics was performed using IBM's SPSS v22 software. A one-way ANOVA with a significance level of $\alpha = 0.05$ was used to test the null hypothesis that the means of gait parameters are the same between the MS and CO groups.

Results

The full set of metrics for the comparative analysis is presented in Table 1.

Table 1. Temporal gait parameters

Parameters	Groups	Mean	SD	CV, %
Stance phase time, s	CO	0.419	0.07	17.4
	MS	0.662	0.134	12.7
Swing phase time, s	CO	0.404	0.08	20.9
	MS	0.542	0.087	20.2
Step time, s	CO	0.824	0.135	16.4
	MS	1.204	0.153	16.2
Approximate motion time, s	CO	6.909	0.792	11.5
	MS	11.142	1.597	14.3
Cadence, steps × min^{-1}	CO	94.74	13.811	14.6
	MS	72.351	11.456	15.8
Stride length, m	CO	1.409	0.189	13.4
	MS	1.164	0.217	18.6
Velocity, m × s^{-1}	CO	1.099	0.125	11.4
	MS	0.686	0.094	13.7

A one-way between subjects ANOVA was conducted to compare the means of the gait metrics for analysis of MS and CO groups. When analysing T25-FW gait task, we found that there was a statistically significant difference in duration of the stance phase [$F = 47.42$, $p = 0.0002$], duration of the swing phase [$F = 25.88$, $p = 0.0008$], step time [$F = 66.39$, $p = 0.0003$], approximate motion time [$F = 50.87$, $p = 0.0006$], cadence [$F = 18.5$, $p = 0.0003$], stride length [$F = 4.88$, $p = 0.0391$], velocity [$F = 65.51$, $p = 0.0009$].

Conclusions

Analysis of 25-Foot walk showed that the duration of stance phase is approximately 1.6 times greater in MS group than in CO group, while the duration of swing phase in MS group is 1.3 times longer than in CO group. However, the coefficient of variability is greater in CO group during the stance phase time than indicating that there is some degree of inconsistency among the CO subjects, while the coefficient of variability of the swing phase duration is almost the same in both groups. Similarly, the variability of step time is the same in both groups, but in general, the MS patients are walking approximately 1.6 slower.

References

[1] Pau, M., *et al.* 2014. Novel characterization of gait impairments in people with multiple sclerosis by means of the gait profile score, *Journal of Neurological Sciences* 345(1–2): 159–163. http://dx.doi.org/10.1016/j.jns.2014.07.032

[2] Pilutti, L. A., *et al.* 2013. Gait and six-minute walk performance in persons with multiple sclerosis, *Journal of Neurological Sciences* 334(1–2): 72–76. http://dx.doi.org/10.1016/j.jns.2013.07.2511

[3] Spain, R. I., *et al.* 2014. Body-worn sensors capture variability, but not decline, of gait and balance measures in multiple sclerosis over 18 months, *Gait & Posture* 39(3): 958–964. http://dx.doi.org/10.1016/j.gaitpost.2013.12.010

[4] Roeing, K. L., *et al.* 2015. Gait termination in individuals with multiple sclerosis, Gait & Posture 42(3): 335–339. http://dx.doi.org/10.1016/j.gaitpost.2015.06.192

[5] Kalron, A. 2016. Gait variability across the disability spectrum in people with multiple sclerosis, *Journal of Neurological Sciences* 361: 1–6. http://dx.doi.org/10.1016/j.jns.2015.12.012

[6] Monticone, M., *et al.* 2014. Reliability of spatial-temporal gait parameters during dual-task interference in people with multiple sclerosis. A cross-sectional study, *Gait & Posture* 40(4): 715–718. http://dx.doi.org/10.1016/j.gaitpost.2014.06.015

[7] Kotiadis, D.; Hermens, H. J.; Veltink, P. H. 2010. Inertial gait phase detection for control of a drop foot stimulator inertial sensing for gait phase detection, *Medical Engineering & Physics* 32(4): 287–297. http://dx.doi.org/10.1016/j.medengphy.2009.10.014

[8] Rueterbories, J., *et al.* Methods for gait event detection and analysis in ambulatory systems, *Medical Engineering & Physics* 32(6): 545–552. http://dx.doi.org/10.1016/j.medengphy.2010.03.007

11TH INTERNATIONAL CONFERENCE
BIOMDLORE 2016
OCTOBER 20–22, 2016, DRUSKININKAI, LITHUANIA
BIOMDLORE.VGTU.LT

eISSN 2345-0630
ISBN 978-609-457-959-2
eISBN 978-609-457-958-5
DOI: 10.3846/biomdlore.2016.22

The influence of barbell's weight, lifting technique and skills on weightlifter's blood pressure and heart rate

Mečislovas Mariūnas[1], Julius Griškevičius[2], Gintaras Jonaitis[3]
[1, 2, 3] Vilnius Gediminas Technical University, Lithuania
E-mails: [1] *mecislovas.mariunas@vgtu.lt (corresponding author),* [2] *julius.griskevicius@vgtu.lt,*
[3] *gintaras.jonaitis@vgtu.lt*

(Received 1 July 2016; accepted 15 July 2016)

Abstract. Article presents hodographs of the arterial blood pressure relation to heart-rate enabling to evaluate organism sensitivity of trained weightlifter to the magnitude of lifted weight, lifting technique and weight repeatability. Variation regularities of the latter relation have been explained and approximate criterions of relative stability and skill level were formulated. Analysing variations of the relation of the arterial blood pressure to the heart-rate and barbell's lifting accelerations and velocities the weaknesses of trained weightlifters have been explained. It has shown that in most cases the blood pressure of the weightlifter can increase 8–13% after the barbell drop.

Keywords: blood pressure, heart rate, snatch, clean and jerk, lifting accelerations and velocities, organism reaction to weight, indexes of relative stability and technique, hodograph.

Introduction

The reaction of weightlifter's organism to the lifted weight and lifting technique can be evaluated analysing the variations of the arterial blood pressure and the heart-rate. Regularities of variations can give insight on weightlifter's skill level. High competition results can be achieved having mastered optimal trajectories of barbell's lifting, i.e. its kinematics. Barbell's lifting kinematics during snatch and clean and jerk has been fairly explored in various scientific works [2, 3, 4, 5, 6, 7]. For example, in the article [5] authors have analysed the parameters of elite athletes' lifting trajectories during 2010 weightlifting championship. They've determined relation of the final result to common barbell's trajectories of the women weightlifters. Despite many research works on kinematics of the barbell only few pay attention to variations of arterial blood pressure and heart-rate after the barbell drop, however presented results are only descriptive [1, 3, 8, 10]. In these work regularities of arterial blood pressure and heart-rate variations are not explored. Some authors attempted to analyse the regularities of time variations of arterial blood pressure and heart rate in response to constant load [9]. A lack of works studies reaction of the organism to load and lifting manner.

The goal of present research is to investigate relationship between the arterial blood pressure of the weightlifter and heart rate after dropping the barbell, understand the variation tendencies of latter parameters and to formulate criterions of organism's sensitivity reaction to lifted weight and technique. By analysing barbell's lifting accelerations and velocities to investigate weaknesses of the athlete and approximately evaluate his prospective abilities in chosen sport.

Methods

Research was carried out in the weightlifting gym of the Vilnius University "Health and sport centre" under the guidance of the coach Rimantas Cijūnėlis. Total six athletes were recruited for the study and were divided in two groups: three beginners and three advanced weightlifters. The barbell's weight was varying from 60 to 80 kg. Inertial sensors with ±1.5g – 6g Three Axis low-g micromachined accelerometer were fixed on the hand and forearms of the weightlifters and one on the barbell. Weightlifters were instructed to perform snatch and clean and jerk lifting

techniques. The heart rate and arterial blood pressure was measured using Siemens and Space Lab Medical monitoring and data processing system before (at 0 sec) and after each attempt after 60, 180, 300, 480 and 540 seconds. All data was registered and stored on the PC.

Results

The arterial blood pressure and heart rate graphs alone are not informative enough. Combining them in a hodograph $p(t) = f[h(t)]$ it is possible to note two important phenomena. First, variation of the area of the hodograph with respect to the lifted weight (Fig. 1). Secondly, location of latter hodographs on the plane, i.e. what area on the plane they are covering after repeated lifting of the barbell (Fig. 2).

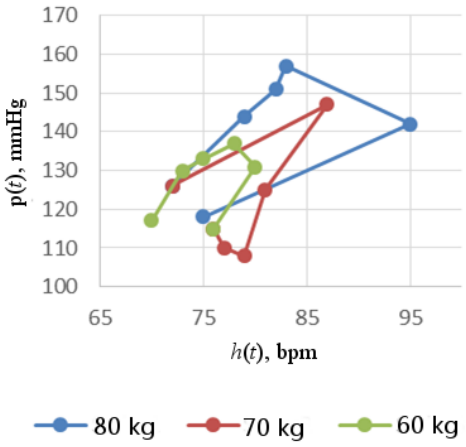

Fig. 1. Hodographs of the beginner athlete

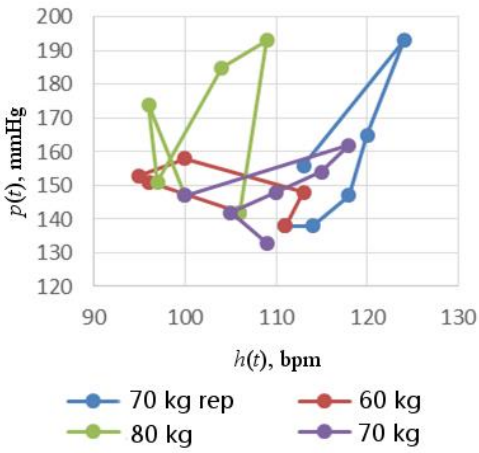

Fig. 2. Hodographs of the advanced athlete (rep means the load was lifted repeatedly)

Fig. 1 and 2 shows that hodographs are located unevenly on the plane. In Fig. 1, the area of the largest weight's hodograph approximately overlaps areas of hodographs corresponding to lower weights. In Fig. 2, hodographs of barbells' during the lifting of different weights and repeatedly 70 kg weight are distributed in bigger area and hodograph of the largest weight does not cover hodographs of lower weights. Therefore, analysing distribution area of the hodographs on the plane of the repeats it is possible to evaluate reaction of the athlete organism to repeated lifts. Magnitude of the distribution of the hodograph on the plane $[p(t); h(t)]$ during lifting barbell of different weight can be described by the ratio:

$$S_d = \frac{Q}{q_{\max}}, \text{ where } Q = \sum_{i=1}^{m} \int_{p(t)_{iap}}^{p(t)_{ivir}} f\left[h(t)_i\right] d(t)_i + Q_t, \quad (1)$$

where Q – total area of the hodograph; Q_t – empty area between the hodographs; q_{max} – area of the largest hodograph; m – number of hodographs; $h(t)_i$ – heart rate time dependence; i – index indicating which hodograph is being analysed; $p(t)_{iap}$ and $p(t)_{ivir}$ – integration limits.

The higher the value of S_d criterion, the higher the distribution of the hodograph's on the plane. Suggested criterion is summary: it is accounting the sensitivity of the organism to the increased load of the barbell, lifting technique and repeatability of the lifting and normal reaction of the organism to the increased load. The value of this criterion would always be $1 \leq S_d < \infty$. When

$S_d \approx 1$, the area of the hodograph of the largest lifted weight covers all other hodographs corresponding repeated lifts with lower weights and it would indicate stable organism reaction to the magnitude of lifted weight.

The natural reaction of the organism to the increased weight and lifting technique can be evaluated with following criterion:

$$S_{st} = \frac{\max\limits_i \left\{ \int\limits_{p(t)_{iap}}^{p(t)_{ivir}} f\left[h(t)_i\right] d(t)_i \right\}}{\min\limits_i \left\{ \int\limits_{p(t)_{iap}}^{p(t)_{ivir}} f\left[h(t)_i\right] d(t)_i \right\}}. \quad (2)$$

The value of this criterion is $1 \leq S_{st} << \infty$. When the value of the latter criterion is very large, it is indicating that the skills of the athlete needs to be improved.

Discussion

Presented hodographs in the Fig. 1 and Fig. 2 represent possible distribution of the hodographs on $p(t)$ and $h(t)$ plane (Fig. 1) and constant reaction of the advanced athlete to the lifted weight (Fig. 2). Carried out calculations on the presented above hodographs are showing that the criterion value of the advanced athlete is $S_d \approx 3.1$, while for the beginner it is $S_d \approx 1.24$. It shows that the organism of the advanced athlete reacts very sensitively to the repeated lifts and lifting weight magnitude. When comparing values of second criterion $S_{st} \approx 4.0$ and $S_{st} \approx 2.0$ for beginner and advanced athlete respectively, they're differ almost two times. The beginner athlete needs to improve his skills, while the reaction of his organism is more stable to the repeated lifts. The coach should evaluate the features of the athletes.

The criterions are integral and they do not identify particular weaknesses of the athletes. For example, the $S_d \approx 4.0$ for beginner athlete could mean that his lifting technique is low, but does not clearly shows what is wrong. Further analysis of the weightlifter's biomechanics parameters might provide related to the technique additional and missing information. Inertial measurements of athlete's hands accelerations during the lifting revealed that there is uneven distribution of the strength between the arms in beginner athlete. The advanced athlete is showing more even distribution of the arm velocities during snatch than it is for the beginner athlete. Therefore, additional analysis of accelerations and/or velocities can contribute to better evaluation of athlete's weaknesses and coach, combining values of S_d and S_{st} criterions, could develop more personalized training methodology and to help increase athlete skills.

Conclusions

Results of experimental research and their analysis allowed making following conclusions:

1. Based on explained regularities of arterial blood pressure relation to heart rate it is possible to evaluate sensitivity of the weightlifter's organism to the magnitude of the weight, lifting technique and repeated lifting.
2. Formulated integral criterions for the evaluation of sensitivity of the athlete organism and his skills. However, criterions need to be used in combination with additional information about the biomechanics of the athlete performance.
3. There is now unambiguous relationship between heart rate and arterial blood pressure. It has been shown that in most cases the blood-pressure of the weightlifter can increase 8–13% after the barbell drop.

References

[1] Mostofsky, E., *et al.* 2011. Physical activity and outset of acute ischemic stroke, *American Journal of Epidemiology* 173(3): 330–336. http://dx.doi.org/10.1093/aje/kwq369

[2] Moon, Y.-J. 2005. Determination of performance determinant factors in snatch weightlifting, *Korean Journal of Sport Biomechanics* 15(2): 21–29. http://dx.doi.org/10.5103/KJSB.2005.15.2.021

[3] Vladimir, P.; Violer, U. M.; Carmen, T. O. 2014. Spatial–temporal aspects of the influence of the ability to concentrate on the execution of snatch style in performance weightlifting, in *Procedia – Social and Behavioral Sciences* 117: 210–215. http://dx.doi.org/10.1016/j.sbspro.2014.02.203

[4] Nejadian, S. L.; Rostami, M.; Naghash, A. 2010. Cost evaluation of different snatch trajectories by using dynamic programing method, in *Procedia Engineering* 2(2): 2563–2567. http://dx.doi.org/10.1016/j.proeng.2010.04.032

[5] Akkus, H. 2012. Kinematic analysis of the snatch lift elite female weightlifter's during the 2010 World Weightlifting Championship, *Journal of Strength and Conditioning Research* 26(4): 897–905. http://dx.doi.org/10.1519/JSC.0b013e31822e5945

[6] Gourgoulis, V., et al. 2009. Unsuccessful vs. successful performance in snatch lifts: a kinematic approach, *Journal of strength and conditioning research* 23(2): 486–494. http://dx.doi.org/10.1519/JSC.0b013e318196b843

[7] Isaka, T.; Okada, J.; Funato, K. 1996. Kinematic analysis of the barbell during the snatch movement of elite Asian weightlifters, *Journal of Applied Biomechanics* 12(4): 508–518. http://dx.doi.org/10.1123/jab.12.4.508

[8] Martinelli, F. S., *et al.* 2005. Heart rate variability in athletes and nonathletes at rest and during head-up tilt, *Brazilian Journal of Medical and Biological Research* 38(4): 639–647. http://dx.doi.org/10.1590/S0100-879X2005000400019

[9] Mariūnas, M.; Kuzborska, Z. 2011. Influence of load magnitude and duration on the relationship between human blood pressure and flow rate, *Acta of Bioengineering and Biomechanics* 13(2): 67–72.

[10] Poderys, J., *et al.* 2005. Mobilization of cardiovascular function during the constant-load and all-out exercise tests, *Medicina* 41(12): 1048–1053.

11TH INTERNATIONAL CONFERENCE
BIOMDLORE 2016
OCTOBER 20–22, 2016, DRUSKININKAI, LITHUANIA
BIOMDLORE.VGTU.LT

eISSN 2345-0630
ISBN 978-609-457-959-2
eISBN 978-609-457-958-5
DOI: 10.3846/biomdlore.2016.23

Estimation of the parameters of barbell' lifting law of motion

Mečislovas Mariūnas[1], Julius Griškevičius[2], Gintaras Jonaitis[3]
[1, 2, 3] Vilnius Gediminas Technical University, Lithuania
E-mails: [1] *mecislovas.mariunas@vgtu.lt (corresponding author),* [2] *julius.griskevicius@vgtu.lt,*
[3] *gintaras.jonaitis@vgtu.lt*

(Received 1 July 2016; accepted 16 August 2016)

Abstract. Characteristic points of the law of motion were determined based on the results of experimental study on the velocities and accelerations of the lifted barbell. Relationship between the height of the athlete, lifted weight, maximal velocity and acceleration was estimated analytically. It was shown, that at the initial time moment the athlete must apply approximately 1,5 times larger force than lifted weight. The values of the parameters of the barbell' law of motion and lifting force approximate law of change were estimated.

Keywords: dynamics, maximal velocities, accelerations, parameters of motion, maximal force, law of motion, height, weight, mass.

Introduction

The biomechanical analysis of the motion of bar in weightlifting was analysed in various scientific research works [1, 2, 3, 4, 5, 6, 7, 8, 9, 10, 11]. The trajectory of barbell motion and accelerations and velocities were measured. Experimentally estimated maximal velocities of the barbell for the experienced athletes and it is equal to ~1.0 m/s. In the study [11] it was explained, that maximal acceleration for different level athletes can vary from 2.8 to 5.13 m/s^2. When analysing time dependency of the motion velocity during the snatch of highly skilled athletes, it was estimated, that it varies continuously, almost symmetrically and without sudden oscillations [4]. The magnitude of the lifted weight depends on the height of the athlete [5]. The taller the athlete, the lower weight he is able to lift. Some research works present studies on the kinetostatics of the barbell using Newton law of motion. However, there is lack of works devoted to development of analytical estimation of the dependency of the maximal velocity on the lifted height and needed acceleration to guarantee maximal velocity.

Therefore, the goal of present research is, based on the experimental results, estimate relationship between the height of the athlete, lifted weight, maximal velocity and acceleration. Also, determine characteristic points of law of motion of the barbell and values of parameters in those points.

Methods

Research was carried out in the weightlifting gym of the Vilnius University "Health and sport centre" under the guidance of the weightlifting coach. Total six athletes were recruited for the study: three beginners and three advanced weightlifters. The barbell's weight was varying from 60 to 80 kg. The height of the athletes was 1.62–1.86 m. The barbell's lifts were the snatch and the clean and jerk. Inertial sensors with ±1.5g – 6g Three Axis low-g micromachined accelerometer were fixed on the hand and forearms of the weightlifters and one on the barbell. Weightlifters were instructed to perform snatch and clean and jerk lifting techniques. All data was registered and stored on the PC.

Results

Some results of the experimental measurements are shown in Table 1 and Fig. 1 and Fig. 2. Table 1 presents athlete-characteristic data of the barbells' velocity and acceleration. Analysis of the influence of the height to maximal velocity v_{max} showed that the taller athlete must generate larger maximal velocity in order to lift the same weight and they can lift lower maximal weight than smaller athlete can. This was estimated also by Jaya et al in [5].

Table 1. Details about the weightlifter

Subject N	Height h, cm	Age	Human weight, kg	Lifted weight Q, kg	a_m, m/s^2	t, s when $a_m \approx 0$	v_{max}, m/s	h / v_{max}	t, s when $v = v_{max}$
1n	186.0	23	74	70	3.85	0.6	1.50	124.00	0.6
2n	178.5	22	76	70	4.05	0.55	1.46	122.26	0.55
3n	169.5	24	80	70	3.68	0.6	1.42	119.37	0.6
4p	162.0	22	73	70	3.33	0.55	1.05	154.28	0.55
5p	175.0	21	75	70	3.58	0.5	1.16	150.87	0.5
6p	172.5	23	77	70	3.16	0.55	1.10	156.82	0.55

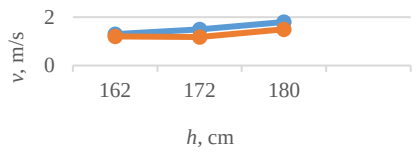

Fig. 1. Influence of the height to barbell (70 kg) velocity: blue – one subject, orange – averaged data of 3 subjects

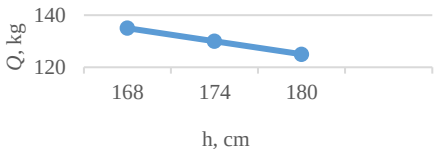

Fig. 2. The influence of height to the lifted weight, according to [5]

From the Fig. 1 it can be noted that there is non-linear relationship between maximal velocity and athlete height, because $v_1/h_1 < v_2/h_2 < v_3/h_3$ and it can be expressed as second order polynomial.

Analysing changes tendencies of barbell's velocities and accelerations during snatch and clean and jerk it was noted that maximal velocity 1.1–1.75 m/s is reached after 0.9–1.2 s, while maximal acceleration 3.16–3.85 m/s^2 is reached after 0.21–0.3 s (Table 1). Their velocity is increasing continuously and after it reaches maximal value starts to decrease (Fig. 3, 4). Fig. 3 shows graph of the 70 kg weight barbell clean and jerk, the height of the athlete 172 cm, maximal velocity $v_{max} \approx 1.75$ m/s, and Fig. 4 – during snatch of the same weight, $h = 162$ cm, and velocity is only $v_{max} \approx 1.1$ m/s. While analysing velocities and accelerations of barbell's motion weaknesses of the athlete can be noted and one can suggest how to improve.

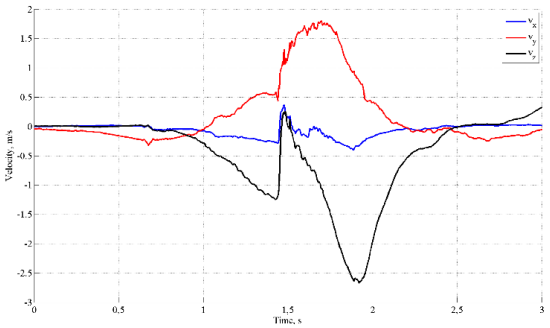

Fig. 3. Barbell' lifting velocity of beginner athlete

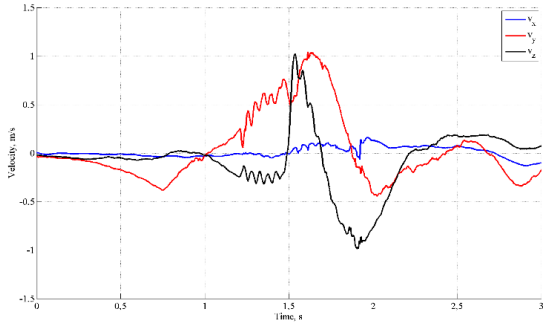

Fig. 4. Barbell' lifting velocity of advanced athlete

The characteristic points of the barbell law of motion and their values were estimated: first – when $t = 0$, the velocity $v(t) = 0$, acceleration $a(t) = 0$ and the lifting height of the barbell $h(t) = 0$; second – when $a(t) = a(t)_{\max}$, $0 < t < T$ and $v(t) \neq 0$; third – when $a(t) \approx 0$, $F(t) \approx 0$ and $0 \leq t \leq T/4$, the value of the velocity is maximal $v(t) \approx v_m$ and $0 < h(t) < h_m$ and, fourth – when $t = T$, $a(t) = 0$, $v(t) = 0$ and $h(t) = h_m$, (where T – barbell lifting time; h_m – barbell lifting height).

The dynamics of the barbell motion will be investigated further after the evaluation of values of characteristic points of barbell's law of motion. Barbell's motion in the direction of 0x axis under action of external force can be described as:

$$m\ddot{x}(t) + k\dot{x}(t)^2 + Q = F(t), \text{ when } a(t) \neq 0 \text{ and } t > 0, \; F(t) = F(t)_d + Q, \tag{1}$$

where $\ddot{x}(t)$ is second time derivative, $\dot{x}(t)$ – first time derivative; $F(t)$ – force applied to the barbell; k – coefficient of the environmental drag; m – barbell's mass, $F(t)_d$ – variable part of the force, Q – barbell's weight.

When $a(t) \approx 0$ and $0 < t < T$, then $F(t) \approx 0$ and equation (1) becomes:

$$m\ddot{x}(t) + k\dot{x}(t)^2 + Q = 0. \tag{2}$$

Equation (2) shows that when the barbell is under action of $F(t) \approx 0$, it will move due to inertia. Based on the barbell velocity (Fig. 3, 4) and acceleration graphs, time varying functions of the kinematic barbell's parameters can be expressed using functions of Fourier series and taking only first elements the solution of equation (1) is:

$$F(t)_d = \frac{\pi m}{T} v_{\max} \cos(\omega t - \varphi) + k\left[v_{\max} \sin(\omega t - \varphi)\right]^2, \text{ when } 0 \leq t \leq \frac{T}{4}, F(t) = F(t)_d + Q;$$

$$F(t)_{d\max} \approx \frac{\pi m v_{\max}}{T} \text{ and } a_{\max} \approx \frac{\pi v_{\max}}{T}, \tag{3}$$

where ω – angular velocity; φ – initial phase.

When $\omega t - \varphi = 0$, then $\sin(\omega t - \varphi) = 0$. In such way, the magnitude of the force when lifting the weight at initial time moment would be described according to the first member of (3) expression. When $t \approx T/4$, then $\cos(\omega t - \varphi) = 0$ and only second member remains in (3) expression. Therefore, the force applied by the skilled athlete at initial time moment and during the lifting should vary approximately according to cosine law.

When the value of the acceleration $a(t) \approx 0$, $0 \le t \le T$ and $v(t) \ne 0$, the lifted barbell moves due to inertia (2). It is important to provide required velocity to the barbell in order to reach desired lifting height. Evaluating estimated characteristic points of the law of motion, dependencies of the lifted height, barbell's weight and maximal velocity were obtained analytically:

$$h_0 \le \frac{k}{2gm} \ln\left[\frac{\left(1+\frac{k}{gm}v_m^2\right)}{\left(1+\frac{k}{gm}\dot{h}(t)^2\right)}\right], \tag{4}$$

where g – gravitational acceleration; v_m – maximal velocity; h_0 – height of the barbell's due to inertia, i.e. when $a(t) \approx 0$, and $v_m \ne 0$; $\dot{h}(t)^2$ – derivative squared.

Assuming, that the environmental drag during the lifting of the barbell is low, the approximate solution of (2) equation can be written as follows:

$$h_0 \le \frac{v_m^2}{2g} \text{ or } v_m > \sqrt{2h_0 g}. \tag{5}$$

The last expression (5) shows the approximate dependency of barbell's maximal velocity on the lifting height when $a(t) \approx 0$ and $v_m \ne 0$, i.e. what height it will reach due to inertia. Calculations performed according to (3) and using data from Table 1 has showed that the barbell must have reached approximately 114.7 mm due to inertia for the taller athlete (h = 186.0 cm), while in case of the smaller athlete (h = 162.0 cm) – 56.2 mm. Therefore, for taller athlete barbell should have lift 2 times more. The larger the athlete, the larger must be the height h_0 and therefore the higher velocity will be required for covering such a distance due to inertia. Which in turn means, that taller athlete must apply higher force to the barbell than the smaller athlete must or he will lift the barbell lower. The difference between calculated maximal velocities according to (3) and experimentally estimated (Table 1) is approximately 8–10%. Experimental data also confirms that taller athlete must apply higher force to the same weight.

Conclusions

After analysis of barbell' motion velocities, acceleration results weightlifters, the relationship between main parameters was determined experimentally and analytically and we can summarize:

- It was shown, that taller athlete must generate larger maximal velocity for lifting of the same weight than the smaller athlete.
- Estimated that the barbell moves not the whole path under action of the external force. When the barbell' acceleration approximately is equating to zero, then action of external force approximately equals to zero, and the velocity is maximum and after this moment barbell is moving further due to the inertia.
- Presented analytical dependencies describe relationship between maximal barbell velocity and covered path length due to inertia, maximum acceleration and applied force at initial time moment.
- At the initial time, the force applied to the barbell must be approximately 1,5 times larger than the barbell's weight and it was estimated that the force magnitude is approximately varying according to a cosine law for advanced athlete.

References

[1] Frounfelter, G. 2009. Triple extension: the key to athletic power. *NSCA's Performance Training Journal* 8(1): 14–15.

[2] Gourgoulis, V., et al. 2009. Unsuccessful vs. successful performance in snatch lifts: a kinematic approach, *Journal of strength and conditioning research* 23(2): 486–494. http://dx.doi.org/10.1519/JSC.0b013e318196b843

[3] Hedrick, A.; Wada, H. 2008. Weightlifting movements: do the benefits outweigh the risks?, *Strength & Conditioning Journal* 30(6): 26–35. http://dx.doi.org/10.1519/SSC.0b013e31818ebc8b

[4] Jones, J. R.; Taylor, J. 2010. *The biomechanical analysis of the Olympic snatch lift* [online]. Western Oregon University [cited 1 July 2016]. Available from Internet: http://www.wou.edu/~jrjones09/biomechanicsfinalpaper.pdf

[5] Rao, P. J., *et al*. 2015. Kinematic analysis of snatch technique in weightlifting, *International Journal of Law, Education, Social and Sports Studies* 2(3): 14–17.

[6] Stone, M. H., *et al*. 2006. Weightlifting, a brief overview, Strength & Conditioning Journal 28(1): 50–66. http://dx.doi.org/10.1519/1533-4295(2006)28[50:wabo]2.0.co;2

[7] Lloyd, R., *et al.* 2012. Long-term athletic development and its application to youth weightlifting, *Strength and Conditioning Journal* 34(4): 1. http://dx.doi.org/10.1519/SSC.0b013e31825ab4bb

[8] Isaka, T.; Okada, J.; Funato, K. 1996. Kinematic analysis of the barbell during the snatch movement of elite Asian weightlifters, *Journal of Applied Biomechanics* 12(4): 508–518. http://dx.doi.org/10.1123/jab.12.4.508

[9] Kim, Y.-J.; Seo, K.-W. 2002. Ground reaction force of the snatch motion and kinesiological analysis by photography, *Journal of Sport biomechanics* 12(1): 89–104.

[10] Haug, W. B.; Drinkwater, E. J.; Chapman, D. W. 2015. Learning the hang power clean: kinetic and technical changes in four weightlifting naive athletes, *Journal of Strength & Conditioning Research* 29(7): 1766–1779. http://dx.doi.org/10.1519/JSC.0000000000000826

[11] Bauer, T.; Isaac, L. 1996. Biomechanical analysis for the coach of Olympic weight lifting, *Journal of Sports Medicine and Physical Fitness* 9(4): 263–268.

11TH INTERNATIONAL CONFERENCE
BIOMDLORE 2016
OCTOBER 20–22, 2016, DRUSKININKAI, LITHUANIA
BIOMDLORE.VGTU.LT

eISSN 2345-0630
ISBN 978-609-457-959-2
eISBN 978-609-457-958-5
DOI: 10.3846/biomdlore.2016.24

The study of extraneous conditions that affect tilt-based pointer movements

Artūras Serackis[1], Darius Miniotas[2], Andrius Katkevičius[3], Audrius Krukonis[4], Darius Plonis[5]
[1, 2, 3, 4, 5] Vilnius Gediminas Technical University, Lithuania
E-mails: [1] *arturas.serackis@vgtu.lt (corresponding author)*, [2] *darius.miniotas@vgtu.lt*, [3] *andrius.katkevicius@vgtu.lt*, [4] *audrius.krukonis@vgtu.lt*, [5] *darius.plonis@vgtu.lt*

(Received 19 September 2016; accepted 21 September 2016)

Abstract. Introduction: With the rapid evolution of mobile devices, there is also a tremendous growth in their applications. This triggers new research on more efficient techniques of human-computer interaction. To point at an object of interest seen on the screen of a mobile device, various new methods were suggested recently.
Methods: This paper presents the results of a user study that employed tilting as a technique for entering text. The independent variables in the user study were mobility (sitting, walking, sitting in the moving bus) and keyboard size (5×3, 10×4). The experiment involved 50 participants aged from 22 to 65.
Results: In the walking condition, it took on average 11.3% more time for participants to complete the task compared to the sitting condition with 5×3 keyboard, and 45.1% more time compared to the sitting condition with 10×4 keyboard. Keyboard size had a marked influence on task completion time. In addition, task completion time while traveling by bus was 3.2% longer than that observed for the walking condition with 5×3 keyboard. Surprisingly, task completion time with 10×4 keyboard while traveling by bus was 10.4% shorter compared to the walking condition. Error rate and movement efficiency were investigated additionally to find out the explanation for such performance data.

Keywords: mobile text input, tilt input, keyboard size, performance measurement.

Introduction

Research area of human-computer interaction (HCI) is becoming increasingly important because of the development of mobile technologies and the rapid growth in their usage. The task of the research is to make the usage of mobile devices user friendly by focusing on quality, effectiveness and efficiency of the graphical user interface (GUI). These objectives can be achieved in different approaches: studies of better hierarchy of information presentation [1], studies of better data input type [2].

According to [3], there are three main input facilities for mobile devices that are on the market: the keyboard, the stylus with the touch screen, and the scroll wheel. However, there are other input types such as tilt-based input, facial tracking input [4], and voice input [5]. Tilt-based input is commonly used for maintaining correct screen orientation when the device is rotated; this is also a popular input method for gaming with mobile devices [6], or it can be used for remote control in other embedded devices [7]. Exploration of possibilities for tilt-based interaction still requires research effort.

Our research focuses on the investigation of the abilities to perform practical tasks by applying the tilt-based control of the pointer. Two independent variables explored in this study were mobility (sitting, walking around a circular table, travelling in the moving bus) and keyboard size (5×3, 4×10) giving six different conditions for experimental investigation. The study is concluded with a report on the user feedback [8].

Methods

The various factors that can influence tilt control, separately along the three axes of wrist movement showed that users could control comfortably at least 16 levels on the pronation/supination axis [9]. Tilt-based input enhances the user experience when compared to key-based input [10].

Participants. All participants were from Vilnius, the capital of Lithuania, and aged between 22 and 65 years. The total number of participants was equal to 50. Anybody who expressed willingness to participate in the experiment was allowed to do that with no restrictions. It was only required that at least two participants were from the following four age groups: 20–30 years old (the youngest), 31–45 years old (younger middle-aged), 46–60 years old (older middle-aged), and 61–80 old (the oldest). Participants were categorized to four groups according to [11]. Participants from different age groups were chosen because user age is an important criterion and people adapt differently to new user interfaces [12]. All participants were unpaid volunteers in the study. Experience of participants in working with mobile devices was taken into account. All the participants had been trained on how to work with the tilt-input before the study began.

The experimental interface. In this study, the tilt of the device was directly mapped to the position of the ball. This allowed quick and easy control of the ball's position. The zero position of the interface (corresponding to the ball is in the centre of the screen) occurs when the device is parallel to the ground in both the pitch and roll axes (Fig. 1). To avoid an unintended start, each task commenced with the ball resting in one corner of the screen. The application controlled the sequence of the tasks presented to the participants. They had to select 10 targets in turn from either a 5×3 or 10×4 grid. To complete the selection, the participant was to move the ball to the target square and dwell upon it for a period of 500 ms. A target was approximately 3 cm × 2.5 cm in size to resemble a real character. The application selected the targets at random; the target was identified by highlighting it. The highlight became more intense when the ball appeared in the target's area. A beep could be heard after each successful selection.

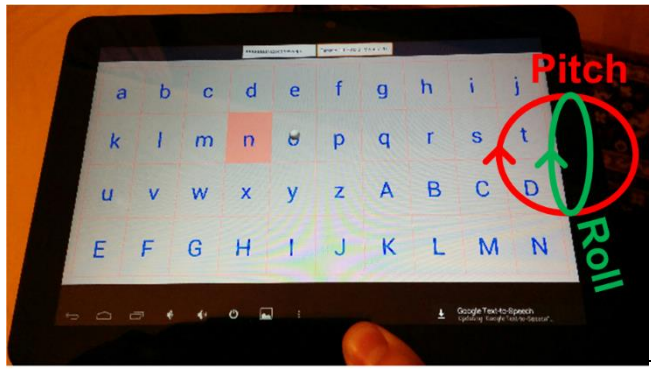

Fig. 1. Participant completing tilt input task (pitch and roll axis indicated)

The application allowed all "characters" on the interface to be selected throughout the task, with erroneous selections recorded. After each successful selection, the corresponding character appeared at the top of the screen. The number of remaining targets was displayed on the interface along with the task condition.

Procedure. For each participant the brief demonstration and key information about the task was provided. Participants were then given a device each and allowed to complete a practice task sitting on the chair and selecting 10 targets. The data from practice phase was recorded but was

not used in this paper. After the practice task, the participants completed six tasks (each task was fulfilled 5 times with 10 inputs per task) in each condition before moving on to the next one.

The study was performed with each participant individually with the changing sequence of conditions. Some participants fulfilled the task sitting on the chair first, some walking around the table and some participants started from fulfilling the task sitting in the bus. Task execution order was changing for every participant in order to get adequate results because participant gets some experience after each fulfilled task. Participants fulfil the task 5 times in every condition (sitting, walking, and travelling in bus) with two different keyboard sizes (5×3 or 10×4). Over all every participant fulfils the task 30 times.

Walking path was around a circular table. Participants were asked to walk at normal speed, at which they usually walk. It is difficult to maintain the same conditions while traveling in bus for experiments but in order to maintain conditions as uniform as possible the same bus route was used during peak hours from 5 till 6 pm.

Each participant used an identical Android device Exynos4412 Prime Quad Development Platform ODROID-Q2. In the sitting condition, participants used chairs. The study was designed to last no longer than 20 minutes per participant (the time required to wait for the proper bus was not included) to ensure that the participant did not tire or lose interest.

Results

Three simplest performance metrics were used: task completion time, the error rate and the efficiency of ball movement. Error rate in this context is the ratio of inadvertent, or extra, selections to correct selections. As there were always 10 correct selections per task, two extra inadvertent selections would result in an error rate of 2 / 10 = 20%. Efficiency of ball movement is the ratio of the minimum distance between targets and the actual distance moved by the ball. 100% efficiency implies a straight-line movement from the centre of each target to the next target.

From the data collected, the shortest task completion time was obtained while sitting. Task completion time was 11.1% longer while walking with a 5×3 keyboard size and 14.5% longer while walking with the 10×4 keyboard size (Fig. 2). Unexpectedly, the task completion time decreased while travelling in the bus comparing with task completion time while walking and using the 10x4 keyboard size.

The smallest error rate was while walking (Fig. 3). It was equal to 51.6% with 5×3 keyboard size and 51.6% with 5×3 keyboard size. The error rate was bigger while travelling in the bus and unexpectedly the biggest error rate was while sitting comparing with walking and travelling in the bus.

The biggest distance efficiency was received while sitting and the smallest efficiency while walking with both 5×3 and 10×4 keyboard sizes (Fig. 4). These results correlate with estimated task completion times and error rates. If the time of task completion is less it gives with the smaller error rate and higher efficiency.

The investigation also showed that age of participants has influence to the task completion time, error rate and distance efficiency.

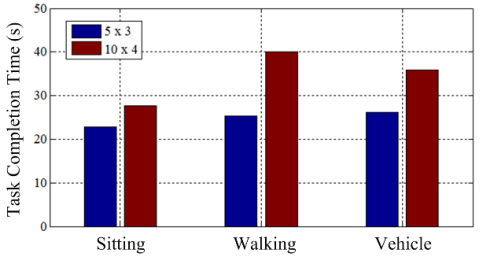

Fig. 2. The participant performs the task while walking around a circular table

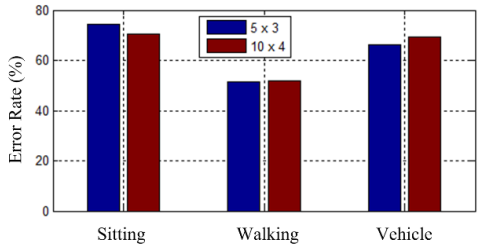

Fig. 3. Mean error rates for all conditions

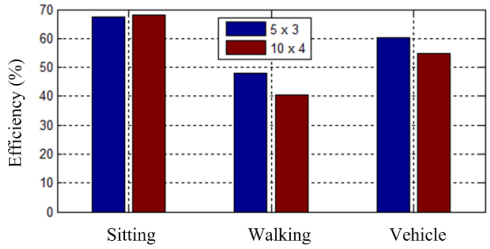

Fig. 4. Mean efficiency rates for all conditions

The older middle-aged and oldest participants had bigger task completion time and error rates. In respect of each participant individually youngest and younger middle-aged participants adapted to conditions of the game faster than others.

Unexpectedly the task completion time while travelling in bus almost unchanged and increased 3.2% (an additional ~ 0.8 seconds) with 5×3 keyboard size and decreased 10.4% (an additional ~ 4.18 seconds) with 10×4 keyboard size compared to walking. Participants had less distraction and had better control over the movement of the device while sitting in the bus compared with walking.

The movement of the body is partly transmitted to the device to make accurate tilt-input more challenging while walking. The attention of the participants also was triggered by the additional navigation tasks around the course and turn in the corners. The quality of the results could be influenced by factor that participants more concentrate on more complex task. Therefore, lower error rate is obtained while walking or travelling in the bus while comparing with sitting.

Conclusions

As demonstrated by this experiment, participants from all the four age groups investigated were able to successfully select targets on mobile devices using the text entry method described here. Investigation under the six different conditions revealed that disturbances of the real settings such as shaking while sitting on a bus do not significantly affect user performance. The age of participants influences the task completion time, error rate, and efficiency. The oldest participants had a longer task completion time and a higher error rate. The youngest participants were able to adapt to the conditions of the game faster than the other groups. The performance data could be influenced by the factor that participants tended to concentrate more on a more complex task.

Acknowledgements

We would like to thank Scott MacKenzie from York University in Canada for his valuable comments, insights, and sharing his experimental software with us. This research was funded by a grant (No. MIP-083/2015) from the Research Council of Lithuania.

References

[1] Hao, J., *et al.* 2010. Visualizing and navigating hierarchical information on mobile user interfaces, *International Journal of Advanced Intelligence* 2(1): 81–103.

[2] Huang, K. Y. 2009. Challenges in human-computer interaction design for mobile devices, in *Proceedings of the World Congress on Engineering and Computer Science*, October 20–22, 2009, San Francisco, USA. Hong Kong: Newswood Limited, 20–22.

[3] Muhanna, A. 2007. *Exploration of human-computer interaction challenges in designing software for mobile devices. Master's thesis.* Reno: University of Nevada. 104 p.

[4] Newman, K. E.; Hobbs, E.; Blei, M. 2013. A tablet based hands free interface to nurse communication in the standard hospital room for limited mobility patients, *Information Engineering Letters* 3(3): 50–56.

[5] Hwang, Y. *et al.* 2012. Developing a voice user interface with improved usability for people with dysarthria, in *Proceedings of 13th International Conference ICCHP2012*, July 11–13, 2012, Linz, Austria. Berlin Heidelberg: Springer-Verlag, 117–124. http://dx.doi.org/10.1007/978-3-642-31534-3_18

[6] Marzo, A.; Bossavit, B.; Hachet, M. 2014. Evaluating controls for a point and shoot mobile game: augmented reality, tilt and touch, in *IEEE International Symposium on ISMAR-MASH'D*, September 10–12, 2014, Munich, Germany. Piscataway: IEEE, 59–62. http://dx.doi.org/10.1109/ISMAR-AMH.2014.6935439

[7] Boring, S.; Jurmu, M.; Butz, A. 2009. Scroll, tilt or move it: using mobile phones to continuously control pointers on large public screens, in *Proceedings of the 21st Annual Conference of the Australian Computer-Human Interaction Special Interest Group (CHISIG)*, November 23–27, 2009, Melbourne, Australia. New York: ACM, 161–168. http://dx.doi.org/10.1145/1738826.1738853

[8] MacKenzie, I. S.; Teather, R. J. 2012. FittsTilt: the application of fitts' law to tilt-based interaction, in *Proceedings of the 7th Nordic Conference on Human-Computer Interaction NordiCHI 2012*. October 14–17, 2012, Copenhagen, Denmark. New York: ACM, 568–577. http://dx.doi.org/10.1145/2399016.2399103

[9] Partridge, K., *et al.* 2002. TiltType: accelerometer-supported text entry for very small devices, in *Proceedings of the ACM Symposium on User Interface Software and Technology UIST2002*, October 27–30, 2002, Paris, France. New York: ACM, 201–204. http://dx.doi.org/10.1145/571985.572013

[10] Gilbertson, P.; Coulton, P.; Chehimi, F. 2008. Using "tilt" as an interface to control "no-button" 3-D mobile games, *Computers in Entertainment*, 6(3): 1–13. http://dx.doi.org/10.1145/1394021.1394031

[11] Wilkowska, W.; Gaul, S.; Ziefle, M. 2010. A small significant difference – the role of gender on acceptance of medical assistive technologies, in *Proceedings of 6th Symposium of Human-Computer interaction and Usability Engineering USAB2010*, November 4–5, 2010, Klagenfurt, Austria. Berlin Heidelberg: Springer, 82–100. http://dx.doi.org/10.1007/978-3-642-16607-5_6

[12] Arab, F.; Malik, Y.; Abdulrazak, B. 2013. Evaluation of PhonAge: an adapted smartphone interface for elderly people, in *Proceedings of 14th IFIP TC 13 International Conference*, September 2–6, 2013, Cape Town, South Africa. Berlin Heidelberg: Springer, 547–554. http://dx.doi.org/10.1007/978-3-642-40498-6_44

SHORT COMMUNICATION

11TH INTERNATIONAL CONFERENCE
BIOMDLORE 2016
OCTOBER 20–22, 2016, DRUSKININKAI, LITHUANIA
BIOMDLORE.VGTU.LT

eISSN 2345-0630
ISBN 978-609-457-959-2
eISBN 978-609-457-958-5
DOI: 10.3846/biomdlore.2016.25

Challenges in adapting technical assistive products individually for people with mobility disabilities

Ilona Ogurcova
Centre for Technical Assistance to Persons with Disability under the Ministry of Social Security and Labour, Lithuania
E-mail: *ilona.ogurcova@tpnc.lt*

(Received 29 February 2016; accepted 27 June 2016)

Keywords: technical assistive products, individual adapting, mobility disabilities.

Introduction

Situation Analysis. The CTAPD is a budgetary institution established by the Ministry of Social Security and Labour for the purpose of organizing provision of technical assistive products to people with disability.

According to the Law on Social Integration of People with Disability and the action plan approved by the CTAPD in 2015, the CTAPD implements provision of technical assistive means to Lithuania's citizens with mobility, vision, or hearing impairments.

The CTAPD implements the following legal measures instituted by the programme "Social Integration of People with Disability" managed by the Ministry of Social Security and Labour responsible for allocated funding:

1) obtain and provide technical assistive means to persons with disability and repair said means;
2) establish conditions for activities of the Centre for Technical Assistance to Persons with Disability;
3) expand the infrastructure of the Centre for Technical Assistance to Persons with Disability.

The purpose of the CTAPD is to ensure implementation of current social integration measures, activities, and projects for people with disability intended for improvement of their medical, social, and professional rehabilitation as well as to ensure provision of technical assistive products to citizens satisfying their special needs.

Terms and Definitions:

- The main terms and definitions coincide with those used in the standard LT EN ISO 9999:2011 Assistive Products for Persons with Disability.
- TAP – technical assistive products.
- CTAPD – Centre for Technical Assistance to Persons with Disability under the Ministry of Social Security and Labour.

Programme measure – obtain and provide technical assistive means to persons with disability and repair said means.

This measure was implemented by obtaining electrical wheelchairs and mobility, vision, and hearing TAP for people with disability. Specialists of the CTAPD have chosen, adapted, and issued mobility, vision, and hearing TAP and accepted personal requests for compensation of expenses incurred in obtaining technical assistive products.

According to the approved methodology for estimation of the number of TAP necessary for people with disability, annual demand for TAP in the country was estimated at 60 078 pcs. at the beginning of 2015. In 2015 CTAPD departments and municipal establishments have issued 48 340 TAP (new, returned, obtained as aid), paid 1 794 compensations (391 470 Eur), and provided services to 34.9 thousand of people. In 2015 the total demand for TAP was satisfied to 83.45%.

Commissions established by the director of CTAPD, of which there are four, considered personal requests and made decisions in regard of adding the applicants to the queue of persons

seeking compensation. Compensations for mobility, vision, and hearing TAP obtained by persons were paid. Certificates were issued granting persons the right to obtain TAP through enterprises and information provided on enterprise invoices and other documents submitted by individuals was checked to established whether said individual had the right to compensation of expenses incurred in obtaining a TAP through an enterprise. After studying the use of TAP obtained by individuals through enterprises, it was discovered that having bought a wheelchair for the first time the person would then have difficulties in replacing it because changes in the person's condition or inappropriate choice of the product. When buying a wheelchair for the first time a person would rely more on the options offered by a supplier then their personal opinion and would consider neither possible future medical or physical changes nor the structural peculiarities of the wheelchair. The best results were achieved when a person would obtain their first wheelchair from the CTAPD as it would then be possible to return it to the CTAPD and, having their medical and physical condition stabilized and clearly knowing their needs, the person would turn to an enterprise for a TAP with the CTAPD paying a compensation to the enterprise. People who had prior experience using wheelchairs and then chose a wheelchair through an enterprise were more satisfied with the products they obtained as they knew their own news well and had enough experience evaluating peculiarities and advantages of wheelchair designs offered by suppliers. Individual selection and adaptation of mobility TAP is very important not only for the effective use of budgetary funds but also for restoring a person's ability to function normally and aiding in the process of their integration into the society.

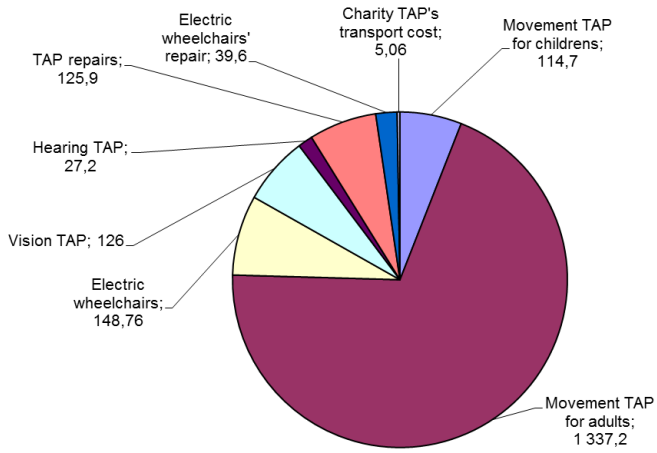

Fig. 1. Distribution of the funds used for the obtaining (exclusive of paid compensations) and repair of TAPs in 2015 (in thousands of euros)

The relevance of the situation was highlighted by the growing tension among the involved parties: the user, the TAP supplier and the Centre. It should be noted that the Centre did not find the publicly announced information about the studies of the quality of the service of selection of TAP. The Centre has established that it is not known what factors or causes may encourage the certain behaviour of the users and the TAP suppliers. Therefore, it was decided to conduct the qualitative research, the essential purpose of which is to formulate the statements and hypotheses, as well as to establish the causes of this phenomenon. It is sought to establish the essential criteria with the help of which the suitability of the selected TAP for a person could be assessed; and to form the survey algorithm for adapting TAPs individually, as the methodical instruction to the employees of CTAPD. The following methods were invoked for the conduct of this research: the in-depth and semi-structured interviews, and focus-group interviews.

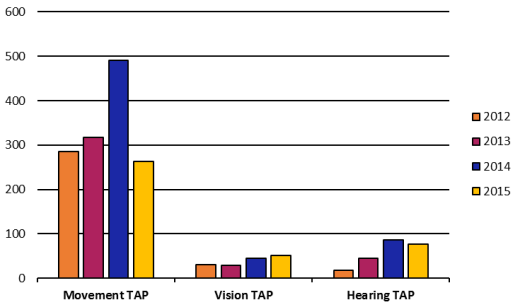

Fig. 2. Budget funds used by the Centre for the obtaining and repair of TAPs (in thousands of euros)

Methodology

During the conduct of the research, the structural peculiarities of the wheelchairs, the possibilities of interchangeability of components and assemblies, and the impact of use of additional accessories on the efficiency of operation of TAPs were researched. By applying the type of survey, such as the in-depth and semi-structured interviews, it was sought to obtain the non-structured information about the issue being researched as much as possible. The process and style of the interviews depended on the goals set by the researcher for himself; however, in all cases, the researcher and the surveyor interacted. Such method provided the possibility to find out the intensity of this topic, and the representation of the issues, in the selected data source. The focus-group interviews were also held in this manner – it is one of the qualitative methods of data selection used mostly in the world. During this research, a conversation with a small group of respondents was held on a foreseen topic of conversation. On 25/9/2015, in the Landscape Therapy and Recreation Centre, CTAPD, along with the social partners involved in the research, seeking to establish the universal technological structure of the basic model of the active type of the wheelchairs, which could be adapted individually for each user, by using the various accessories and/or other additional/alternative parts offered by the manufacturer, organized and performed the research and practice seminar. During this seminar, the focus-group interviews distinguished themselves by the synergic effect which enabled a variety of opinions, ideas, and experiences. The research on the focus-group interviews was useful; while looking for the new information (e.g. the opinion about TAPs and their usage), it was sought to hear different opinions on the same topic, by illustrating them with the words of the very Respondents; it is desired to learn why the Participants behave one way or another, what their motives and attitudes are; it is sought to reveal the ways by which the individuals affect each other; and it was to obtain more various information in a greater number.

Respondents

The research involved the members of the Paraplegic Associations of the Republic of Lithuania, who tested TAPs that were provided to them, and gave feedback; as well as the Suppliers of the Centre who, in accordance with the valid procedure of providing the persons with TAPs, supply various wheelchairs (of different manufacturers, types and models), the kinesiotherapists and the rehabilitologists of the Health Care Institutions. The research involved total 20 persons who were using the wheelchair. The participants were divided into 3 groups. All groups discussed on the indicated topic: “Possibilities of adjustment of the wheelchair and their importance to the correct seat posture: possibilities of adjustment of the seat width and foot support; adjustment of the height and tensioning of the back support; and possibilities of adjustment of the height of hand supports.” During the first task, the members of each group had, by mutual agreement, to express in one word what, in their opinion, is most necessary for the user of the wheelchair from the specialists of the Centre. The topics of open discussions were named

in these words, which formed the contents of the second task. During the second task, the respondents took part in the open discussions which were held by the moderators appointed by the organizer, who asked the prepared open questions. The wheelchairs of different manufacturers and the possibilities of their adjustment were demonstrated during discussions. TAPs of the following companies were examined: Meyra, Ottobock, Vermeiren, Offcarr, Kuschell, Panthera.

Results

Essential conclusions and suggestions are given in the table 1. The necessary requirements for TAPs for the better integration of the person in the society were specified.

Table 1. Essential conclusions and suggestions

Section No.	Group name and specified requirements for TAPs		
	TOLERANCE	RESPECT	TRUST
Section I	• Flexible wheel protections • Fork frame folding mechanism • Good cohesion of arcs with the palm	• We know how to sit correctly, but we sit conveniently • The correct seat posture from the very beginning • The tensioning of the backrest for the stable seat posture • The footrests create the load for the joints	The very user shall like it.
Section II	• The weight of TAP is the very significant criterion for transportation • The check of technical condition every 12 months during the warranty period • The adjustment of the height of the backrest by passing to the more active usage	The tilt of the seat is adjusted by 3 belts	• The lighter ones are less adjusted, but the more experienced users shall use them • For the beginners, max. adjustment, from 1 to 6 months
Section III	• Adjustment of the footrest angle, stiffening of the backrest from 46 cm • Tensioning of the seat is adjusted not only by the stripes	• Covered front wheel caster bearings • Fork frame mechanism • Front caster fork angle • Total height is adjusted by the wheel beam • Adjustable armrests	I've seen it and I like it, and the rest may be tamed

Conclusions and suggestions

It has been concluded that the essential criterion for evaluation of effective TAP use is personal energy commitment. This is to say that a person using different products of the same type to perform the same kind of action commits a different amount of energy because of product design peculiarities and choice of accessories. In other words, several TAP are offered to a person after assessing their everyday needs and impairments. The TAP that is the most suitable for the person is the one using which they commit the least amount of energy.

Currently, the CTAPD and DWCAO (Disability and Working Capacity Assessment Office), using the International Statistical Classification of Diseases and Related Health Problems (ICD) and International Classification of Functioning, Disability and Health (ICF), are working on functional ability identification tests that could be used to determine energy commitments when using this or that TAP.

AUTHORS INDEX

NOTES

Proceedings of 11th International Conference BIOMDLORE 2016
October 20–22, 2016, Druskininkai, Lithuania
Print-on-Demand
Published by Vilnius Gediminas Technical University press Technika
Saulėtekio al. 11, LT-10223 Vilnius, Lithuania
Printed by UAB “Ciklonas”
J. Jasinskio g. 15, LT-01111 Vilnius, Lithuania